U N I V E R S I T Y O F L O N D O N

IMPERIAL COLLEGE OF SCIENCE AND TECHNOLOGY

Department of Physics

Applied Optics Section

THE APPLICATION OF A THERMOPLASTIC RECORDING MATERIAL TO HOLOGRAPHIC FILTERING

by

Peter Frank Gray B.Sc., M.Sc., D.I.C.

Thesis submitted as part of the requirements
for the degree of Doctor of Philosophy

February 1977

Abstract

A review is given of work in the fields of xerography and associated subjects from which thermoplastic xerography and holography stemmed, and the path by which this development occurred is traced.

The techniques and results of other workers with thermoplastic hologram plates are surveyed in order to identify the approach most likely to yield success in the present application.

A description is given of the apparatus constructed for the production of thermoplastic hologram plates, accompanied by an account of the behaviour of the plates in the relatively uncomplicated situation of recording holographic gratings.

To carry out holographic filtering it is necessary to record a hologram of the Fourier transform of a transparency, and the difficulties arising in this (due to the large intensity range to be recorded) are considered. This is done both by computation upon a simplified theoretical model of the process and by examination of the behaviour of thermoplastic hologram plates in the more complex practical situation.

The results of optical cross correlation and autocorrelation are then given for a variety of images from satellite and aerial photography, using both phase-modulated transparencies and the more normal absorption-modulated transparencies. Possible methods of forming conclusions from the resulting correlation responses are then considered.

CONTENTS

contd.

CHAPTER 1

THE HISTORICAL DEVELOPMENT OF TECHNIQUES

1.1 Origins of Thermoplastic Recording

The use of thermoplastic films as a material for image recording began in the field of electrography. This subject is concerned with the production of a latent electrostatic charge pattern on a suitable surface by a non-photographic technique (such as using an electron beam or electrical discharge) for the ultimate purpose of forming a visible image (ref.1 p.111 & ref.2). The earliest publication on thermoplastic recording is by Glenn (3) who recorded images on a moving thermoplastic-coated conducting tape. The electrostatic image was formed by an electron beam which was scanned across the moving tape in a raster pattern. The lines of static charge laid down on the thermoplastic surface induced lines of opposite charge in the underlying earthed conducting base material, so that when the tape was heated by R.F. induction the surface of the thermoplastic was depressed into parallel grooves by the mutual attraction of the lines of charge.

The electron beam intensity was modulated by the brightness of the original scene, so that the groove depth was modulated in a corresponding pattern. The monochrome image was then reconstructed by a schlieren technique.

The advantages mentioned by Glenn of the thermoplastic material are erasure, reusability and freedom from chemical processing. The bandwidth for the recording system is

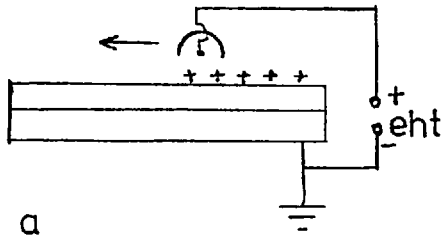

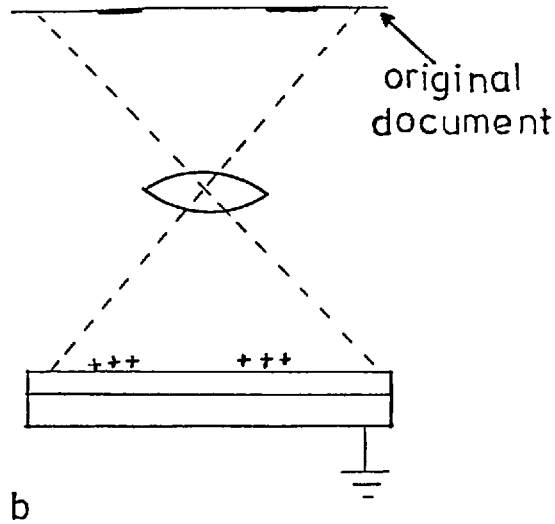

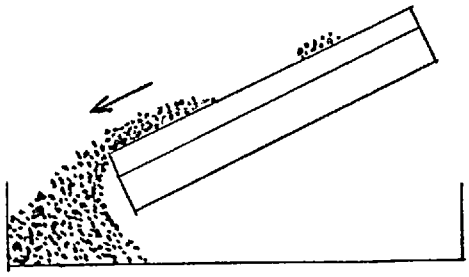

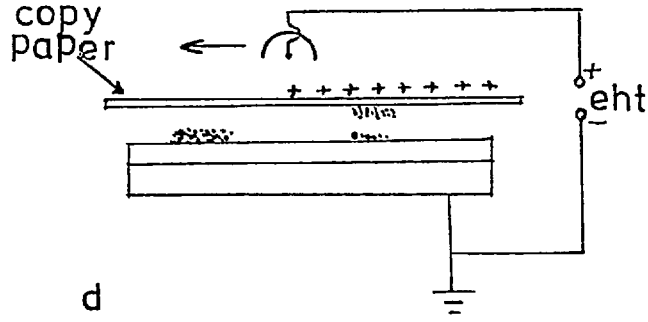

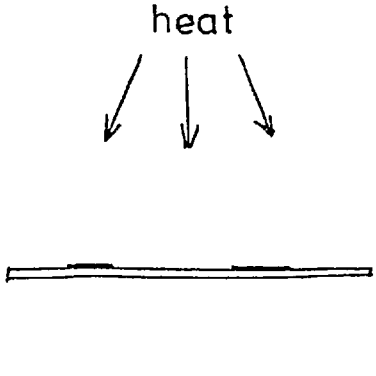

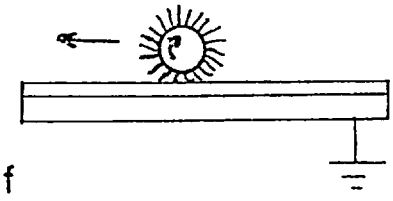

Figure 1. The Xerographic Process.

claimed to be more than adequate for video recording. "Development" of the surface deformations by R.F. heating pulse is said to be complete within 0.01 second.

1.2. Normal Xerographic Recording

Xerography is the production of a visible image by means of an electrostatic charge pattern which has been directly modulated by the action of light on a photoresponsive material. It is a branch of electrophotography.

The commonest application in which the principles of this subject are encountered is the familiar Xerox process for rapidly producing dry paper copies of documents. The basic stages of this process are shown in Fig. 1.

The xerographic plate, which is used as an intermediate store for the image in a latent form, consists of a thin layer of a photoconductive material supported on a conducting base. Amorphous selenium is often used for the photoconductor layer, thicknesses of 20 to 100 microns being usual (ref.1, p.22). The resistivity of the photoconductive layer in darkness must be very high (10^{12} to 10^{14} ohm. m) as it is required to retain very small amounts of charge on its surface without appreciable leakage in darkness. The term "photoconductive insulator" is sometimes used here. The conducting substrate is earthed.

The first stage of the recording process (Fig. 1a) is carried out in darkness and consists of laying a uniform charge on the free surface of the photoconductor. Usually, this is done by moving a high voltage corona discharge device (consisting of a thin wire partially surrounded by an earthed

shield) steadily across the plate at a short distance from it. This is known as sensitization of the xerographic plate, as the plate is now capable of recording a latent image.

An optical image of the original to be copied is then allowed to fall on the plate, causing the photoconductor to conduct in those regions which are exposed to light (Fig. 1b). The surface charge in these areas leaks away to the underlying earthed conductor leaving a surface charge pattern whose SPATIAL modulation is the same as that of the image.

The next stage is to develop the latent image into a visible one. Particles of a fine powder, or "toner" are brought very close to the surface of the xerographic plate and adhere to the surface by electrostatic attraction (Fig. 1c). The adhesion is greatly increased if the toner particles are first given an electric charge of opposite polarity to the charge forming the image on the plate. The particle sizes are usually in the range 1 to 20 microns and only a few charges are necessary to hold a particle to the plate (ref. 2).

The developed image is then transferred to paper (Fig. 1d) to form the final copy. This is often done by placing the sheet of paper in contact with the xerographic plate and applying a charge of the same polarity as that present in the latent image to the back of the paper by corona charging. The attraction of the toner particles by this charge is greater than that by the image charge and the particles adhere to the paper when it is removed from the plate.

The image is then fixed (Fig. 1e) by, for example, momentarily heating the paper so that the toner particles

melt and, on cooling, form a permanent ink image on the paper.

Finally, the xerographic plate is cleaned of particles and its image charge is neutralized to prepare it for the next image to be recorded.

There are many variations in the details of how these principles are applied. For example, to develop the latent image the toner particles may be blown in a fine cloud across the surface of the plate (aerosol, or powder cloud development), or they may be mixed with larger granules (0.3 mm diameter, say) of a different material (the "carrier") and poured over the plate. The granular carrier material adds to the mass of the mixture and increases the proportion of toner particles which reaches the plate. This is known as cascade development.

1.3 Organic Photoconductors in Xerography

A variation which was introduced in the late 1950's and has been extensively experimented with is the use of organic photoconductive materials in Xerography. Many organic compounds have been considered for this role. For example, Lardon et al. (4), Hayashi et al. (5) and Hoegl (6) consider a number of photoconductors. In many cases the conductivity of a compound can be increased by mixing it with an electron donor or acceptor (a "dopant") and its spectral response may be adjusted by adding an organic dye (a "sensitizer"). The field of organic photoconductors is thus very large.

The characteristics of these materials which have been found attractive in xerography are concerned with the ease

with which they can be formed into thin films, and their transparency and mechanical flexibility. Also, they are virtually free of granularity, and by dye sensitization, can be tuned to respond to the desired part of the spectrum.

1.4 Thermoplastic Xerography - The approach of the General Electric Company

In the early 1960's techniques were developed which brought together xerography and the work of Glenn on thermoplastic recording. The object was to produce a device which would record an optical image directly (without the intermediate step of converting the image to an electron beam signal) and yet from which the recorded image could be projected optically. Dispensing with electron beam recording would mean freedom from the need, which Glenn encountered, for an evacuated chamber in which to carry out the recording. Also, it was hoped that in copying applications where a permanent paper copy was not required, it would be possible to use a recording technique which employed entirely reusable materials and needed no inks, powders or paper. This would simplify operation and remove supply problems.

This work involved the use of a photoconductor layer to modulate spatially a charge pattern laid down on the surface of a thermoplastic layer. The thermoplastic surface would then be heated to allow deformation under the forces acting on the charges. The final recording would be in the form of thickness modulation of the thermoplastic. The first publications on this work appeared in 1963 (7and 8) and indicate two slightly different approaches.

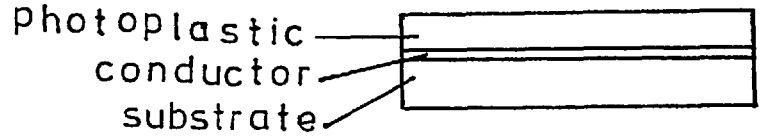

Figure 2. Structure of the Recording Plate used by Gaynor and Aftergut.

The method of Gaynor and Aftergut (7) at General Electric involved the use of a single material which had both photoconductive and thermoplastic properties. They use the term "photoplastic" for this type of substance. A thin layer (in the range 13 to 51 microns) of the photoplastic was deposited on one side of a glass substrate which had previously been given an electrically conductive coating of stannic oxide (Fig. 2).

The recording cycle began with the earthing of the conductive film and the laying of a uniform electric charge on the surface of the photoplastic in darkness by a corona discharge device. The plate was then exposed to the optical image, allowing the charge to leak away in the illuminated areas. So far the process is similar to that of xerography, described previously. However, to develop a visible image, a heating current was passed briefly through the conductive film and the photoplastic surface deformed under the forces of attraction between the surface charges and those induced on the earthed conductive film. The recorded image was viewed by projection with a schlieren projector.

The thermoplastic is effectively incompressible, and is unable to flow for large distances across the plate because of friction and viscosity. Only at the boundaries of charged areas (where there is an uncharged area nearby which is under no compressive force and to which the material displaced by the compression of the charged region can therefore flow locally) will compression of the film take place.

Thus the deformation of the surface is confined to regions where the surface charge density is strongly

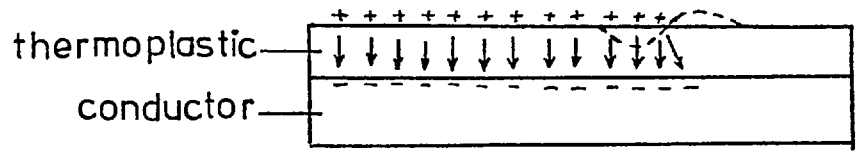

Figure 3. Thermoplastic Surface Deformation in "Relief Imaging."

non-uniform across the plate. Such a condition is found at the edges of illuminated regions in the recorded image, so that the recorded image tends to be a line diagram showing the edges of objects in the original. A qualitative description of the deformation which occurs in these situations was given by Gundlach and Claus (8) who use the term "relief image" for the resulting recorded image. They depict the deformation in the region of the boundary of a charged (unilluminated) area as that shown in Fig. 3. They point out that, in addition to the frictional forces which prevent wholesale movements of the thermoplastic across the plate, another cause of relief imaging is that at the charge boundary there is an unresolved lateral component of force acting on the surface charges which tends to pull the surface into a ridge as shown (broken line).

Relief imaging is no problem where the original to be reproduced is a line diagram, but it means that all areas of appreciable size and uniform tone will be reproduced with the same brightness whatever their density in the original. This would be unsuitable for continuous tone reproduction, but can be overcome as Gaynor and Aftergut show, by the well known technique of "screening" the original image. The type of screen used here is usually a fine regular square mesh of opaque lines whose spacing is less than the size of the smallest detail in the original image and yet which is large enough to be resolved by the recording technique. The screen is placed in the plane of the original (or its projected image) and its effect can be described qualitatively as breaking up the areas of uniform tone into a finely detailed

structure so that even in a region of originally uniform tone no point is now far from a density boundary. The magnitude of the change in image charge density across these boundaries depends on the density of the uniform tone in the original so that now even in places corresponding to originally uniform areas of the image, deformation of the photoplastic will take place and will do so to an extent determined by the original density. Continuous tone reproduction can thus be achieved, or, at least, approximated.

Gaynor and Aftergut considered numerous materials for the role of photoplastic. Transparent photoplastics were produced both by dissolving organic photoconductors in thermoplastic materials and by polymerizing organic photoconductors. They also formed opaque photoplastics by mixing inorganic photoconductive materials such as cadmium sulphide in finely divided form with thermoplastics.

Images recorded on opaque photoplastics were projected by reflection schlieren optical systems. They claim a higher sensitivity for this type of photoplastic than for the transparent materials, although it is not clear how the surface charge could leak away to ground through the photoplastic film during the recording exposure if the opacity of this film prevents the penetration of light to the lower levels of the film. Possibly, as Queener suggests, the explanation is that the free charge carriers are generated only in a thin surface layer of the photoconductor and then swept through the bulk of the material by the electric field without a significant degree of recombination taking place (ref. 16).

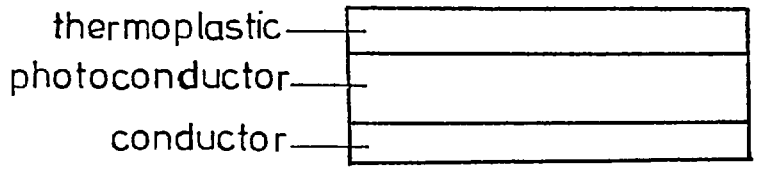

Figure 4. Structure of the Recording Plate used by Gundlach and Claus.

1.5 Thermoplastic Xerography - The approach of the Xerox Corporation

The other approach to image recording on light-sensitized thermoplastics which emerged at this time was that of Gundlach and Claus (8) at the Xerox Corporation. This was based on the observation that if the surface of a thin thermoplastic film is charged by a corona discharge while the film is hot and in a soft condition, the surface takes on a "frosted" appearance. This is due to its being deformed into a fine wrinkled structure. It was also found that this occurred if the film surface was charged to a high potential while cold (presumably, somewhat higher potentials than those used by Gaynor and Aftergut) and was then softened by heating.

It was observed that the depth of these surface Frost deformations increased as the applied surface charge density was increased. This enabled Gundlach and Claus to devise a method for recording continuous tone images without the need for screening.

They employed the arrangement shown in Fig. 4, using both the selenium xerographic photoconductor on an opaque conducting substrate and organic photoconductors on glass substrates coated with a transparent, electrically conducting layer of stannic oxide deposited chemically by the NESA process (see, for example, ref. 9, p. 493). In both cases a top layer of a transparent thermoplastic was used. This material was a good insulator (10^{12} ohm. m minimum) over the range of temperatures to be used in image recording. Whichever type of photoconductor was being used, two modes

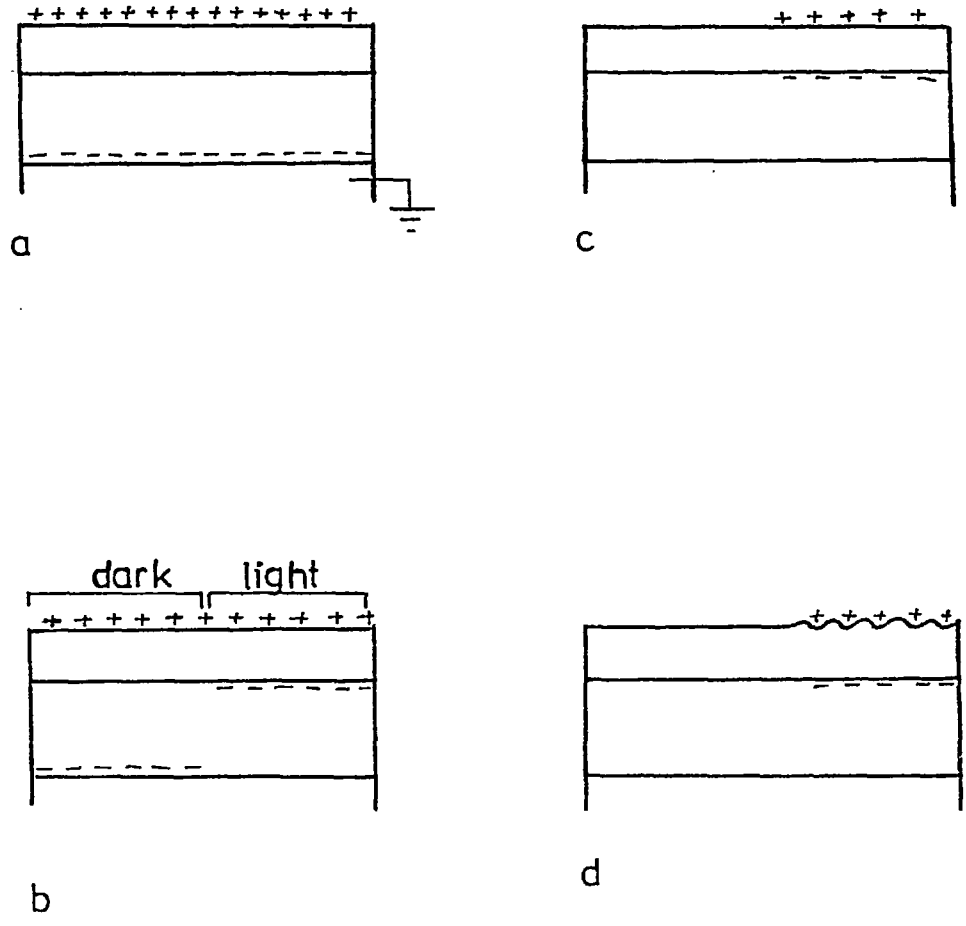

Figure 5. The "Sequential" Processing Mode, according to Gundlach and Claus.

of operation were possible.

The first of these was described by Gundlach and Claus as the "sequential" mode and is depicted in Fig. 5. The conducting substrate (or, in the case of organic photoconductors, the thin conducting film on the surface of the glass substrate) was earthed and to sensitize the device a uniform positive charge was laid on the free surface of the thermoplastic by a corona charging device. This would induce an equal negative charge on the underlying earthed conductor (Fig. 5a).

The corona device was then removed and the films were exposed to the optical image (Fig. 5b). Let us consider a binary image (i.e. one containing black and white areas only with no intermediate grey tones) for simplicity. In the dark regions of the image the photoconductor will be unaffected. However, where the photoconductor is illuminated it will conduct, allowing the charges induced on the conductor layer to drift up to the photoconductor-thermoplastic interface under the forces of electrostatic attraction towards the charges on the free surface of the thermoplastic. The image illumination is then removed and the photoconductor becomes insulative again.

The next stage is to move an A.C. corona discharge across the free surface (Fig. 5c). Gundlach says this device has the effect of neutralizing (or grounding) a surface. Presumably it produces both positive and negative ions in roughly equal numbers and as these are free to drift under electrostatic forces arising from any potential gradient they are in, the tendency is for all nearby

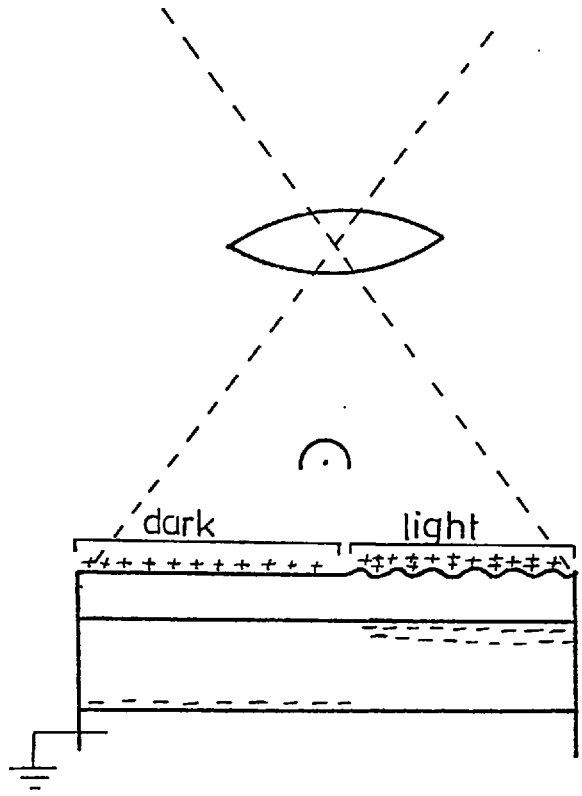

Figure 6. The "Simultaneous" Processing Mode, according to Gundlach and Claus.

insulating surfaces to acquire a uniform potential.

The final step is to soften the thermoplastic by heat or exposure to solvent vapour. If the charging potential, exposure and degree and duration of thermoplastic softening have been chosen suitably the free thermoplastic surface deforms into the Frost structure. Gundlach and Claus note that the depth of the deformations depends on the exposure if the other parameters are properly adjusted so that continuous tone images can be recorded as modulations of the depth of the Frost deformations.

The Frost images have the property of scattering light out of a transmitted light beam (or out of the specularly reflected beam in the case of reflection illumination) so that if the image is viewed by an optical system which accepts only a narrow cone of rays from the transmitted light, the various depths of Frosting will cause various degrees of scattering and, thus, intensity modulations and will form a continuous tone reconstructed image.

The alternative mode of use described by Gundlach and Claus is referred to as the "simultaneous" mode of operation. This is shown in Fig. 6. The conducting substrate is again earthed and the plate is exposed to the optical image whilst the free thermoplastic surface is being charged by a D.C. corona device. The thermoplastic is also softened by heating or by solvent vapour at the same time. The photoconductor becomes conducting where it is illuminated so that in such regions the photoconductor-thermoplastic interface effectively achieves earth potential. In the unilluminated areas the free thermoplastic surface is still

separated from the earthed surface by the thickness of both the thermoplastic and the photoconductor films, whereas in the illuminated areas only the thickness of the thermoplastic layer separates the free surface from the earthed surface. Thus in the illuminated areas, the capacitance to earth is greater than in the unilluminated areas.

However, the corona device will bring the free surface to a uniform potential, so the charge density on the free surface in the illuminated area will be higher than that elsewhere.

As was the case in the sequential mode, Gundlach and Claus reported that it was possible, by adjusting the critical parameters, to obtain tonal gradation in the form of continuous modulation of Frost deformation depth when using a continuous tone original. Reconstruction was by the modified schlieren method used before.

The techniques developed by Gaynor and Aftergut, Gundlach and Claus in image recording are the immediate practical basis of the later work carried out on thermoplastic holography.

CHAPTER 2

DEVELOPMENT OF IDEAS FROM IMAGE RECORDING TO HOLOGRAPHY

2.1 Preliminary Observations of Frost Properties

Gundlach and Claus (8) completed their paper on Frost imaging with a brief description of some of the light scattering properties of Frost. As it was from studies of Frost that thermoplastic holography was later to emerge, it is of interest to review the development of knowledge of the behaviour of Frost.

Gundlach and Claus were concerned especially with the ability of Frost imaging faithfully to record areas of uniform tone in continuous tone originals without the need for a screen. To learn more of this, they recorded a Frost image of a density step wedge and examined the properties of the image. They appear to have used a thermoplastic film of 2.5 microns thickness and a selenium photoconductive layer 20 microns thick. However, they do not state whether the simultaneous or sequential recording mode was used, nor do they give any indication of the optical exposure or the exact development time or temperature used in the recording stage, although thermoplastic viscosities around 10^{4} $N.s.m^{-2}$ and temperature in the range 50° to 100° C are said by them to have been used generally in the work.

To some extent, these omissions are the consequence of their being interested primarily in demonstrating the dynamic range of exposure to which the system will respond and the contrast attainable in the final projected image,

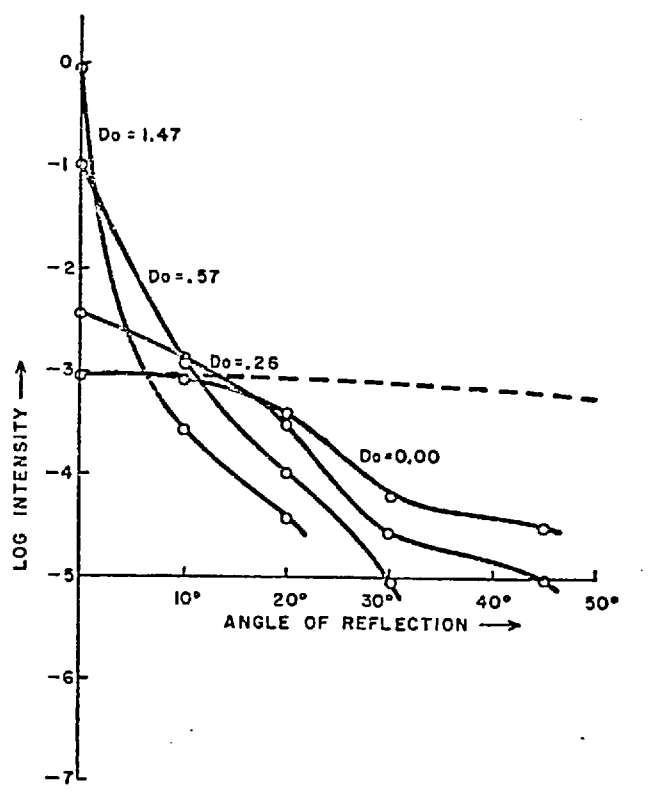

Figure 7a. Backscattered Intensity as a function of angle for Frost recordings of the various densities D_o of a step wedge. (According to Gundlach and Claus)

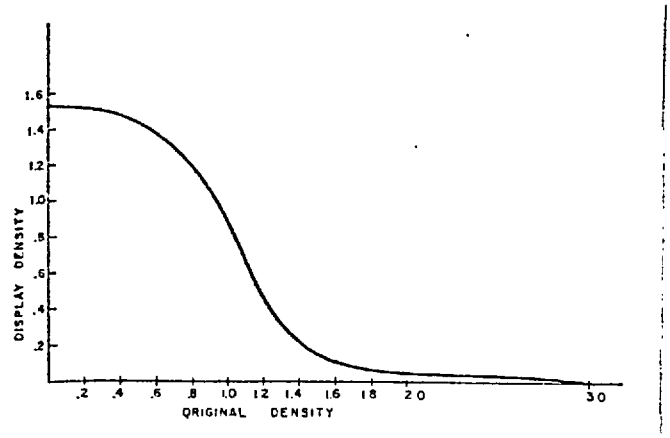

Figure 7b. Display density as a function of original density for a Frost recording system. (According to Gundlach and Claus)

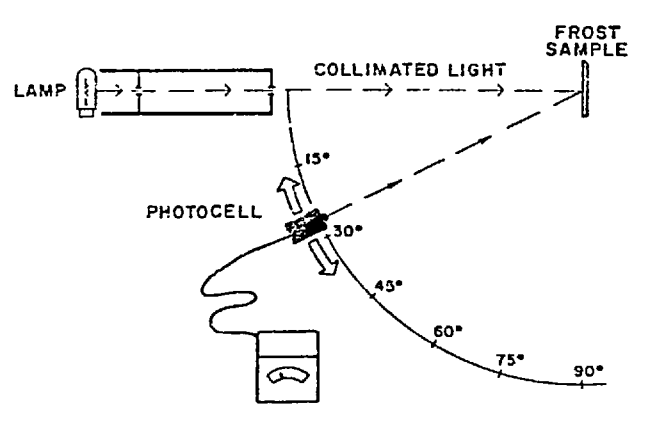

Figure 8. Arrangement used by Gundlach and Claus in Frost scattering measurements.

rather than in forming a theoretical framework relating the various parameters involved in the process. This was reasonable as, at the time, they were announcing a new recording technique and the possibility of the comparison of their results with those of other workers had not yet arisen. Nevertheless, it does limit the support which can be sought in their results for any particular model of thermoplastic behaviour.

Their main results in this area are reproduced in Fig.7. Fig.7a was obtained using the apparatus shown in Fig.8. This consisted of a source of collimated light illuminating the recorded Frost image at normal incidence. The intensity of the light scattered at various angles out of the specularly reflected beam was measured by a photocell which was moved around an arc of a circle centred on the Frosted plate. The scattered intensity was plotted as a function of the scattering angle separately for each area of the plate which had been exposed to a single step of the original density wedge, producing the family of curves of Fig.7a. The data points for the specularly reflected intensity (reflection angle of zero) were obtained by making the collimated beam incident at 5^{o} to the normal and placing the photocell at 5^{o} on the other side of the normal.

We can see from this data that a range of three orders of magnitude in the intensity of the specularly reflected beam was achieved. Gundlach and Claus suggest that an average commercial projector will form its image from light up to about 10^{o} either side of the normal to the plate, and used a projector such as is used in more normal xerography

to obtain the curves of Fig.7b. This projector had an aperture of f/4.5.

The curve is, in effect, a sensitometric curve for the Frost recording system, showing, in the words of its authors, display density as a function of original density. The "original density" is the density of the step wedge used in the exposure. Although they do not define the term "display density", it presumably refers to the ability of the Frost recording to scatter light out of the specular beam by implying an analogy with a photographic image, which absorbs light from a beam and may truly be said to possess density. Thus, although the Frost recordings have the power only to redirect light and cannot appreciably absorb it, the "display density" of a Frost recording may nevertheless be defined as the density that an absorbing structure would possess if it reduced the intensity of a transmitted beam by the same amount that the Frost recording reduces the intensity of a specularly reflected beam.

The display density of a given Frost recording depends on the aperture of the lens through which it is projected, as this determines the proportion of the scattered light which reaches the final image. Also, the contrast in a projected Frost image depends on the aperture of the projecting lens as, from Fig.7a, the intensities in areas of the projected image which correspond to different densities in the original do not increase at equal rates while the acceptance angle of the lens is increased. This situation is an extreme case of that encountered in photographic emulsions, and some of the concepts used there are useful to us.

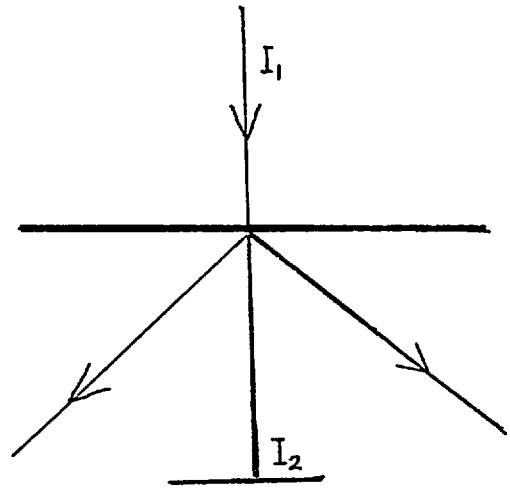

$$T_S = \frac{I_2}{I_1}$$

$$D_S = \log_{10}\left(\frac{1}{T_S}\right)$$

Figure 9a. The definition of specular density D_S in terms of the specular transmission T_S.

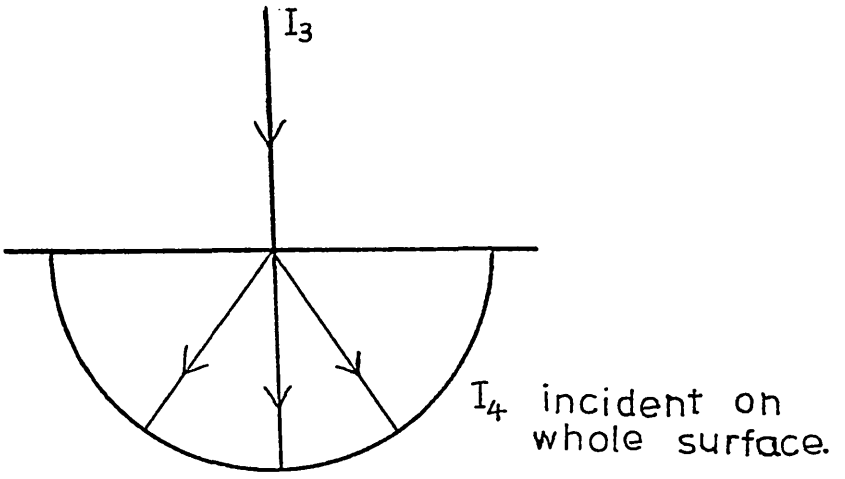

$$T_d = \frac{I_4}{I_3}$$

$$D_d = \log_{10}\left(\frac{1}{T_d}\right)$$

Figure 9b. The definition of diffuse density D_d in terms of the diffuse transmission T_d.

2.2 A Comparison of Frost and Photographic Images

When light is transmitted through a photographic emulsion, some is, in general, absorbed, but some is scattered out of the beam by the silver grains. This is known as the Callier effect. To assist in quantifying this property of emulsions, two different forms of density are defined, known as specular density and diffuse density. (A third form, known as double diffuse density also exists but is of no significance here). Specular density (D_s) (see Fig.9a) is defined as

$$D_s = \log_{10}\left(\frac{1}{T_s}\right)$$

where T_s is the ratio of the intensity of the unscattered transmitted light to the intensity of the incident collimated light.

The diffuse density (D_d) (Fig.9b) is defined as

$$D_d = \log_{10}\left(\frac{1}{T_d}\right)$$

where T_d is the ratio of the intensity of all the transmitted light, scattered and unscattered, to the intensity of the incident collimated light.

The magnitude of the Callier effect is indicated by the extent to which D_s and D_d are unequal, and the Callier coefficient (Q) is defined as

$$Q = \frac{D_s}{D_d}$$ (See ref.10,p.226)

For a normal photographic emulsion, Q is around 1.4, whereas for a relatively grainless structure, such as a thin evaporated metal film on glass, Q is effectively unity. For a Frosted thermoplastic plate, Q will clearly be higher

in general than these figures because of the large proportion of the incident light which is scattered. Values in the range 3 to 9 are quoted (ref.11) for scattering images of a similar kind.

In the case of the printing of a photographic negative, it is found that the contrast of the resulting image is slightly higher if only the unscattered transmitted beam is used (as in a condenser enlarger) than if all the transmitted light is used (as in contact printing). This is because the denser parts of the negative scatter more light than do the less dense areas. If the scattered light is not allowed to contribute to the image, the contrast will be increased. To a less extent, the aperture of the enlarger lens determines how much of the scattered light reaches the image and thus also slightly affects the image contrast. This is equivalent to the much stronger dependence of projected image contrast upon projection lens aperture noted by Gundlach and Claus for Frost images having much higher values of the Callier coefficient.

In the photographic case, the Callier coefficient is used as a measure of the extent to which this effect takes place. It is not, however, a theoretically perfect indicator as one cannot necessarily assume that the intensity of the light scattered at any particular angle is linearly related to the diffuse transmission (T_d) as density varies; nor that the form of the dependence of the intensity of the scattered light upon angle of scattering is independent of the diffuse density. This means that the various ranges of density present in the recorded image may

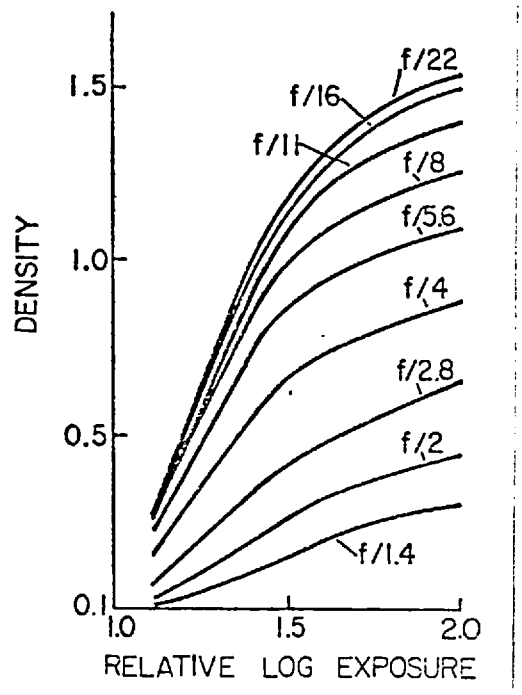

Figure 10. Projection Density as a function of Relative Log Exposure for a Frost image projected through a lens set at various apertures. (According to Urbach)

have their contrast influenced to different degrees by any given lens aperture. In the case of a photographic negative where the Callier effect is small this secondary phenomenon is of little significance, but in the projection of Frost images where the Callier coefficient is larger, higher order effects may limit the usefulness of the coefficient as a means of describing the influence of projection lens aperture on image contrast. Nevertheless, the behaviour of the coefficient does serve to illustrate a distinction between photographic and Frost imagery.

2.3 The Image-forming Properties of Thermoplastic Frost

In 1964, Urbach (11) considered in some detail the properties of Frost as an image forming structure. He, too, noted the strong dependence of image contrast upon projection lens aperture which accompanies high values of the Callier coefficient such as are found in Frost imaging, and he shows a family of characteristic curves (Fig.10) of Projection (or Display) Density as a function of Relative Exposure for various apertures of the projection lens. However, he also points out that although decreasing the projection aperture size increases the contrast in low spatial frequencies of the image (macroscopic contrast) it decreases the contrast at high spatial frequencies (microscopic contrast) because of diffraction by the aperture stop, so that a compromise must be reached in practice.

In order to investigate the macroscopic and microscopic contrast properties of the Frost process Urbach imaged

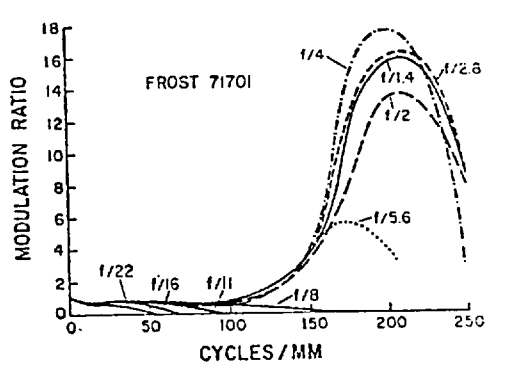

Figure 11. Image Modulation Ratio as a function of object spatial frequency for Frost recordings at various projection apertures. (According to Urbach)

sinusoidal and step function gratings as well as line images on to the recording plate, and observed the recorded image. His paper (ref.11) contains only a report of the findings with sine wave gratings, but these results provide the first reference to a particularly interesting property of the Frost recording plates.

Frost recording plates were exposed to a series of sinusoidal intensity patterns of various spatial frequencies. The modulation of the projected image was measured with a microphotometer and was divided by the image modulation that would have been expected if the deformation properties of the thermoplastic were independent of spatial frequency. The values of the latter modulation were calculated from the data shown in Fig.10. This normalized modulation was then plotted as a function of spatial frequency, for various projection lens apertures as shown in Fig.11.

If the deformation properties of the thermoplastic had been independent of spatial frequency the curves of Fig.11 would all have been straight lines of modulation ratio unity, apart from the progressive high frequency cut-off due to the modulation transfer function of the projection lens. However, at the larger lens apertures there is a very pronounced peak in the region of the higher spatial frequencies. As Urbach says, it is clear that in the high frequency range the behaviour of the thermoplastic layer requires a different model for describing its action from that which is needed in the low frequencies (below, say, 100 mm^{-1} in this case) where the material behaves virtually as was hitherto expected.

Urbach also considered the power spectrum of the Frost.

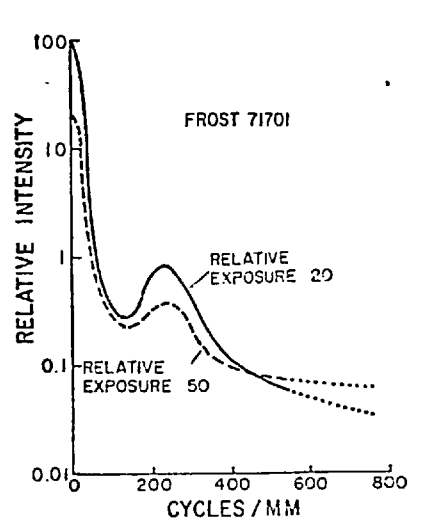

Figure 12. Frost power spectrum for a particular specimen, given two different exposures. (According to Urbach)

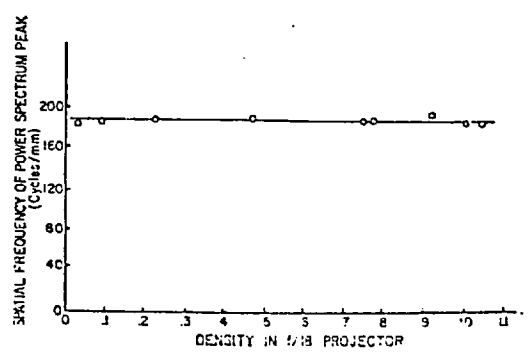

Figure 13. Spatial frequency of secondary peak in Frost power spectrum as a function of projection density (f/18 projector) and, by implication, as a function of exposure.

He obtained this data in much the same way as Gundlach and Claus (8), by measuring the angular distribution of the light scattered by the Frost from a collimated laser beam. An example of the data he obtained is shown in Fig.12, the Frost sample used being the same as that used in obtaining the data for Fig.11. In all Frost power spectrum measurements he found a secondary peak in the curve such as is seen in Fig.12 and he notes that although the shapes of these curves were to some extent dependent upon the exposure given to the recording plate, nevertheless in all cases a secondary peak was found. Also, for a given combination of recording plate and processing parameters, this peak occurred at a remarkably constant value of spatial frequency, whatever exposure was given. (See, for example, Fig.13 which shows the results that Urbach used to confirm this point, although a different recording plate or set of processing parameters was used here from those used for Figs.11 and 12).

Clearly, the presence of a secondary peak in the power spectrum indicates the existence of a preferred spatial frequency in the surface deformations of the thermoplastic, and comparison of Figs.11 and 12 suggests a correspondence between the preferred frequency of the Frost and the frequency to which the surface deformed most strongly when given sinusoidal intensity grating exposures. Urbach confirms that, although alteration of the processing parameters shifted the peak in Fig.11 and the secondary one in Fig.12, these two peaks always occurred at almost exactly the same frequency as each other if identical processing was used.

From all these results Urbach concluded that from the

point of view of image recording, the thermoplastic surface responds to sinusoidal image exposures in one of two separate ways, depending on the spatial frequency of the grating used. At low frequencies the material responds in the manner reported by Gundlach and Claus, the image information being recorded as an amplitude modulation of the Frost deformation depth. However, as the spatial frequency of a grating image exposure approaches the preferred frequency of the Frost the randomly oriented Frost deformations tend to disappear, being replaced by a cleanly defined, relatively Frost-free sinusoidal grating deformation whose orientation and spatial frequency are those of the image grating. The replacement is largely complete when the image exposure has the same spatial frequency as the preferred Frost frequency.

The failure of small projection aperture sizes to show the high image modulation available from these Frost-free gratings (Fig.11) is due purely to the inability of the projection lens to resolve them at the smaller apertures.

Urbach found that Frost-free gratings of this type behaved strongly as diffraction gratings, showing four or five diffraction orders. Gundlach and Claus did not obtain a secondary peak in their measurements of power spectra. In the light of later work in this area, it seems likely that this was due to their using thicker thermoplastic layers (2.5 microns) than did Urbach, so that the secondary peak would occur at a lower spatial frequency. It seems quite likely that in their case the secondary peak merged with the larger one centred on zero frequency which represents the specular beam.

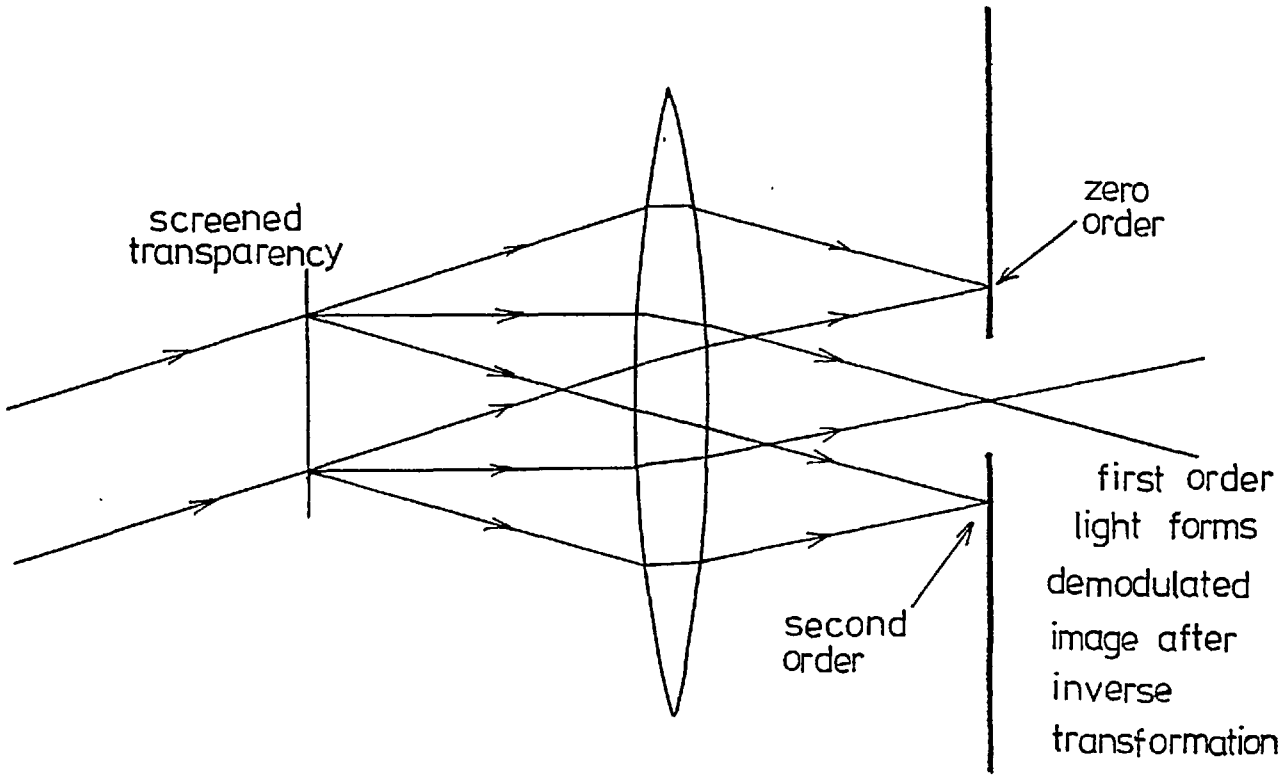

Figure 14. Schematic representation of spatial filtering to remove screen frequencies from an image (demodulation). (According to Urbach)

2.4 The Demodulation of Screened and Frost Images

In 1966, Urbach (12) further extended understanding of the thermoplastic recording process. He observed that in using it to record continuous tone images either periodic screening in the conventional way, or a quasi-random screen pattern could be employed.

The latter mode is, of course, thermoplastic Frost xerography. This situation can, as he says, alternatively be described as the use of a periodic or quasi-random carrier of information whose amplitude is modulated by the signal frequency. In this, Urbach drew an analogy between thermoplastic recording and the one dimensional communication theory of, for example, temporal electrical signals.

Also, where a periodic carrier frequency is used (screening) whose frequency lies above that of the highest image frequencies, it is possible in principle to demodulate the recorded image by separating the image information from the carrier frequency when projecting the image. With optical images this can be done by spatial filtering (see, for example, reference 13 and Fig. 14 which shows the schematic representation of spatial filtering by Urbach). As with other fields where amplitude modulated carrier frequencies are used, separation of image from screen is only possible if their power spectra do not overlap in frequency. In optical separation by spatial filtering this requirement manifests itself as the need for the signal information surrounding each order of the screening power spectrum not to overlap that surrounding

other orders so that the screen information alone can be obstructed by the spatial filter. With a Frost image, demodulation could be attempted by obstructing the Frost diffraction ring and reconstructing the image from the zero order and its immediate surroundings.

2.5 Screening, Demodulation and Holography

Towards the end of his paper (12) on the use of screening in thermoplastic recording, Urbach mentions that he has carried out some attempts at recording holograms on thermoplastic recording plates. (The earliest publication concerning thermoplastic holography seems to be a short letter by Urbach and Meier (14) dated a few months earlier in the same year, 1966).

It is clear from Urbach's remarks that he was regarding the sideband hologram as an image signal recorded using the holographic interference fringes as the information carrier - a periodic grating-type carrier, therefore. In this he was following the ideas of Leith and Upatnieks (15) in their early discussion of sideband holography, or the carrier frequency method of holography as they call it.

However, as we have seen, it was Urbach's investigations of the image recording properties of thermoplastic recording which led him to expose the material to periodic sinusoidal image structures, thereby discovering their high degree of modulation achievable with grating images. His consideration of this property as a useful bonus in the recording of periodically screened images then brought him to the point where sideband holography was a natural advance.

The nature of this advance is that whereas "multiplying" an image wavefront by an absorbing periodic carrier produces a screened image whose amplitude can be recorded efficiently on a thermoplastic plate, if the image wavefront is instead added coherently to an off-axis reference wavefront a periodic carrier will again result, but in this case the carrier will be frequency-modulated as well as amplitude-modulated by the image wavefront. In general it is the phase information from the image wavefront that will be mainly encoded in the frequency modulations and its amplitude that will be encoded in the amplitude modulation of such a carrier grating. The holographic method is thus seen as a more sophisticated form of image screening whereby additional image information (concerning phase) can be recorded, as well as providing the usual advantage of screening whereby image areas of uniform tone (low spatial frequency, amplitude information) can be recorded on a material such as the thermoplastic plate which is intrinsically responsive only to high spatial frequencies.

A further note by Urbach (12) opens even wider the door leading to thermoplastic holography. This concerns his observation that if a thermoplastic plate is used to record a periodic image structure whose spatial frequency is that of the Frost deformation which that plate normally exhibits, then the amplitude of the Frost will be much reduced. Thus the likelihood arises that holograms relatively free of Frost noise may be produced. Urbach (12) points out that in a silver halide photographic emulsion the halide grains represent a broadband noise carrier of the

image information, the latter being a modulation of the noise. By contrast, in thermoplastic recording the surface deformations which form the Frost tend to be replaced by the optical exposure information deformation if a periodic intensity structure of the correct frequency is used. As Urbach and Meier (14) suggest, thermoplastic holography should therefore be capable of producing images which are relatively free of scattered background light, noise not being an intrinsic part of the recorded image, whereas photographic silver halide emulsions form the image record from an essentially noisy structure and may be expected to scatter considerably more.

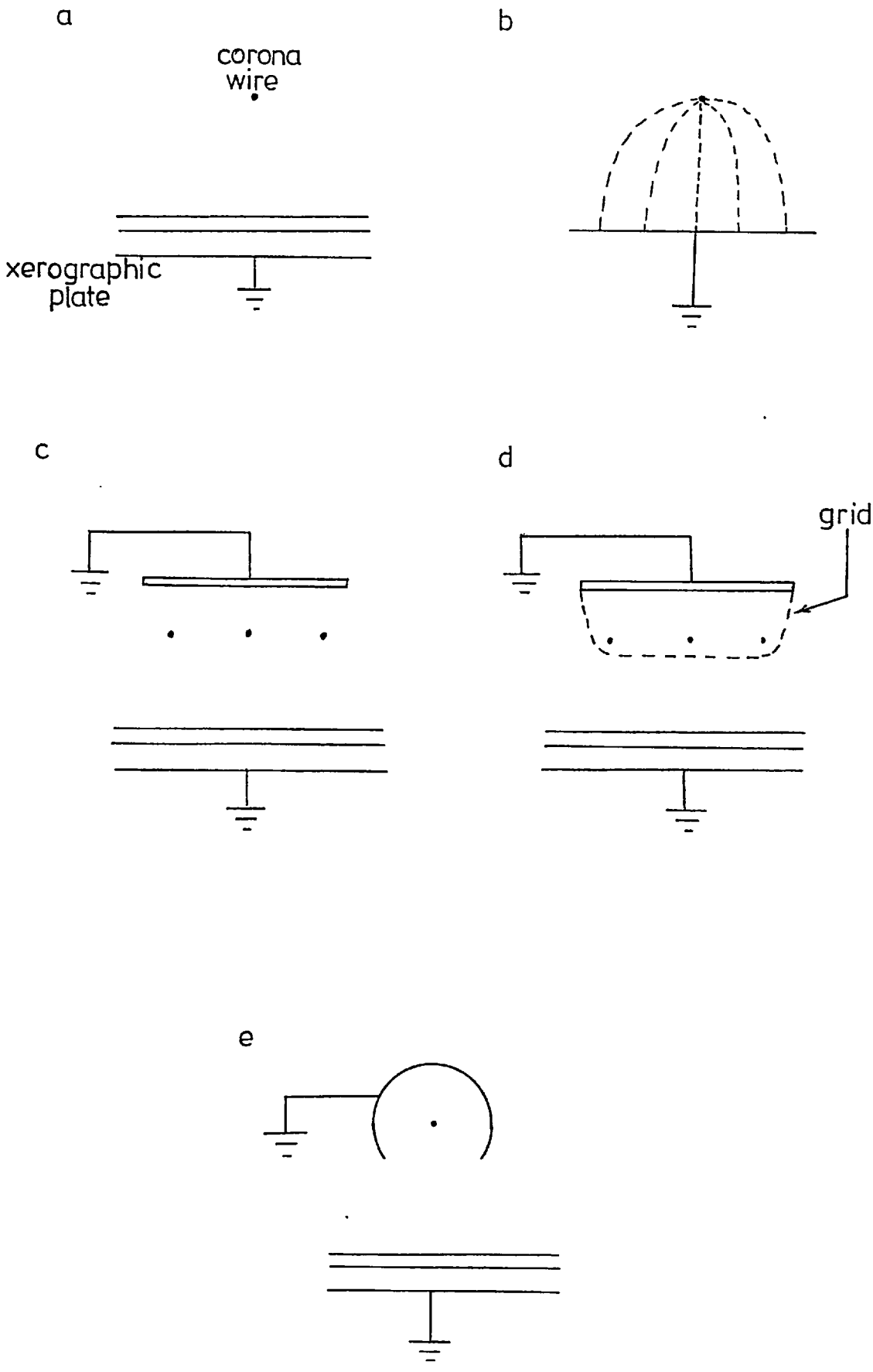

Figure 15. Various designs which have been used for corona charging devices.

CHAPTER 3

REVIEW OF TOPICS RELEVANT TO THERMOPLASTIC HOLOGRAPHY

Because of the close similarity between thermoplastic holography and certain forms of xerography much of the work which has been carried out in the latter field is of direct relevance for us. Let us, therefore, consider a few topics with the assistance of literature from both fields.

3.1 Designs for the Corona Charging Device

Corona charging devices exist in four basic forms, the simplest of which is not generally used in commercial xerographic equipment.

This simple form is mentioned by Schaffert (17), for example, and is shown in Fig.15a. It consists merely of a fine wire which is usually supported for convenience by a frame made from an insulating material which takes no part in the action of the device. To charge an insulating surface, as is required in thermoplastic xerography or holography, the conducting layer beneath the insulating film is generally earthed and the wire of the corona device is connected to a positive or negative D.C. potential of around 7 KV. This causes a high electric field (electric potential gradient) in the immediate vicinity of the wire. This is evident from the distribution of electric field lines which pertains to this electrode geometry (see Fig.15b). The field lines are constrained by the geometry to run close together in the region near the wire

and, as the number of lines of force passing through a unit area which lies normal to the lines of force is equal to the value of the electric field at that point (ref.18 p.7), it is clear that the region of highest electric field must be adjacent to the wire. Note, also, that for a given potential on the wire, higher electric field strengths can be produced near the wire electrode by using wires of smaller diameters. The fields obtainable by this method are sufficient to ionize the gas molecules close to the wire, resulting in a supply of free charge carriers in the vicinity and a rather weak glow discharge around the wire.

Where it is required that a large area be given a uniform charge, it is common, in xerography, to use a corona device containing several wire electrodes running parallel.

An improvement to the simple device is the addition of a plane grounded electrode behind the wires (Fig.15c). This arrangement is known in xerography as the "corotron" device (ref.1 p.25), and is found (ref.17) to give improved performance in the form of a greater supply of free charge carriers for a given applied potential. The improvement is purely a result of the different arrangement of field lines and consequent redistribution of electric field strength arising from the new electrode geometry.

A refinement of the corotron is produced by adding a wire control grid between the wire electrodes and the plate to be charged (Fig.15d). The purpose of the grid is to control the potential which the plate surface ultimately achieves. Without this control the potential on the plate surface may rise to very high values (of the order of the

wire E.H.T. voltage) if the corona device is too close to the plate and electrical breakdown of the films on the plate may occur. Also, if the area to be charged is large, the control grid promotes more uniform charging than is the case otherwise and in any event allows the plate potential prior to exposure of the plate to be adjusted easily. These two points are particularly useful in continuous tone Frost xerography and may improve consistency in thermoplastic holography.

The potential applied to the control grid is intermediate between that of the wire potential and the earth potential of the plate conductor layer. The grid potential is set to approximately the potential required on the plate surface and charging is allowed to proceed long enough for a steady voltage to be achieved on the plate. The disadvantage of this design is the relatively long charging time required which limits its use in commercial xerographic machines, although this would not be such a drawback in development work. It is in any case the latter situation that is likely to require adjustable control of the charging potential. This device is known as the "scorotron" (ref.1 p.25).

The most efficient of the four basic electrode designs for this type of device is the "shielded corotron" (Fig.15e) in which the earthed electrode is of cylindrical form with a gap at one side.

3.2 Charge Transfer in Coronas

The subject of corona discharges is an extensive field

and the basic theory is to be found in the standard texts (such as reference 19). Shahin (20) has considered their behaviour with specific reference to xerography.

In both positive and negative coronas the discharge is initiated by breakdown of the air near the wire electrode as a result of the very high electric field existing in that region. The polarity refers to the potential on the wire electrode but is also that of the free charge carriers generated by operating the device. If the centre wire potential is positive, the electrons freed by the breakdown accelerate towards the wire and acquire sufficient energy to ionize further molecules, producing an avalanche effect. Meanwhile the positive ions drift towards the cylindrical earthed electrode and it is SOME OF THESE CARRIERS which are released from the device. The electrons are retained by the wire. The discharge is probably maintained by the photoionization of air molecules by ultraviolet radiation from the glow discharge itself. The electric field is still necessary to accelerate the electrons. The positive ion carriers released in the positive corona have been shown by Shahin (21) to be hydrated protons of the general formula

$$(H_2O)_n H^+$$

where n is 1,2,3 etc. depending on the relative humidity. He found that n mainly took the value 6 for a relative humidity of 20% and a temperature of 27°C.

In the negative corona the initial breakdown of the air is followed by the acceleration of electrons away from the wire and ions towards it. Further ionizations of gas molecules occur as a result of collisions with the electrons.

In summarising the knowledge of the negative corona, Shahin (20) tells us that the main source of electrons for maintaining the discharge is the wire electrode, as a result of positive ion impacts and consequent secondary emission together with photoelectric emission due to radiation arriving at the wire surface from the glow discharge. He also found (25) that the main charge carriers released from the negative corona discharge device and which are used in the charging of an external surface are mainly of the formula

$$CO_3^-$$

when the discharge is operated at atmospheric pressure, although at 50% relative humidity about 10% of the ions are hydrated according to the formula

$$CO_3^-(H_2O)_{1,2}$$

As Shahin points out, the presence of water vapour has a greater effect on the nature of the released charge carriers in the positive corona than in the negative case.

3.3 Theory of the Corona Charging of an Insulating Surface

There seems to be broad agreement about the general behaviour of electric charge, potential and fields within the three layer (conductor-photoconductor-thermoplastic) sandwich of the thermoplastic plates during the charge-expose-recharge-develop cycle of Gundlach and Claus described earlier (Section 1.5). For example, Sullivan and Kneiser (22) and Schaffert (17) both consider the three layer structure. Sullivan is specifically concerned with thermoplastic xerography, whereas Schaffert describes a

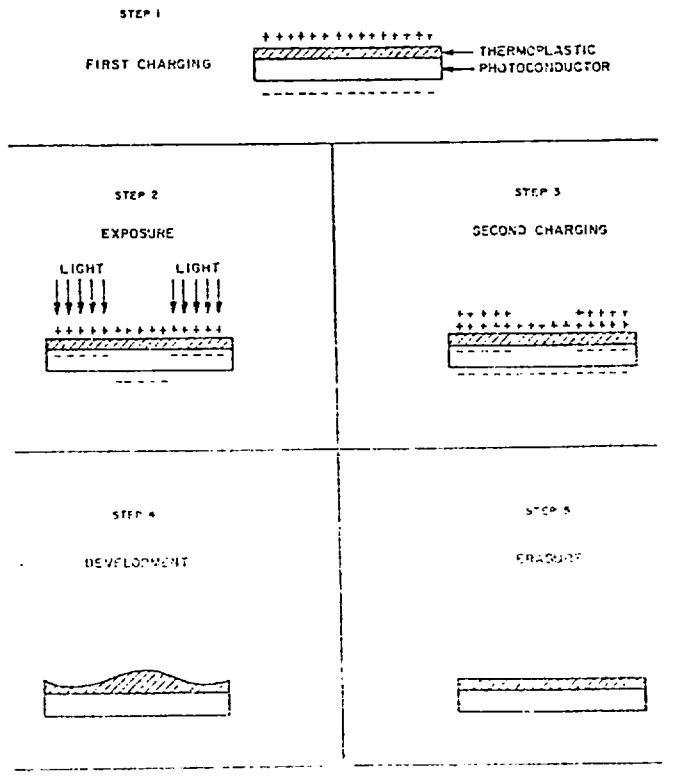

Figure 16. The steps of the sequential mode for operating a thermoplastic plate.
(According to Gundlach and Claus).

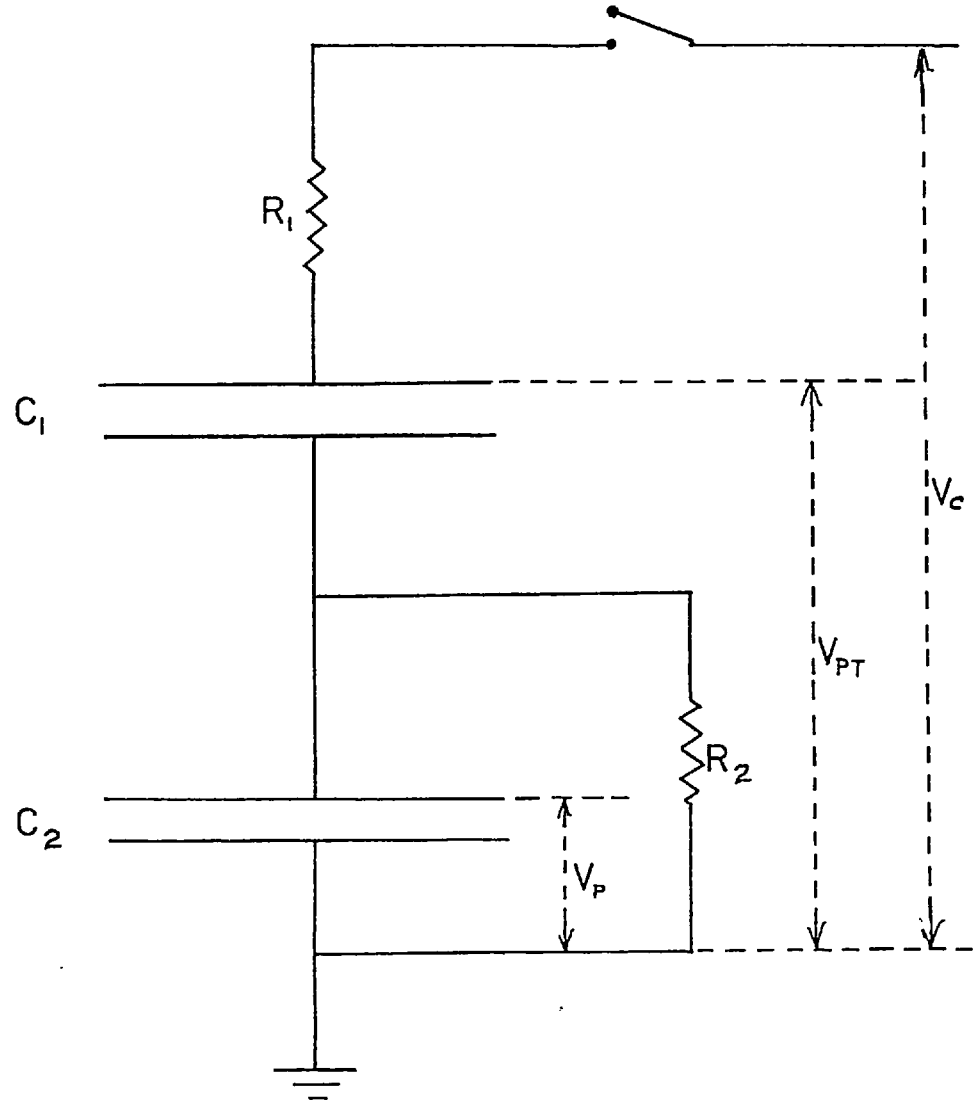

Figure 17. Equivalent circuit for three layer thermoplastic plate.

three layer (conductor-photoconductor-insulator) sandwich in a general xerographic context without relating it to particular materials.

Fig. 16 shows the steps in the sequential mode of operation first mentioned by Gundlach and Claus, and Fig. 17 is the equivalent circuit which is generally assumed electrically to represent the three layer thermoplastic plate. The capacitances C_1 and C_2 (Fig. 17) are those from the free thermoplastic surface to the photoconductor-thermoplastic interface and from this interface to the earthed conductor layer respectively. Resistance R_1 refers to the air gap separating the corona device from the thermoplastic surface and R_2 is the resistance presented by the photoconductor to the passage of charge between the conductor layer and the photoconductor-thermoplastic interface. The value of R_2 is therefore dependent upon the intensity of the light to which the plate is exposed. The circuit elements C_1, C_2 and R_2 should, of course, strictly be considered as representing a unit area of the plate.

During the first step of the processing cycle (the sensitising stage, Fig. 16a) a uniform charge is placed on the free surface of the thermoplastic using a corona voltage V_C. This gives rise to a voltage (V_{PT}) across the thermoplastic and photoconductor layers together.

The second step (Fig. 16b), the exposure, causes some areas of the plate to receive light. Where the plate receives no light the value of R_2 remains very large, but where light falls its value decreases allowing some reduction of the voltage (V_P) across C_2. The amount of the

decrease depends on the duration and intensity of the exposure. This will have the effect of reducing the potential of the free thermoplastic surface with respect to earth although the charge density on this surface is unchanged as no current has flowed to or from this insulated surface during the exposure. Thus at this stage we have a potential distribution across the free surface which corresponds in magnitude and spatial form with the intensity of the image exposure, but the surface charge density here is uniform still.

When, in step 3 (Fig. 16c), the free surface is recharged by the corona device, its potential is restored to a uniform value which is determined by the corona voltage V_c. (Gundlach and Claus used an A.C. corona to achieve a neutral potential, but other authors commonly use the same corona potential here as they use in step 1). During this recharging, the capacitance to earth of the free thermoplastic surface is uniform and is given by

$$\left(\frac{1}{C_1} + \frac{1}{C_2}\right)^{-1}$$

if the step is carried out in darkness. If uniform illumination (room lighting, as opposed to image exposure) is present during this step the value of this capacitance will be different because of the leakage resistance R_2, but the capacitance will nevertheless be uniform across the plate. A uniform potential across the free surface of the plate will result from the recharging as during this step free charge carriers are released by the corona discharge and the air adjacent to the free thermoplastic surface becomes, effectively, an electrical conductor, allowing the dissipation of potential differences across the surface.

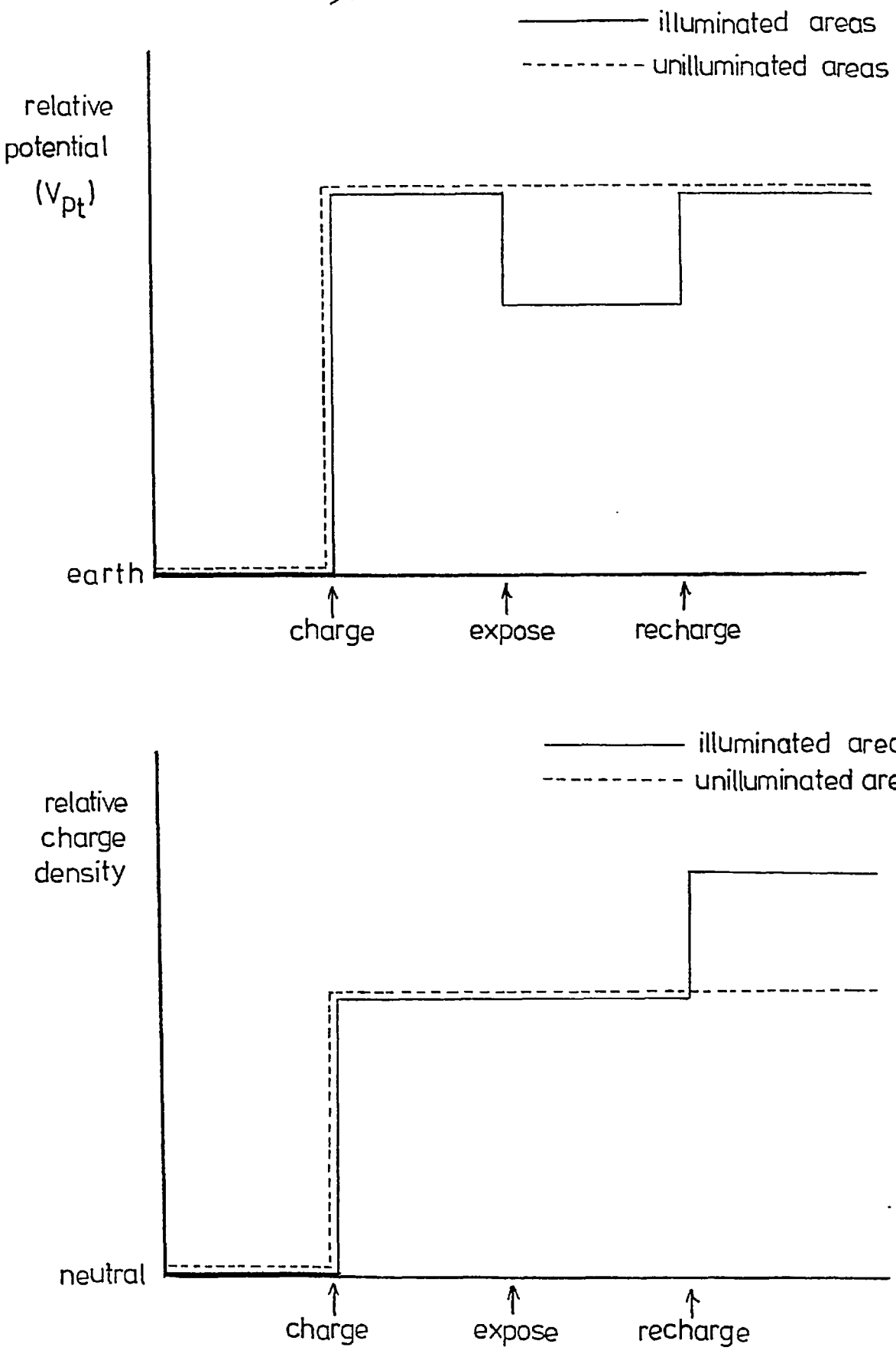

Figure 18. The behaviour of surface potential and charge density of the free thermoplastic surface during the sequential processing cycle.

Because the potential across the free surface was modulated by the image exposure in step 2, it is necessary for various amounts of charge to be added to the various parts of the thermoplastic surface during recharging (step 3) if the potential of this surface is to become uniform.

The amounts of charge added to the free surface will be in proportion to the surface potential drop caused by exposure in step 2 so that the image intensity modulation has now been translated into a modulation of charge density on the free thermoplastic surface.

Fig. 18 summarises the behaviour of the potential and charge density of the free thermoplastic surface during the cycle, the extent of the changes in these parameters during exposure being dependent on the intensity and duration of exposure.

The theory of the simultaneous mode of operation described by Gundlach and Claus and since used for thermoplastic holography does not appear to have been discussed separately by any author except Schaffert (17) and is generally assumed to depend upon the same physical principles as the sequential mode described above. Precise mathematical models of the two modes of operation would be rather different as in the sequential case the modification of electric fields and potentials within the thermoplastic plate by the image during exposure depends upon the truncation of a capacitor discharge transient; if the exposure duration were too long nearly all contrast would be lost from the resulting recorded charge density image as the potential variations across the plate following

exposure would be very slight. In the simultaneous mode on the other hand the potentials and charge densities increase throughout the combined charge-exposure-development operation, up to values determined either by the operator in terminating the process or by charge leakage or electrical breakdown in the organic layers; excessive exposure should produce no degradation of the recording as charging is also maintained.

This difference between the necessary mathematical formulations is not, however, of immediate practical significance since the attempts such as those of Sullivan and Kneiser (22) and Schaffert (17) to produce mathematical models have not yet proved accessible to experimental verification.

It seems likely that the above electrical models, although originally formulated in connection with Frost image recording, are equally applicable to the recording of holographic fringes on these plates.

3.4 A Surface Model for Frost Deformation

The earliest investigations of the immediate cause of Frost appears to be that of Cressman (23). For his experimental results, he evaporated a film of copper on to a glass slide and overcoated this with a layer of a thermoplastic. He then placed an electric charge on the free thermoplastic surface using a corona device but varied the corona voltage as the device travelled across the surface. This produced a surface potential which was uniform with respect to the shorter dimension of the plate

but which varied nearly linearly with its longer dimension. This might be described as a potential "wedge". Having established and measured this potential distribution he softened the thermoplastic by heating to produce the Frost.

He varied the thickness of the thermoplastic but found in all cases that the Frosted area was bounded by a sharp line and was confined by this line to the end of the plate which had corresponded to the higher potentials. He concluded that there existed a well defined threshold charge density below which Frost would not occur with a given thermoplastic material.

Cressman suggested that the presence of a surface charge had the effect of tending to make all points in the surface mutually repulsive, in opposition to the normal force of surface tension. The existence of a threshold potential (or charge density) for Frost supports this view in that this potential would correspond to the charge density at which the electrostatic repulsion and surface tension forces were equal. At higher charge densities the surface would attempt to increase its surface area by deforming (Frosting), thereby reducing the charge density until the repulsion caused by the charge was again equal to the surface tension. This simple view neglects, of course, viscosity, friction and other perturbations.

The quantitative results roughly supported this hypothesis by showing that the forces involved were around the necessary magnitude. The dependence of threshold potential (V_T) upon thermoplastic thickness (d) was shown closely to follow the form

$$V_T = a + b \cdot d^{\frac{1}{2}}$$

where a and b are constants. The above theory assumes that the threshold potential is that which causes the electrostatic surface energy per unit area to equal the surface energy density due to surface tension. This leads Cressman to the conclusion that the relationship between threshold potential and film thickness should be

$$V_T = \left(\frac{2 \gamma_0 d}{\varepsilon} \right)^{\frac{1}{2}}$$

where γ_0 is the normal surface tension of the thermoplastic material and ε is its dielectric constant.

Thus the simple theory predicts the constant a to be zero, whereas its experimental value was around 70 volts. Also, it suggests a value of about 60 volts.(microns)$^{-\frac{1}{2}}$ for the constant b using the appropriate physical constants, although its experimental value was about 46 volts.(microns)$^{-\frac{1}{2}}$. At least the functional dependence of threshold voltage upon thermoplastic thickness is of the predicted form.

3.5 The Surface Model, in an Attempt to Account for a Predominant Spatial Frequency

Cressman observed that in cases where the thermoplastic thickness lay in the range 40 to 120 microns the ratio of the predominant deformation wavelength of the Frost to the thermoplastic thickness was in the range of one to two.

To try and account for this Cressman expressed the total energy of the thermoplastic surface in the form of an integral involving the electrostatic energy and the surface energy due to surface tension. He then minimised the value of this integral subject to the condition that

the total volume of the thermoplastic was constant. Again the effects of viscosity and friction were neglected.

This approach resulted in the prediction that the ratio of predominant deformation wavelength (λ) to thermoplastic thickness (d) would be 4.4 for deformations occurring at the Frost threshold potential. The experimentally observed figure of 1 to 2 suggests that from this point of view the simple theory is not too bad an approximation for such a complex process as Frost formation.

However, Cressman points out that the behaviour of deformation wavelength with the applied charge gives rise to a greater difficulty as his theory predicts that the wavelength will decrease with increasing voltage, whereas the experimental case is the opposite. This experimental result is confirmed by Ost and Moraw (26). He points out that this may be due to the contravention in the practical case of the assumption made in the theory that the surface potential remains constant during deformation. Also, increasing the initial surface potential (PRESUMABLY) takes the practical case further away from the Frost threshold voltage which is contrary to another of the theoretical assumptions.

3.6 A Hydrodynamic Theory of Frost Formation

Budd (24) has produced a considerably more complex theory for thermoplastic Frost deformation in an attempt to obtain a more realistic model, although this is not accompanied by experimental work in verification of the results.

He approaches the subject by assuming that the fluid

thermoplastic is incompressible and that the layer of the material which is in contact with the substrate is stationary. Then, using a form of the Navier-Stokes equation to describe the viscosity, he derives an expression which describes the "growth rate" (ω) of the Frost deformations during their development, as a function of the deformation wavelength (λ) and the effective surface tension (T^*), the last of which in turn involves the normal surface tension of the material and the changes which occur in the electrostatic and mechanical surface energy as the surface deforms. The expressions he obtained are

$$\omega = -\frac{T^* K}{2\mu} \cdot \frac{\left[(\sinh 2Kh)/2 - Kh\right]}{(\cosh^2 Kh + K^2h^2)}$$

and

$$T^* = T_M - \frac{\sigma_o^2}{\varepsilon_1 K}\left[\frac{\cosh Kh}{\sinh Kh + \left(\frac{\varepsilon_1}{\varepsilon_2}\right)\cosh Kh}\right]$$

where $K = \frac{2\pi}{\lambda}$

h is the mean thermoplastic thickness

μ is the coefficient of viscosity

T_M is the surface tension coefficient for the uncharged surface

σ_o is the initial surface charge density

ε_1 is the dielectric constant of the thermoplastic

ε_2 is the dielectric constant of the air.

Fortunately, Budd shows that these can be simplified by the assumption that, while the deformation is proceeding, the thermoplastic surface is an equipotential (i.e. a good

conductor) or carries a uniform charge density (i.e. is an insulator).

For both of these cases he finds that the Frost growth rate (ω) is predicted to increase rapidly with an increase in the initial charging potential, and that the predominant wavelength of the deformations is predicted to decrease slowly with increasing voltage. The latter is also a suggestion made by the theory of Cressman (23) but Cressman and Ost and Moraw (26) tell us it does not agree with experiment.

Budd also predicts that if the surface is assumed to be a conductor, then for low initial voltages the fastest growing wavelength in the deformations during development will be around twice the mean thickness of the thermoplastic, and he suggests that this wavelength will be the predominant one in the developed Frost. The consequence of assuming the surface to be an insulator is a longer predominant wavelength so Budd felt that the experimental evidence such as that of Cressman (23) supported the model using a conducting surface.

However, it should be remembered that Cressman's thermoplastic films were from 40 to 120 microns thick and Budd considered only surface deformation depths which are small compared to the film thickness. Whilst these two conditions are quite consistent with each other and Budd's conclusions may well be valid for the relatively thick films used by Cressman, nevertheless when using the much thinner films (0.2 to 1 micron thickness) which have been found suitable in thermoplastic holography it is highly probable that the deformation depth can no longer be

considered small by comparison with the film thickness. This suggests that an even more thorough analysis of at least the hydrodynamic aspect of thermoplastic Frost would be necessary before the influence of Frost upon thermoplastic holography is properly understood.

3.7 Review of Thermoplastic Deformation in Relief Image and Hologram Recording

As explained earlier (Section 2.5) thermoplastic image recording by Frostless techniques such as described by Gaynor and Aftergut (7) and Urbach (12) is closely similar to thermoplastic holographic recording, especially if screening is used in the case of image recording. We shall take these two recording processes together for the purpose of considering the mechanism by which thermoplastic deformation takes place in Frostless recording.

It seems to be generally agreed by authors in the field (refs. 27, 28 & 29 for example) that the electrostatic forces which act on the thermoplastic surface to cause deformation during the development stage of Frostless recording are directed perpendicularly to the surface and arise from attraction between the charges on the free surface and the induced charges on the underlying conductor. This is the same as the mechanism described by Glenn (3) to account for the action of his thermoplastic electron beam recorder, and is quite distinct in the literature from the explanations of Frost image recording which invariably consider only the forces of mutual repulsion between charges on the free thermoplastic surface.

In the case of thermoplastic relief image recording and holography the existence of force variations acting on the free thermoplastic surface is generally accounted for (e.g. refs. 7, 27 & 29) by the charge density variations which exist on the free surface after the recharging step (in the sequential mode of operation). It is argued that where the surface charge density is high the electric field density (directed perpendicularly to the surface) between the free surface and the conductor layer is higher than elsewhere, so that a greater force of attraction exists here between these two surfaces.

Interestingly, Bergen (29) points out that if the room lights (or, in the case of holography, the reference beam) are turned on after the recharging step then the photoconductor becomes uniformly conducting all over the plate. Once the recharging step is complete the image information is stored in the form of charge density modulations on the free thermoplastic surface and these are not removed by the illumination. However, as a result of the "fogging" exposure the photoconductor-thermoplastic interface is now uniformly at ground potential so that the electric field due to the charge on the free surface now crosses the thermoplastic layer alone whereas previously it crossed both the thermoplastic and photoconductor layers. Thus the forces acting on the free surface will be greater than before and so will the modulations of those forces which represent the image information. The contrast (in relief imaging) or diffraction efficiency (in holography) after heat development should therefore be increased.

3.8 Discussion of Deformation Mechanisms

Cressman's observation (23) that a threshold value of surface charge density must be exceeded for Frosting to start suggests that mutual surface charge repulsion is the mechanism mainly responsible for Frost initiation, as the existence of a threshold is consistent with the need for surface tension to be overcome before a net mutual repulsion exists within the surface. Cressman and Budd (24) agree that the quantitative evidence supports this view.

However, it is quite possible that once the threshold has been exceeded and Frost deformations have started to develop, the deformations may be accelerated by the greater forces of attraction that exist between the conductor layer and the thermoplastic film at the bottom of the depressions than exist elsewhere. The force on the free surface where it is depressed would be greater than elsewhere as a result of the smaller separation between the conductor layer and the free surface here. This mechanism for the acceleration of deformation is mentioned by Credelle and Spong (30) in the context of Frostless recording.

It is also quite possible that mutual repulsion between surface charges helps to pile the thermoplastic into ridges when a sinusoidal surface charge density distribution is present as in the relief (Frost free) recording of a screened image or in thermoplastic holography.

It seems there is no reason why a sharp distinction should be drawn between the mechanisms operating in Frost recording and non Frost recording. Comparison of the mechanisms for these two recording techniques is found in

the literature only in the context of the competition which occurs between Frost deformations and image structure (or grating) deformations in the recording of thermoplastic holograms. In this case the aim is always to minimise the Frost deformations and maximise the grating structure deformations.

Lee (28), for example, tells us that the driving forces producing the grating deformation are much greater than those for the Frost so that the grating will predominate. However, he does not explicitly state the physical cause of these forces. The equations he quotes for Frost formation have the same form as those of Budd (24) implying that Frost results from mutual surface charge repulsion alone whereas when discussing grating deformations Lee mentions only electric fields within the thermoplastic (as opposed to along the surface) so that he assumes each of these types of deformation is caused by only one of the two mechanisms. He gives no reason for this belief, though, and it is probably best not to make any such simplification to the theory.

CHAPTER 4

THE DEVELOPMENT OF THERMOPLASTIC HOLOGRAPHY

4.1 The Attractions of Thermoplastic Holography

From the earliest suggestion of the use of thermoplastic materials as a holographic recording medium it was apparent that they offered several advantages over the more usual photographic plates.

Clearly, the thermoplastic plates should provide the higher diffraction efficiency common to all phase hologram materials in comparison with amplitude materials. Also, this high efficiency should be obtained without the lengthy processing necessary in the development of bleached photographic emulsions. Indeed the development stage of the thermoplastic material is, in principle, simpler even than the processing of an amplitude hologram on a photographic emulsion. Furthermore, development in the case of thermoplastics involves electrical processes and so should lend itself more readily to automation than does chemical development.

Another point concerning thermoplastics also stems from their use of electrical development steps. This is the possibility of in situ processing: the ability to develop the image without removing the plate from the position in which it was exposed or even bringing a material substance into contact with it. This is ideal in applications such as holographic interferometry and matched filtering where the hologram must be accurately located during certain

stages of the operation cycle. Also, problems of emulsion shrinkage due to contact with chemical solutions are removed. (The possible difficulty arising from thermal expansion of the thermoplastic plate during heat development should become negligible if substrates of low expansion materials are used or if the sequential mode of operation is adopted so that the recording and reconstructing exposures are both made while the substrate is at room temperature).

Another attraction of the thermoplastic materials is the possibility of erasing a hologram by reheating the substrate, and forming another recording on the same area of the plate. This was seen to offer a means of producing a write-read-erase optical memory device (see, for example, ref. 27) as well as the rather more mundane advantage of speed and convenience of operation, and the reduction in cost and supply difficulties, which might be expected from any reusable recording system in a field hitherto served almost exclusively by "disposable" photographic plates.

It was mainly as a result of these potentialities that development work was carried out on the thermoplastic materials for holography.

4.2 The First Specific Development Efforts

After the initial description of thermoplastic holography by Urbach and Meier (14) nothing appears to have been published on the subject for several years, but in 1970 Lin and Beauchamp (27) considered the behaviour of the material in connection with their Optical Memory System.

They tried using plates on which the photoconductor

and thermoplastic were mixed as well as those on which they were in separate layers, but preferred the latter on the grounds of higher diffraction efficiency. The thicknesses of the layers were less than were generally used in thermoplastic xerography, the photoconductor being 2.5 μm. and the thermoplastic 1 μm. thick. These layers were coated on the glass substrate by dipping into solutions of the materials in organic solvents. Thickness was controlled by adjusting the concentration and rate of pulling from the solution. The materials used as photoconductor and thermoplastic respectively were poly-N-vinyl carbazole doped with 2,4,7, trinitrofluorenone and "Staybelite" respectively, the latter being a trade name for a naturally occurring tree resin. As they note, a difficulty encountered using this photoconductor material is the carcinogenic nature of the dopant trinitrofluorenone and the precautions necessary in handling it to prevent contact with the skin or inhalation of the airborne powder.

Lin and Beauchamp were concerned with the application of this recording material to a reusable optical memory and so were concerned largely with erasure and re-recording, and they reported satisfactory holograms after a hundred record-erase cycles. However, the diffraction efficiency they obtained was only 7% which, although better than that obtainable with amplitude holograms on photographic materials, nevertheless suggests that their material was by no means modulated to its optimum depth with respect to diffraction efficiency.

The spatial frequency at which they recorded the holographic grating was 1000 cycles per mm. which was

arranged to be the centre frequency of the band pass response of the thermoplastic layer. They believed this to be the highest centre frequency obtainable.

Although the work of Lin and Beauchamp covers the behaviour of only a single form of recording plate used in one particular application, it does nevertheless provide the earliest example of holographic application for this material and, consequently, the first indication of its potential.

4.3 A More Extensive Examination

A much more comprehensive assessment of a thermoplastic holographic recording material was given in 1972 by Credelle and Spong (30).

After reviewing the state of understanding of the processes involved in the operation of these materials in general, they describe their own experimental work. This is entirely concerned with the separate layer sandwich type of construction for the recording plate but involves both simultaneous and sequential modes of operation. Their recording plates are similar to those of Lin and Beauchamp in the materials used but they use generally thinner films of thermoplastic; down to about 0.2 μm.

A difficulty which they describe as fogging of the photoconductor layer (apparently a disabling opacity of this layer) occurred if the dip-coating was carried out in humidities greater than 25% when the photoconductor solvent employed was a 1:1 mixture of dioxane and dichloromethane. They avoided this difficulty by the use of trichloroethane

as the solvent which tolerated humidities up to 65%. This problem was encountered in the work of the present author also, although an alternative solution was found for it, (See Section 7.6)

The experience of Credelle and Spong concerning the optimum spatial frequency at which to record the holographic information when using the sequential mode of operation was that the spatial wavelength should be twice the thermoplastic thickness, as expected by Cressman (23) and Budd (24). However, when using the simultaneous mode they tell us that the thermoplastic could be considerably thinner than suggested by this relationship. This seems to be the first occasion on which the absolute validity of the "factor of two" rule has been questioned, even though it apparently stemmed from observations by Cressman that were based on thermoplastic films of far greater thickness than those used in holography (See Section 3.5).

By using the simultaneous mode of operation, Credelle and Spong were able to record holographic gratings at up to 4100 cycles per mm. (at down to 1% diffraction efficiency).

With regard to the maximum diffraction efficiency obtainable, Credelle and Spong were able to achieve gratings which diffracted 40% of the transmitted light into each of the 1st orders. This, as they point out, is greater than the theoretical maximum for a thin sinusoidal phase grating, and indicates the presence of non linearity. Even with holograms of non sinusoidal object transparencies 35% was achieved. Both of these were carried out using the simultaneous mode which they considered generally to be preferable to the sequential mode unless there were other

considerations than high diffraction efficiency. Frost noise was also thought to be less with the simultaneous mode.

A further property of the thermoplastic plates which they noted was their relative insensitivity to ambient illumination (illumination of zero spatial frequency) and stray fringe patterns (of low spatial frequency) caused by multiple reflections of the laser light within the glass substrate during the exposure. The spatial frequencies of these light fields would certainly be too low to fall within the bandwidth of the thermoplastic film so that they would not be recorded directly as modulations of the thermoplastic as are the holographic frequencies. The possibility remains, however, of this stray light saturating the photoconductor and interfering with the hologram recording process in this way but according to Credelle and Spong this does not happen even with fairly high ambient light levels.

This is in striking contrast to the case of photographic holograms where stray fringe patterns from dust particles and multiple reflections are often recorded on the plate, and high ambient lighting levels (such as a tungsten filament lamp) cause complete saturation of the holographic recording process so that no hologram is recorded.

This tolerance to ambient lighting, both during storage before use and during the holographic exposure should be a great convenience in the use of thermoplastic plates in practice, as well as facilitating the taking of holograms of self luminous objects (such as light bulbs) for the purpose of, say, holographic interferometry, as Credelle and Spong demonstrated.

4.4 Thermoplastic Holography in Another Memory System

A second attempt at applying thermoplastic holography to the problems of a read-write-erase optical memory was made by Stewart et al (31). In preparation for their construction work they examined the behaviour of thermoplastic plates of the type used by Credelle and Spong.

Stewart et al appear to have used the sequential mode of operation exclusively, but their observations of the centre frequency of the bandpass spatial frequency response conflict somewhat with those of Credelle. Credelle found the ratio of spatial wavelength to thermoplastic thickness to be around 2 when using the sequential mode. Figures of 1.90 and 2.16 for this ratio were obtained when working at 1170 and 1850 $mm.^{-1}$ respectively. However, Stewart obtained ratios of 3.40 and 2.94 at 600 and 1000 $mm.^{-1}$ respectively, and found generally that his results disagreed with the "factor of two" rule.

He was uncertain of the reason for the disagreement, conceding that it may be due to inaccurate measurement of thermoplastic thickness as much as a definite failure of this supposed rule. Nevertheless, he proposed that it is not practicable to predetermine the centre frequency of the response of a plate before fabrication: it must be set empirically to the required value by dip coating a number of trial plates and monitoring the resulting centre frequencies while adjusting the concentration of the thermoplastic solution or the rate of withdrawal of the plate. Stewart added, however, that if very high exposures were used (around 1000 μJ) the material seemed to have a broader bandpass response; a wider range of spatial

frequencies could be recorded as higher exposure levels were used.

On the subject of erasure, Stewart noted the tendency for previously erased images to return when a new recording was made but was unable to decide whether this was due to a residual charge pattern remaining in the thermoplastic or to mechanical stresses remaining in this layer after the erasure.

4.5 The Reduction of a Material to Parameters

A good example of an approach which is quite different from that of Stewart et al and Lin and Beauchamp is the work of Bergen (29). Here, thermoplastic plates of a particular design were subjected to a large number of experiments to obtain quantitative information on their behaviour in holographic use without reference to any particular application.

The material used here was again polyvinyl carbazole (PVK) for the photoconductor, but Piccopale H-2 was used for the thermoplastic. The range of experiments covered was considerable. Measurements of surface voltage and photodischarge of a single photoconductor layer without its thermoplastic overcoat were made, contributing some rather abstract information to the overall picture, but also some interesting techniques were used in the measurements of the effects of beam intensity ratio and spatial frequency upon the response of the photoconductor-thermoplastic combination.

These techniques appear to offer a rapid means of determining these properties of any such plates prior to

using them in a particular application, which would be a useful practical contribution because of the difficulty of predetermining these properties by controlled fabrication, and the great time involved in plotting the properties if a separate recording is needed for each value plotted. These procedures involved recording a range of beam ratios or spatial frequencies respectively on a single plate so that the relative diffraction response of the material was measurable by scanning the plate with a laser beam raster and measuring the diffracted intensity.

A useful simplification of this equipment could be to illuminate the developed hologram with an expanded collimated beam and view the diffracted light with a closed circuit television system. A single line of the T.V. raster could then be displayed on an oscilloscope to form a plot of diffracted intensity against recording beam-ratio or spatial frequency as the case may be. The slightly difficult practical problem of generating a laser beam raster would then be removed, the T.V. raster being used instead.

Probably the most significant difficulty with the techniques of Bergen is the variation of development temperature and of the thickness of the photoconductor and thermoplastic layers across the test area of a single plate. These non-uniformities would tend to be worse with smaller plates as they are largely due to the proximity of the edge of the plate to the test area. Thus the method is not really suitable with small hologram plates, but may well be useful where the test area of the plate is small compared with the dimensions of the whole plate. Bergen does not,

unfortunately, give any indication of the sizes of plates or test areas used in his work.

Thus it is the techniques used in Bergen's work rather than his results which are of significance to later workers. Even if one was working with the same materials as he used, the tendency, noted by other authors such as Stewart (31), of thermoplastic materials to defy predetermination of their behaviour (even though samples made in a particular way may behave repeatably) means that one would probably not rely solely on Bergen's results. The more reasonable course for an experimenter to take would be to measure for his own plates some of the parameters Bergen measured. In this, the actual methods used by Bergen could be useful.

An interesting piece of information which Bergen's work provides is that holograms can be recorded using Polyvinyl Carbazole as the photoconductor without the carcinogenic dopant material Trinitrofluorenone, although the sensitivity of the photoconductor material would probably be reduced.

4.6 The work of T.C. Lee

In two papers, Lee (28, 32) describes his work carried out on thermoplastic holography in connection with its use as a reusable storage medium. He considers especially the characteristics of the growth of the holographic recording and Frost noise during heat development. To investigate this he uses a form of the sequential mode of operation, the charging and exposure being carried out together and a heat pulse of controlled duration and energy content being applied during this operation to carry out the development.

The experimental arrangement he used makes use of the extreme thinness of the thermoplastic layer. As this layer is only 0.4 to 1.5 μm. thick in Lee's work, Bragg diffraction effects, such as may occur with photographic holographic emulsions, are absent and the diffraction orders from the resulting holographic gratings will have intensities which are symmetrical about the central zero order. Thus, for example, the +1 and -1 diffracted orders will be equally bright, so Lee measured the brightness of the -1 order as it developed. The +1 order image was presumably inaccessible to him as it would have been swamped by the light from one of the recording beams.

Lee found that it took his films 80 m.sec. to reach the softening temperature with the heat pulses he was using, after which the deformation amplitude of the thermoplastic surface increased almost linearly with time. This continued until a stage he describes as saturation which he attributed to charge leakage across the progressively more fluid thermoplastic as the temperature continues to rise. The leakage would tend to reduce electric forces existing across the thermoplastic, preventing further enlargement of the surface deformation. Beyond this "saturation", Lee tells us that the image brightness decreased, and he seems to ascribe this to a reduction in the deformation amplitude as the thermoplastic becomes less viscous with further increases in the temperature.

However, he does not tell us whether he has considered the possibility that the "saturation" and subsequent image decay may be due simply to a steady increase in the surface deformation amplitude, causing the image intensity to follow

the first order Bessel function which relates the intensity diffracted into one of the first orders by a thin phase grating to the wavefront deformation produced by the grating. In this case there would be no need to assume that the rate of increase of the deformation amplitude changes or reverses during the development stage.

Whatever the cause of the limitation and decay of image brightness, though, Lee's techniques did enable him to determine the optimum heat development pulse for his hologram plates and to develop holograms (in the sequential mode) having the brightest image possible with respect at least to the development parameters.

With regard to Frost growth Lee noted particularly, that the dominant spatial frequency in the developed Frost tended to be the same as that of any holographic grating that was recorded on the plate, providing the recorded grating had a spatial frequency roughly in the region of the "quasi-resonant" frequency of the thermoplastic. For this part of his investigation he used the technique employed previously by Ost and Moraw (26) of examining the annular diffraction ring caused by the dominant spatial frequency and random orientation of the Frost deformations. Lee recorded gratings of various spatial frequencies on his plates and observed the variation in diameter of the Frost diffraction ring. Interestingly, the diameter of this diffraction ring tended to follow the +1 and -1 diffraction orders of the grating not only in one orientation but in all: the Frost diffraction ring remained circular as the grating frequency was varied, and tended always to pass through the +1 and -1 diffraction orders of the recorded grating. This means that

the grating not only influenced the size of the Frost deformations in an orientation perpendicular to the grating lines, but also their extent along the lines of the grating.

4.7 The Need for Further Work

As we have seen, thermoplastic holographic devices have been investigated by a number of people, most of this work having been carried out in industrial research laboratories with a view to a particular application. The commonest objective has been the use of this recording medium as an erasable and reusable information store for a read-write memory system.

However, its other potential uses seem to have been largely overlooked. A notable exception here is the work of Credelle and Spong (30) who demonstrated its application to holographic interferometry, where the ability to develop the image without mechanically disturbing the recording plate was a considerable practical advantage. Also, the insensitivity of the material to ambient lighting was especially useful to them when incandescent objects were being recorded. In general, though, other uses for the rather unusual properties of this material have not been developed or described in the literature.

One field of applied optics in which there is the need for some of these properties is that of holographic filtering. This is an embodiment (thought by many to be the only practical one yet devised) of the concept of matched filtering which, in turn can be considered a special case of the technique of spatial filtering.

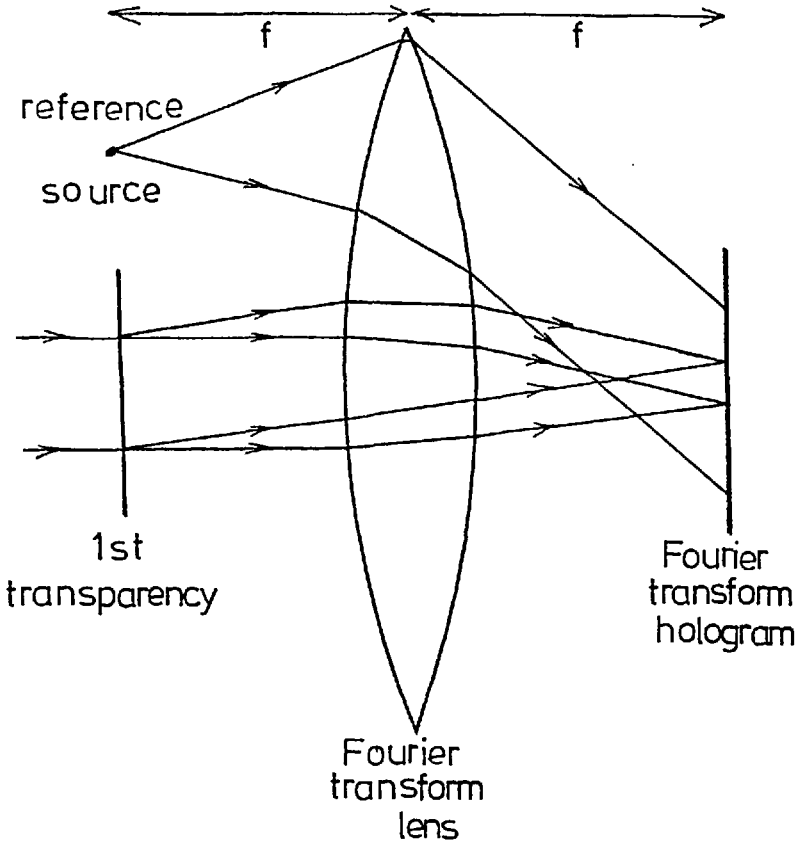

Figure 19a. Vander Lugt filtering, 1st stage - recording the Fourier Transform hologram filter.

Figure 19b. Vander Lugt filtering, 2nd stage - construction of the cross correlation.

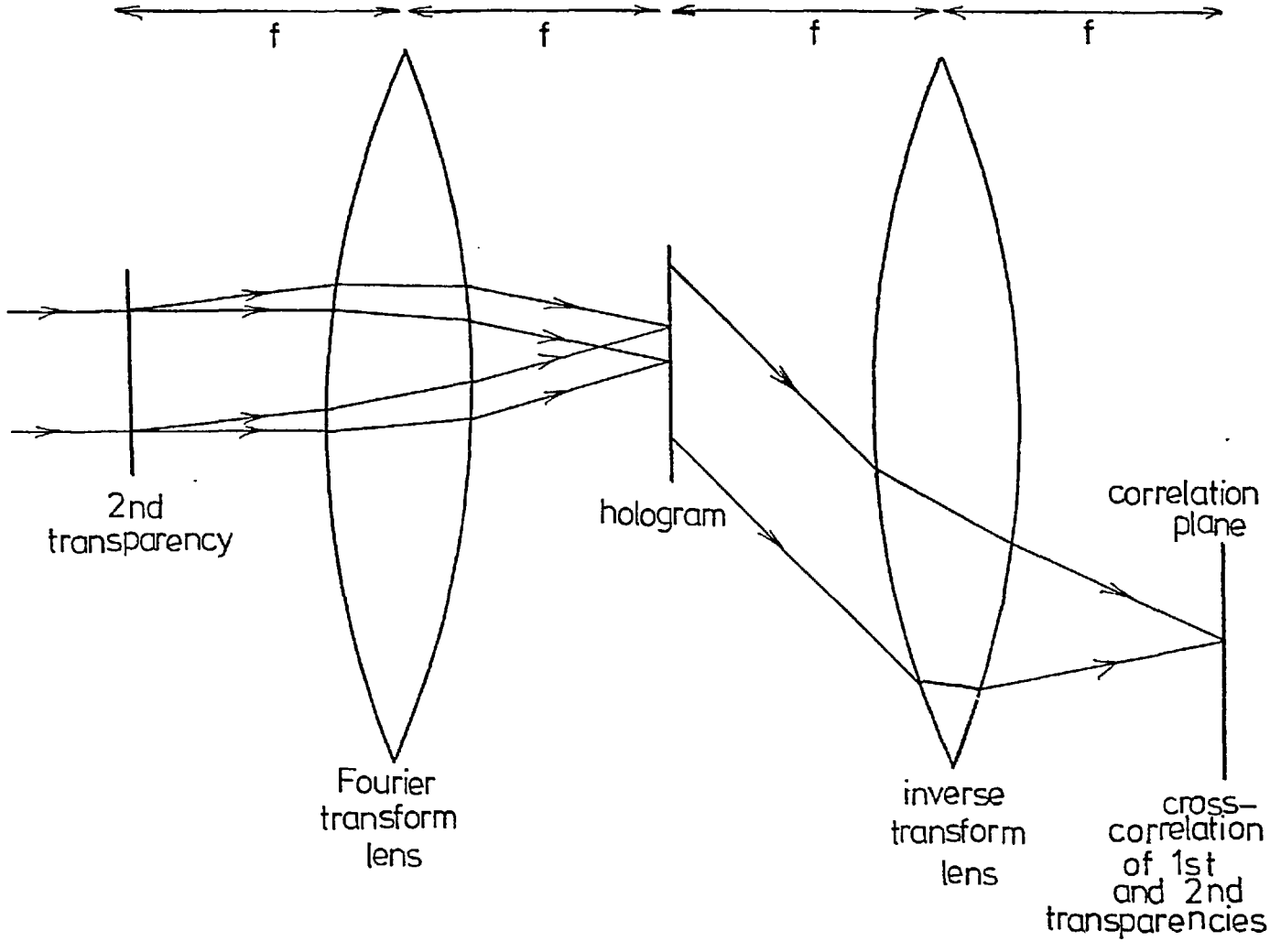

4.8 Practical Aspects of Holographic Filtering

The idea of holographic filtering was first put forward by Vander Lugt (33) and has since been much discussed in journals and text books (see ref. 34, for example). Its purpose is to carry out the two dimensional cross correlation of two sets of spatial data. If the two sets are identical, the autocorrelation of that set is performed.

The technique involves recording a Fourier transform hologram (See Fig. 19a) in the spatial frequency plane of an optical spatial filtering bench, using one of the two sets of spatial data in the form of a transparency in the object plane. The hologram thus, in principle, stores the amplitude and phase components of the Fourier transform of the object transparency.

The cross correlation of this object transparency with the second is carried out (See Fig. 19b) by mounting the latter in the object plane in place of the first transparency. The reference beam used in recording the hologram is removed and the transparency is, as before, back illuminated by coherent light, so that its Fourier transform is now generated in the plane of the hologram. The light diffracted by the hologram is collected by an inverse transform lens and the cross correlation of the two sets of data is displayed as the light amplitude in the back focal plane of this lens.

The principal practical problems which have been encountered by other workers in implementing this technique have been of two types. The first of these is concerned with the large range of intensities which exists across

the Fourier transform plane. When continuous tone photographic data is used as the object (input) transparency the intensity at the centre of the Fourier plane is usually far brighter (by a factor of, say, 1000) than the intensity at the edge of it. This range is far too great to record on real holographic materials and has often resulted in constraints upon experimental arrangements. For example, the cross correlation of sets of alphanumeric characters for character recognition purposes (e.g. page reading machines) is attempted usually only with transparent characters on a black background in the object plane rather than the complementary case. This type of object has a much lower amplitude in the low spatial frequencies than one having opaque characters on a transparent background, so that the intensity at the centre of the Fourier plane is much lower.

Another form of this constraint under which experimental work has been carried out in this field is the having to accept that only one annular ring of the Fourier plane can be recorded more or less linearly on a real holographic material when using continuous tone input data so that in effect only one spatial frequency band of the object will be recorded on the holographic filter. This is clearly a deviation from the ideal case but has been shown to produce results which are at least tolerable (see ref. 35, for example).

The second main difficulty encountered in holographic filtering has arisen from the mechanical tolerances involved. In particular, problems arise when using photographic hologram plates, from the need for mechanical contact of the plate with the liquid developer. If the hologram is

removed from the Fourier plane for processing it must be relocated accurately afterwards. Dickinson and Watrasiewicz (36) tell us that the intensity of the correlation response of the filter will be reduced by 10% for a replacement error of 4 μm, and 50% for an error of 10 μm when replacing the filter after processing.

If, alternatively, processing is carried out while the hologram is still located in the Fourier plane, by using a liquid gate, there remains the problem of swelling and shrinkage of the emulsion which also causes misalignment.

Thermoplastic holography appeared to offer a solution at least to the second of these two problems (the general repositioning difficulty) by virtue of its freedom from mechanical disturbances during development. The behaviour of the thermoplastic material in the face of the first problem (high intensity range across the Fourier plane) is less predictable, but is at least a possible improvement on the photographic case.

CHAPTER 5

PREPARATORY EXPERIMENTAL WORK

5.1 Early Development of Suitable Conductive Films

The first step towards producing a thermoplastic hologram plate in our own laboratory was perceived to be the development of a suitable conductive transparent layer with which to coat a glass substrate in order to form the heating element of the device. Glass substrates already bearing such a film were known to be available from commercial suppliers, but in order to avoid unnecessary expense some effort was directed towards the development of our own.

The requirements for this film are, principally, high optical transmission to minimise light losses from the holographic system and high electrical conductivity so that sufficiently large amounts of heat can be produced in the film to raise the substrate temperature to around 50-60^{o}C, without the need for high voltage heater power supplies.

Also, uniformity of the film's thickness and composition both on the large and small scale were desirable to promote uniform heating of the plate, as temperature was believed to be a critical parameter in the development of the hologram.

Finally, chemical resistance of the film to the materials used in coating the photoconductor and thermoplastic layers on to the substrate was essential, and, of course, good adhesion of the film to the substrate is highly desirable.

A process which is credited in the literature with having many of these properties is the NESA coating technique such as described by Peaker and Horsley (37). In this a film of antimony doped tin oxide is produced by raising the glass substrate to 480°C (for soda glass) and spraying it with a mixture of hydrochloric acid, stannic chloride, alcohol, water and antimony trichloride. Hydrolysis of the stannic chloride is said to take place at the elevated temperature of the glass, forming the tin oxide at the glass surface itself. The resulting films are said (37) to be highly transparent (transmissions around 80%) and highly conductive (down to 20 ohms per square), as well as chemically stable and mechanically tenacious (See also ref.9 p.493).

Two experimental arrangements were attempted with this process in the present work. Firstly the substrate was supported, after cleaning, in an oven and, after a period of about two hours for temperature stabilisation to 480°C, the lid of the oven was opened and a fine spray of liquid directed at the substrate. The composition of the liquid was as described by Peaker and Horsley.

A first attempt by this method yielded a slightly conducting film on the upper side of the substrate. The resistivity was about 5000 ohms per square. This was too high a value for a practical holographic device for operating at low heater voltages: a few hundred ohms per square is more suitable. Also, a more significant problem was that the film produced was cloudy in appearance. For a device which is to be used in coherent light granular or diffusing films should be particularly avoided because of

their strong contribution to the noise (speckle) in the system.

Two contact electrodes were formed on the coated side of the glass by painting a line of copper paint along two opposite edges of the substrate. The paint was then baked for about ½ hr. at 100°C to drive off the last of its solvent. Baking in this manner reduced the resistance of each electrode from about 10000 ohms to around 10 ohms.

After the substrate had cooled a D.C. heating current was passed between the electrodes to allow an estimate on the uniformity of heating. However, it was found that no refined measurement technique was required for the temperature: some parts of the plate were cool to the touch while others were unbearably hot. The degree of uniformity was considered negligible. It seemed that the areas of high resistance low temperature in the film were also those of greatest cloudiness.

Probably the principal inconvenience with this method of film production was the clouds of acrid fumes which engulfed the operator. These would contain hydrochloric acid as well as poisonous antimony compounds, so a change in the method was sought which would enable the spraying to be carried out in a fume cupboard.

This was arranged using a hotplate. A steel plate about 6 inches square was supported about half an inch above the bare wires of the heating element. The plate had a hole about 1½ inches deep drilled into one edge to receive a thermocouple element. The equipment was set up inside a fume cupboard this time.

The cleaning procedure used for the glass substrates

this time was made slightly more thorough, beginning with washes in Teepol and water followed by a chromic acid bath and rinsing with distilled water and alcohol. The substrate was then placed on the cold steel plate whose temperature was then brought to 480°C, the temperature being monitored by the thermocouple.

A variety of styles were tried for the spraying technique this time. A series of short bursts of spray yielded a film which appeared not at all granular or diffusing, a considerable improvement over the oven method that was possibly due to there not being a large volume of very hot air surrounding the substrate when hotplate heating was used. In the case of the oven, there would be a considerable quantity of hot air contained by the walls of the oven while the spray was directed down into it, and this may have been causing the hydrolysis of the stannic chloride to take place in the spray droplets before they reached the substrate surface. This could well have produced the granular films observed when the oven was in use.

The film thickness was, however, still not very uniform, being generally greater in the centre than towards the edges and having small scale variations all over. (At this stage the uniformity was being judged by the interference colours shown by the film). The region of greatest thickness was not central on the substrate, but was displaced slightly in the direction that the spray had been travelling during the coating process.

Some improvement over this situation was obtained by rotating the substrate (and, since the glass was at a temperature near its softening point, the steel plate also)

through 90 degrees between giving each burst from the spray gun. This produced a film which, according to its interference colours was again thinner towards the edges, but this time the thickest part was very close to the centre of the substrate.

An attempt was also made to spray the liquid on to the substrate in one long burst. Unfortunately this cracked the glass. It was interesting to note, though, that the fragments had a film on them which was particularly free of the small scale thickness variations that all other methods seemed to produce. This technique may, therefore, be useful if Pyrex glass substrates are available to prevent shattering due to the sudden large temperature change during the long spray burst. The cost of such substrates did not appear warranted for the present work, as the small scale film variations were expected to be less troublesome in our application than the large scale ones.

The cause of the large scale thickness variations (the film being thicker towards the centre than at the edges) was assumed to be non uniformity of the temperature of the substrate during spraying, arising from the use of the hotplate as a heater. A larger hotplate would probably have reduced these "edge effects" but some of the films produced so far, especially those made by short spray bursts with substrate rotation between to promote symmetry, seemed likely to be sufficiently uniform to use as hologram heater layers. Consequently, a trial batch of holograms was prepared using these substrates in order at the earliest possible time to be able to see the problem of heater film non-uniformity in perspective against other problems that

would undoubtedly arise in later stages of the fabrication work. Thus it would be easier to decide whether, before embarking on the evaluation of the hologram plates, to devote more effort to overcoming the non-uniformity.

5.2 A Trial Batch of Holograms

For a first attempt at producing complete thermoplastic hologram plates, four soda glass plates each about 6 cm. square were given coatings of the NESA tin oxide on one side. The technique used here was the short spray burst method described above, and line electrodes were formed along two opposite sides of each plate using copper paint followed by baking.

The resistance between the electrodes on these plates had values from 480Ω to 810Ω, although these would be only a rough guide to the areal resistivity of the films because of the variation in film thickness across the plate.

To make the organic layers of the plate the method adopted was as described by Collier et al. (ref.34 p.302) and Lin and Beauchamp (27). This involves making solutions of the photoconductor and thermoplastic materials in two different solvents, dipping the substrate into the solutions and withdrawing it at speeds chosen to yield a film of the desired thickness.

The materials and figures given by Collier were followed for a first attempt, the photoconductor material being poly-n-vinyl carbazole (PVK) mixed with an electron acceptor 2,4,7, trinitro-9-fluorenone and the red-sensitising dye brilliant green. The solvent was an equal volume mixture

of dichloromethane and p-dioxane, and the quantities involved were:-

poly-n-vinyl carbazole (PVK)	20 gm.
2,4,7, trinitro-9-fluorenone (TNF)	2 gm.(carcinogenic)
brilliant green	0.2 gm.
dichloromethane	150 cc.
p-dioxane	150 cc.

The two components of the solvent are best mixed together before adding the PVK as otherwise the dichloromethane converts the PVK into a black dense rubbery mass which is quite unsuitable for our purpose.

The PVK dissolves only slowly in these solvents so it was convenient to arrange a mechanical agitator for the bottle containing them. If the mixture was not kept in motion the PVK formed a transparent syrupy layer at the bottom of the solvent and took several days to dissolve completely. The TNF and the dye were added after the PVK had dissolved.

The thermoplastic material was "Staybelite", which is a commercial name for a derivative of natural tree resin. The solvent mentioned by Collier for this is "Super hi-flash Naphtha" which is a commercial American name for naphtha.

The quantities used here were, again following Collier, 75 gm. of resin in 300 cc. of naphtha. One or two other solvents were tried, such as Xylene but none other was found which dissolved the resin but not the photoconductor. The latter requirement had to be met as the substrate would already be carrying the photoconductor layer when it was dipped in the thermoplastic solution.

The dissolution of the thermoplastic in naphtha is a

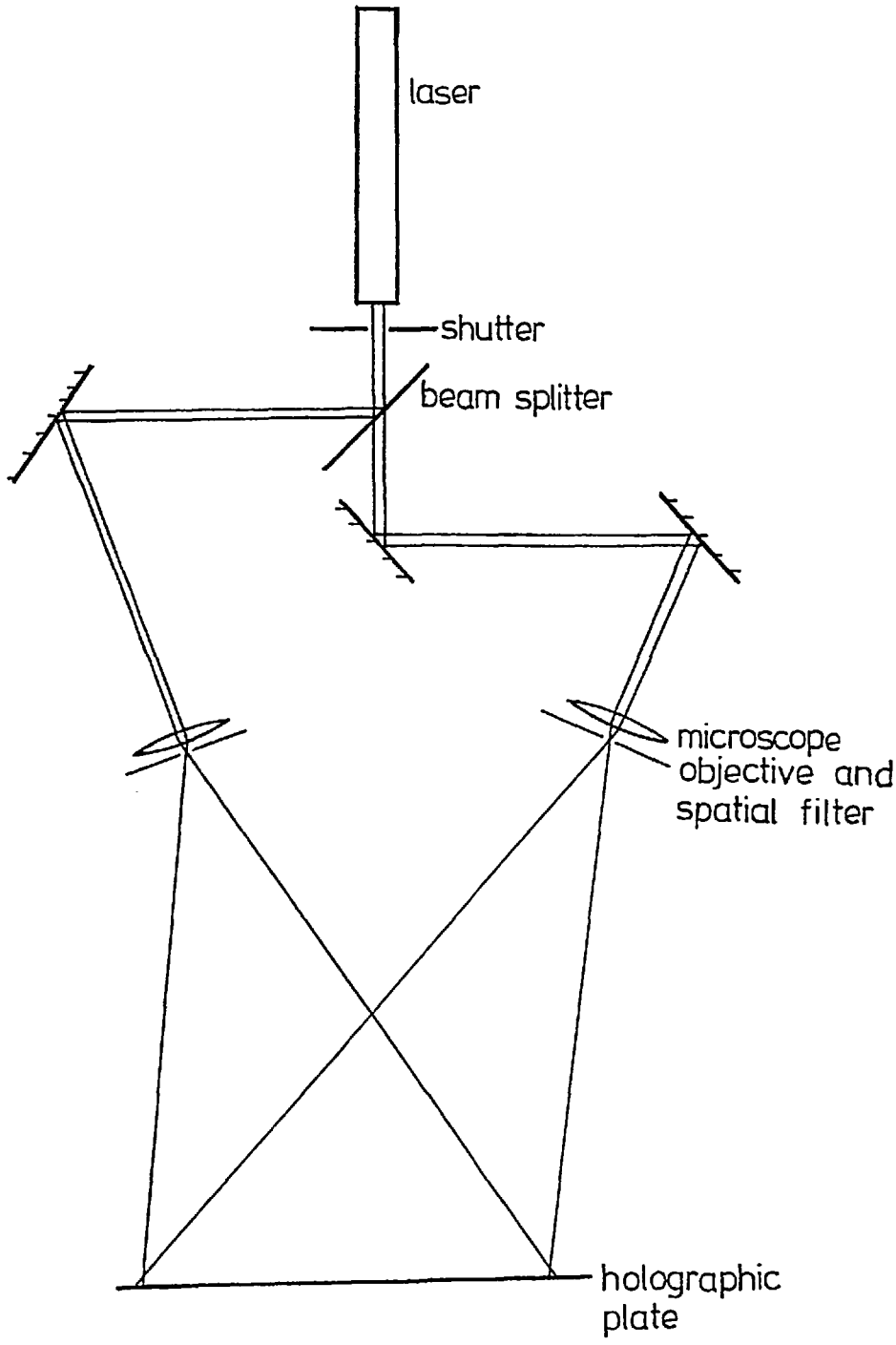

Figure 20. The preliminary holographic arrangement for evaluating thermoplastic recording plates.

rapid affair in comparison with the case of the photoconductor in its solvent.

Collier's method for adjusting the thickness of the organic layers is to exercise control over the speeds at which the substrate is withdrawn from the solutions. In the present work the withdrawal was carried out using a geared-down synchronous electric motor to obtain a smooth movement. Two threads attached by clips to the substrate plate were wound around the final drive spindle of the motor's gearbox, counterbalance weights being attached to the other ends of the threads to keep the threads taut and prevent slipping.

Sleeves of various diameters were fitted on the spindle to produce a variety of winding speeds. The thicknesses of the resulting films drawn from both photoconductor and thermoplastic solutions were measured by scoring a mark in the film and examining it with a Zeiss Linnik reflection interference microscope.

However, little change in thickness seemed to occur as the withdrawal speed was varied. Speeds of 7.5 cm. per min. and 3.25 cm. per min. were adopted for drawing the substrate from the photoconductor and thermoplastic solutions respectively, these figures for the first attempt being based on those of Collier. The corresponding film thicknesses were 2μm and 1μm.

5.3 Holographic Trials

An optical arrangement, shown in Fig. 20, was used to investigate the suitability of the first thermoplastic plates. With this it was intended to record holographic

gratings as a preliminary step.

One frequent source of trouble when recording holograms is vibration transmitted to the optical components from the floor of the building. To avoid this, the components were mounted on a heavy steel table which was supported on four inner tubes from motorcycle tyres. These were laid horizontally on the floor, and a wooden board was placed on each. The legs of the table rested on the boards. The tubes were inflated only sufficiently to lift the boards about an inch clear of the floor, providing a soft suspension with a very low resonant frequency.

In order to check the mechanical stability a holographic grating was first recorded on a photographic plate (Agfa 10E75). The correct density (0.6) of the plate for holography was obtained with a 2 second exposure. This suggests (ref. 50) an energy density of about 2 ergs per sq. cm. at the plate. An angle of 17.6° between the light beams was used, producing an interference grating of 483 lines mm^{-1}.

A successful hologram of the point object was recorded. This was then viewed through a small telescope which was defocussed so that the reconstructed image point appeared as a disc of appreciable size. The original object source was left in position and the recorded (virtual) hologram image was reunited with the original object by careful movement of the hologram plate, so that interferometric fringes appeared across the disc of light seen in the telescope.

The steadiness of these fringes which were produced by interference between wavefronts from the real object point

source and the virtual image point source was taken as an indication of the stability of the holographic arrangement. This seemed to be better than a quarter of a fringe generally providing nearby doors were not slammed, nor any other severe local disturbance committed. This was satisfactory so thermoplastic holography was next set up.

The method of Collier and others for thermoplastic holography involves the use of a corona discharge close to the plate to produce the necessary free electric charges. A device for producing a suitable discharge must, however, have some metal components which are connected to an E.H.T. power supply and which are also exposed to the air. This produces a hazard to the operator's safety, especially as the corona will often be operated in darkness or dim illumination during holographic exposures, when its presence may be temporarily forgotten. Also, as the apparatus was to be mounted on a steel table supported by inflated rubber tubes the possibility would exist of the entire table being raised to E.H.T. potentials if the corona device accidentally touched, say, the supports of the hologram plate while the table was not thoroughly earthed.

Bearing in mind that the supply driving the corona needed to be capable of delivering several milliamps at least, the use of this type of device seemed better avoided if possible.

An alternative which was considered at this stage was the Tesla coil, which produces a discharge in air by high frequency induction but which cannot supply very much current.

The trial batch of holograms was put through the sequence of steps described by Collier and others for

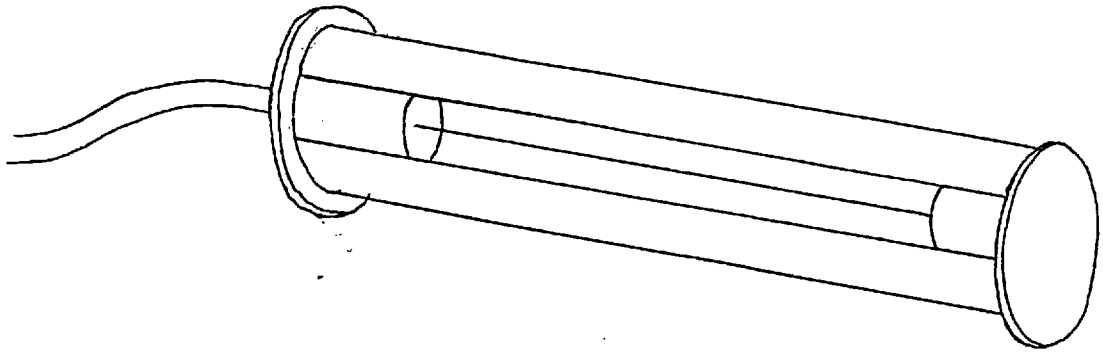

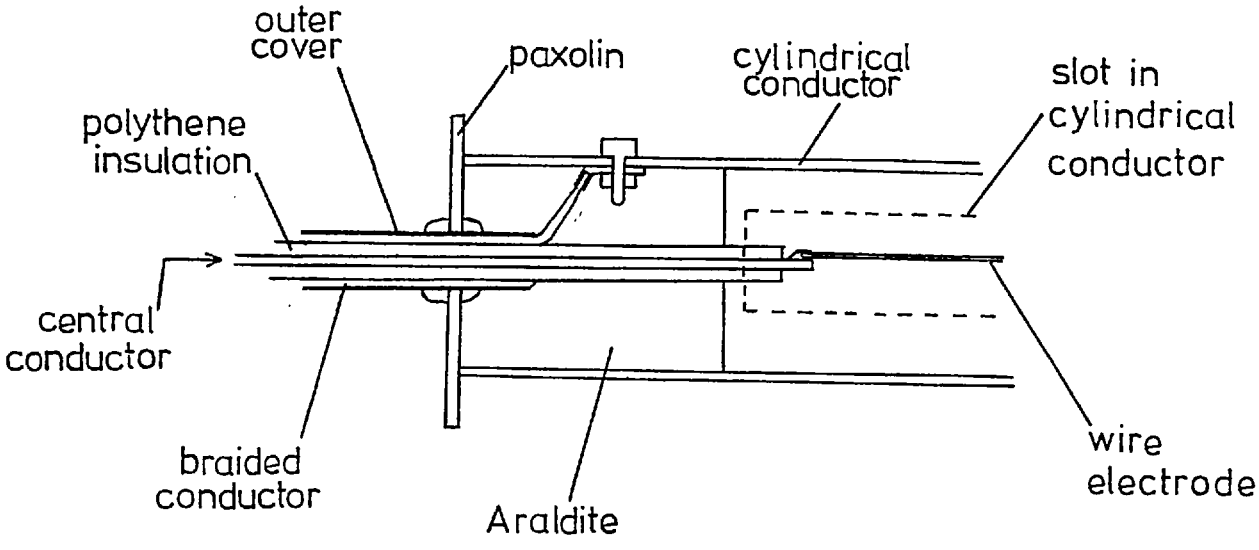

Figure 21. Details of the corona discharge device used for all further work.

thermoplastic holography, using the same optical arrangement as above. This should involve placing a uniform charge on the free thermoplastic surface, exposing the material to the holographic light pattern, recharging the surface to a uniform potential and then softening the thermoplastic by passing a heating current through the conducting layer of the hologram plate. In the present case, the charging and recharging were attempted using the Tesla coil and the heating was carried out with an A.C. current from a Variac variable ratio mains transformer. One side of the output from this was earthed to comply with the need for the conducting layer of the hologram plate to act as a ground plane during the charging and recharging as well as a heater layer.

Unfortunately, no holographic image whatsoever was recorded even after repeated attempts with different exposures, heating temperatures and positions of the Tesla coil. The most likely cause of this was certainly the use of the Tesla coil so an immediate start was made on making a corona discharge device to replace it.

5.4 Improvements to the Recording Technique

The corona discharge device which was produced here is depicted in Fig. 21. The design aimed at was a cylindrical earthed conductor with a wide slot down its length. The E.H.T. electrode was a wire concentric with the earthed cylinder so that a corona would form around the wire, more or less uniformly along its length, as described earlier (Section 3.1). The length of the device needed to be

sufficient for the slot aperture to cover the width of the hologram plates used, which was currently around 7 cm. All insulation in the device needed to withstand potential differences of up to, say, 10 KV as 7 KV was the expected operating voltage.

The construction of the device began with the forming of the cylindrical shield by wrapping a small sheet of tin plate around a solid metal bar of about 2.5 cm. diameter, leaving a gap between the two edges of the sheet. A paxolin sheet, cut to the size of the end of the cylinder, was drilled centrally to take the supply cable and araldited in place. A similar piece drilled with a smaller hole was araldited at the other end of the cylinder. After drilling a hole in the cylinder to take the bolt for securing the braid of the coaxial supply cable, two extra pieces of curved tin plate were araldited in place to complete the cylindrical shape at the two ends of this electrode. The supply cable, cut and stripped to length, was inserted through a rubber grommet in the paxolin, and an araldite mixture (MY753 resin and HY951 hardener), which had previously been briefly evacuated, was poured around the cable end. The purpose of the prior evacuation was to remove air from the mixture to prevent the formation of voids in the material during setting. Corona discharges might otherwise have formed within the voids during use, leading eventually to damage to the resin.

Generally, araldite is a very suitable material for a high voltage insulator as, in addition to being easily formed by casting it has good electrical strength,

withstanding up to 115 KV cm^{-1}. The coaxial supply cable used for the corona device was rated at 14 KV, D.C. so this would also be working well within its capabilities at 7 KV.

The central wire electrode of the device was a single strand of thin copper wire taken from the windings of a coil. The wire diameter is not critical providing it is small enough to produce the corona in the adjacent air by virtue of the high electric field which surrounds a sharply curved charged conductor, as described earlier (Section 3.1).

The device was connected to an E.H.T. power supply (the central wire being connected positive and the surrounding cylinder well earthed), the voltage was brought up slowly. At around 5 KV a visible discharge formed around the wire, spreading to cover its whole length at 6 KV. This produced a hissing sound which increased in intensity as the voltage increased through 7 KV. At 8 KV a spark jumped the gap between the two electrodes, apparently tracking across the surface of the Araldite insulation. This drew so much current that the overload cut-out of the supply operated and terminated the experiment.

This general behaviour seemed quite suitable for our purpose. Voltages of around 7 KV could be supplied and seemed to produce a suitable discharge, taking about 0.5 mA. If this voltage was greatly exceeded, the resulting spark jumped between the electrodes and not to the operator or the optical bench, and the consequence of such overloads was only temporarily to disable the power supply, causing no damage to the circuitry.

The device seemed as safe as could be expected where exposed high voltages are to be found.

It was later found that changes in humidity of the air caused small variations in the current consumption of the discharge at a given potential and in the sparking potential.

To test its effectiveness, a simple comparison was carried out between the corona device and the Tesla coil. A single layer of paper tissue was laid on an earthed conductively coated glass plate, and the Tesla coil moved across its surface. This should have produced a situation similar, in principle, to the charging of the free surface of the thermoplastic (insulating) layer above an earthed conductor.

However, this had no noticeable effect on the paper (except that if the spark from the Tesla coil was allowed to strike through the paper to the earth plane, the paper was inclined to ignite and rise into the air, burning).

A second paper tissue was laid on the glass plate and the operating corona device was moved across it. Immediately, the paper below the device was pulled down firmly on to the glass and, by moving the device around, all of the paper was pulled into contact with the glass. The attractive forces were such that the glass plate could be pulled across the table by the paper tissue.

This suggested that the new device was considerably better at charging the free surface of an insulator than was the Tesla coil.

When the corona was used in the sequential process of Collier for charging the thermoplastic plates a faint recorded image of the point object source was found. The procedure was again the sequential charge-expose-recharge-heat cycle using the corona charging device. A method soon

found to be useful for determining the duration of heat development was to remove one of the holographic light beams during development and view the reconstructed image as it develops. The heating could then be stopped as soon as the image brightness ceased to increase, avoiding any danger of the image's being partially erased by continuing the heating for too long and thereby achieving too high a temperature. The development time needed with a heater voltage of about 160 v (the heating current being around 250 mA) was only about 5 seconds, so the plate would still be increasing in temperature by the time development was completed. Hence the danger of overheating was otherwise significant.

This procedure is an example of the great practical flexibility of the thermoplastic hologram.

CHAPTER 6

INVESTIGATION OF SOME PROPERTIES OF THERMOPLASTIC HOLOGRAM PLATES

6.1 Holographic Requirements

There is a very large number of parameters which can be considered when examining a device such as the thermoplastic hologram, where several different processes are involved in its operation. For example, the operation of these hologram plates relies upon optical interference, photoconductivity, electrostatic forces, the mechanical deformation of a viscous fluid and, finally, optical diffraction from a phase structure.

It is not possible to investigate in a single project the effect of all the parameters which influence these processes, because of the limitation of time. This is especially true if, as is likely in the present case, some of the parameters are not independent of each other. For example, a change in the temperature of development may well alter not only the mechanical properties of the thermoplastic but its electrical ones also so that optimum performance in recording a particular holographic interference pattern could be restored only by readjusting, say, the time of development, the thickness of the thermoplastic layer and the position and potential of the corona device. A change in the materials used in the two organic layers of the hologram plate may be expected to have even wider ranging effects.

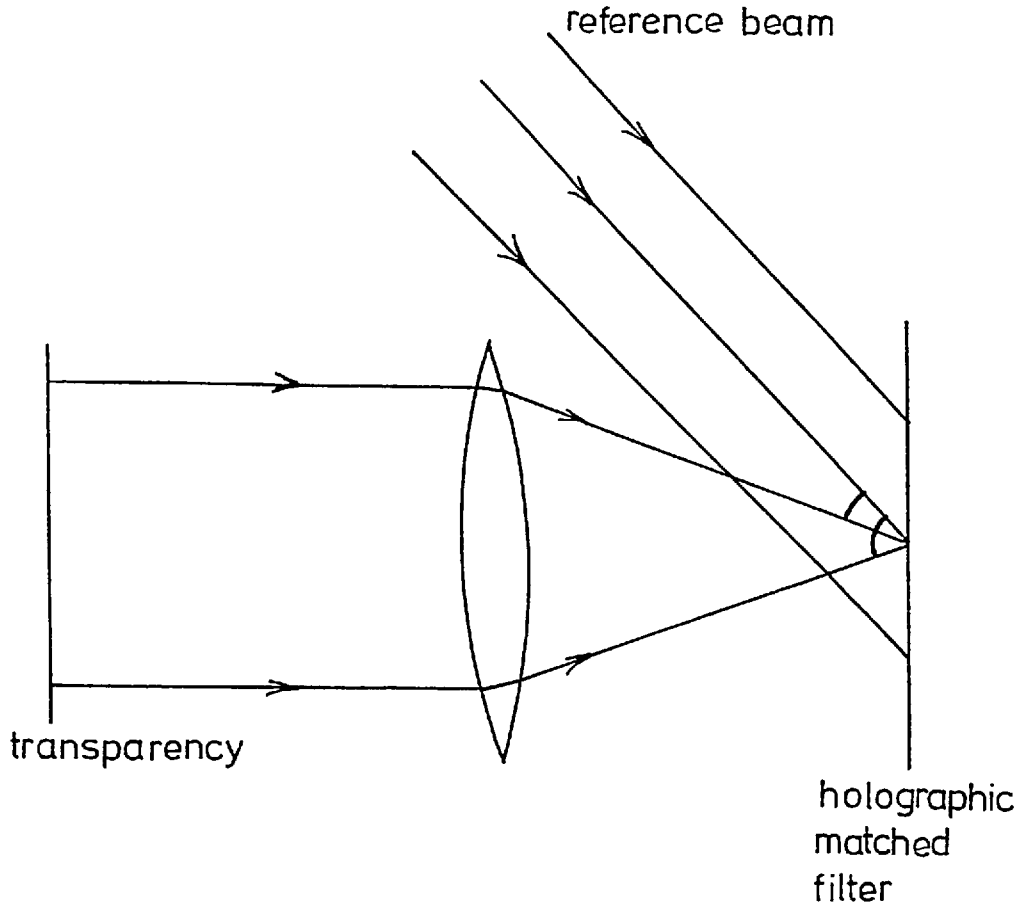

Figure 22. The range of inter-beam angles (and, therefore, holographic frequencies) present during the recording of a holographic filter.

In this type of situation it seems useful to simplify matters by considering the whole set of parameters in the light of a particular application of the thermoplastic device. This enables the selection of a relatively small number of the most significant parameters for examination although even then, the possibility of their interdependence may have to be neglected for simplification.

The present application is to holographic filtering and this gives rise to several particular requirements of our holographic device. Firstly, when carrying out the "reconstruction" stage with our holograms we illuminate the hologram device with a light beam which has already passed through the object transparency, rather than an unobstructed reference (reconstruction) beam. The reason for this is that we are constructing the autocorrelation of the original object transparency, and not reconstructing an image of it. However, in this case the object transparency will absorb energy from the beam.

Because of this we may generally expect a fairly weak autocorrelation response from the system unless the diffraction efficiency of the holographic filter is kept high.

Another characteristic of holographic filtering which is likely to have to be considered carefully if a thermoplastic Fourier transform hologram is used as the filter is the convergence of the light beam reaching the hologram plate from the Fourier transform lens (Fig. 22). This gives rise to a range of spatial frequencies in the holographic fringes at each point on the hologram. If, as

previous authors have stated, thermoplastic plates have a pronounced bandpass spatial frequency characteristic, this could lead to an inability to record all the information present. In particular, the record which the Fourier transform hologram retained of information in the object transparency would no longer be independent of the position in that transparency from which the information came. For example, an image reconstructed from such a Fourier transform hologram may be bright at the centre and fainter towards the sides. This would correspond to a situation where the bandpass spatial frequency response was centred on the frequencies at which the centre of the object field was being recorded, the outlying areas being attenuated in brightness according to the profile of the bandpass response curve and their position in the scene.

Thus high diffraction efficiency and a sufficient width to the bandpass response are desirable. However, there is also at least one constraint under which some other experimeters with thermoplastic plates have necessarily laboured but from which our application for these holographic devices frees us. Much of the work done on these plates has been in connection with reusable holographic storage devices. For these it is essential that images stored on the plates are completely erasable, but in our application to holographic filtering erasability is only useful as a matter of convenience in that it reduces the number of plates which have to be prepared: it is not an essential requirement to us.

6.2 Improvements to the Holographic Technique

A number of techniques have been tried in connection with the processing of thermoplastic holograms. These involve both variations to the order in which charging, exposure and development are carried out (ref. 28 for example) and a supplementary charging step, mentioned by Credelle and Spong (30).

The experiences of Credelle suggested, however, that the highest diffraction efficiency could be obtained from these holograms by the simultaneous mode of operation (charging, exposing and heating simultaneously). This was borne out in the present work by a short series of experiments.

The holograms recorded up to this time (described in Section 5.4) had all been produced by the sequential technique. The diffraction efficiency yielded was estimated to be much less than 1% and was certainly too low to measure with the available equipment.

Some trial batches of holograms were now recorded. The first of these employed charging and exposure at the same time, followed by a separate heating step. The second batch used the simultaneous (charge, expose and heat at the same time). Both of these techniques involved charging the thermoplastic surface while exposure was carried on, so the plate was used with the coated side of the substrate away from the laser. The corona charging device did not then obstruct the light beams before they reached the plate.

The first of these batches yielded a diffraction efficiency rather higher than was obtained with the earlier

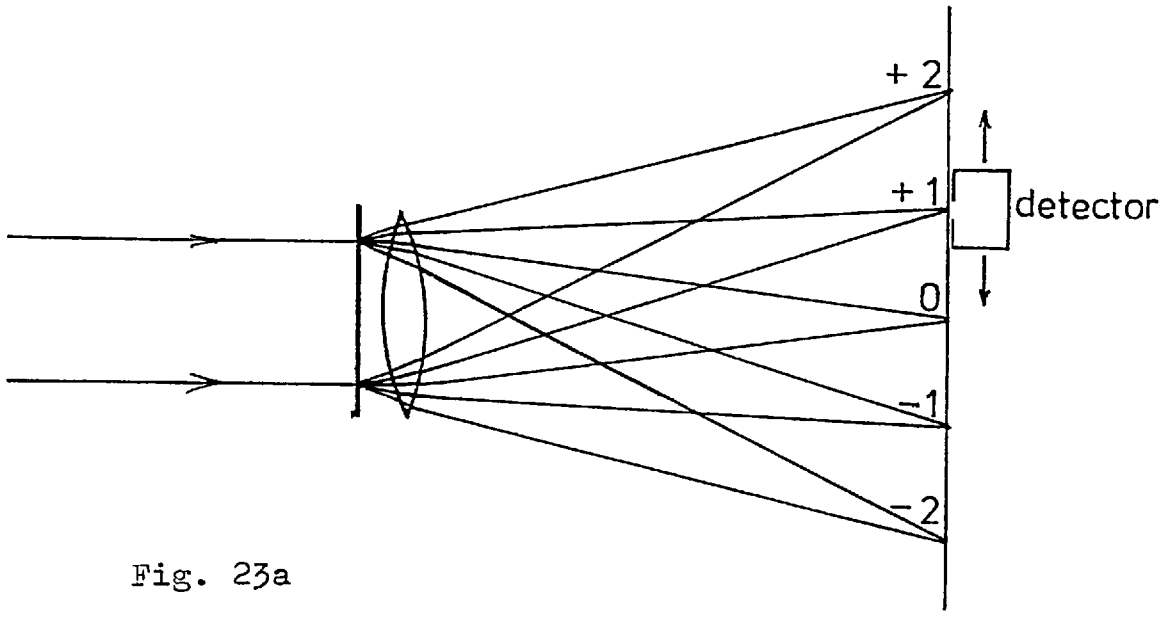

Fig. 23a

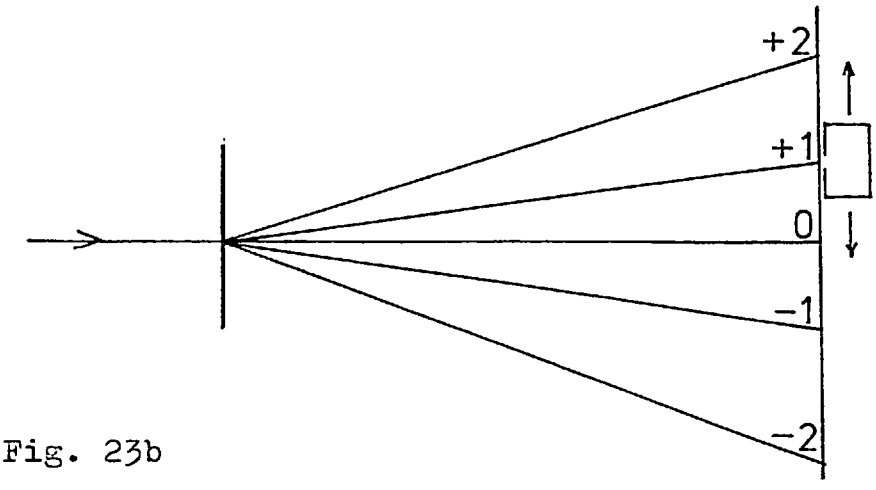

Fig. 23b

Figure 23. Arrangements used to measure the intensities diffracted by thermoplastic holograms.

sequential mode batch. The efficiency was estimated to be around 1%. This was still too low to be useful, and as this was the highest efficiency obtained by this technique even after trying a variety of development times and temperatures, it was not thought worthwhile to study the behaviour of the device in this mode in detail.

The second of these batches, by the simultaneous mode, seemed much more encouraging. The reconstructed point images were obviously brighter than any seen so far, even before any attempt was made to optimise the development of the image, several diffracted orders being visible each side of the undiffracted light. Some Frost noise was also present.

A cadmium sulphide cell was used to measure the diffraction efficiency of a typical grating formed in this way. The arrangement used to do this is shown in Fig. 23. At first (Fig. 23a) a collimated beam was limited in width by an aperture stop, allowed to pass through the hologram at normal incidence and immediately through a converging lens, to produce diffracted point images in the plane of the detector. The brightness of the diffracted orders varied considerably if the beam was passed through different parts of the plate, so it seemed better to use a narrower beam to investigate the plate.

This was arranged as in Fig. 23b, by using an unexpanded laser beam. No lens was then needed to produce diffraction spots small enough to be completely collected by the detector. Also no light was now being cut off by an aperture stop, giving higher intensities generally at the detector.

By this means it was found that within the area of the hologram plate were several separate regions which gave different diffraction efficiencies. These regions were strips, some only a few millimetres wide, lying parallel to the edge of the plate which had been uppermost during the drawing of the organic films during fabrication. The most likely cause of these strips seemed to be vibration of the apparatus or jerkiness in the drawing rate during the film drawing. This would be expected to cause variations in film thickness which, especially in the case of the thermoplastic layer, would modify the behaviour of the film locally. Care was taken to eliminate sources of vibration and make the winding threads run smoothly (by removing all traces of the Staybelite resin which had started to contaminate them) in the production of all later films and this reduced the problem to the point where it was of no practical significance. Its occurrence became sufficiently rare that when it was found, cleaning the plate of the organic films and recoating seemed invariably to produce a good film.

Typical figures obtained for the highest diffraction efficiency exhibited by one of the plates at this stage are shown in Table 1a. Here the diffraction efficiency is expressed as that percentage of the incident intensity which appears in each of the diffracted orders. The sum of these percentages is about 40%, indicating that about 60% of the incident light was being lost from the diffraction spots by absorption in the dye of the photoconductor layer and scattering over a range of angles and directions by the quasi random Frost noise. Also, a little light was being

Table 1a

Diffraction Order	-4	-3	-2	-1	0	+1	+2	+3	+4
Proportion of Incident Intensity	% 0.22	% 1.33	% 5.5	% 7.9	% 9.6	% 7.9	% 5.25	% 1.41	% 0.37

Table 1b

Diffraction Order	-4	-3	-2	-1	0	+1	+2	+3	+4
Proportion of Total Transmitted Intensity	% 0.44	% 2.66	% 11.0	% 15.8	% 19.2	% 15.8	% 10.5	% 2.82	% 0.74

Table 1. Proportions of (a) incident intensity and (b) transmitted intensity appearing in each diffraction order of a thermoplastic holographic grating.

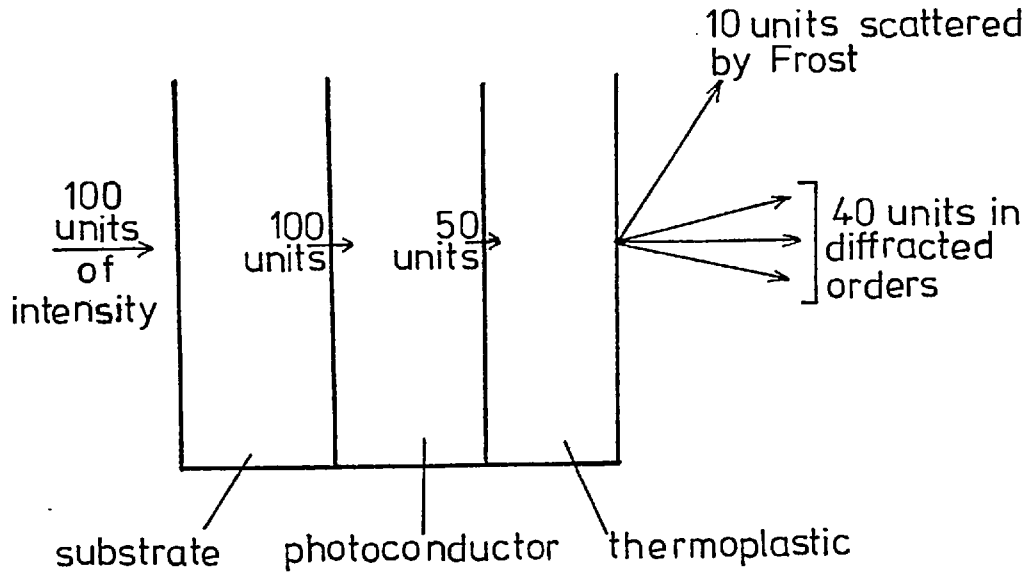

Fig. 24a

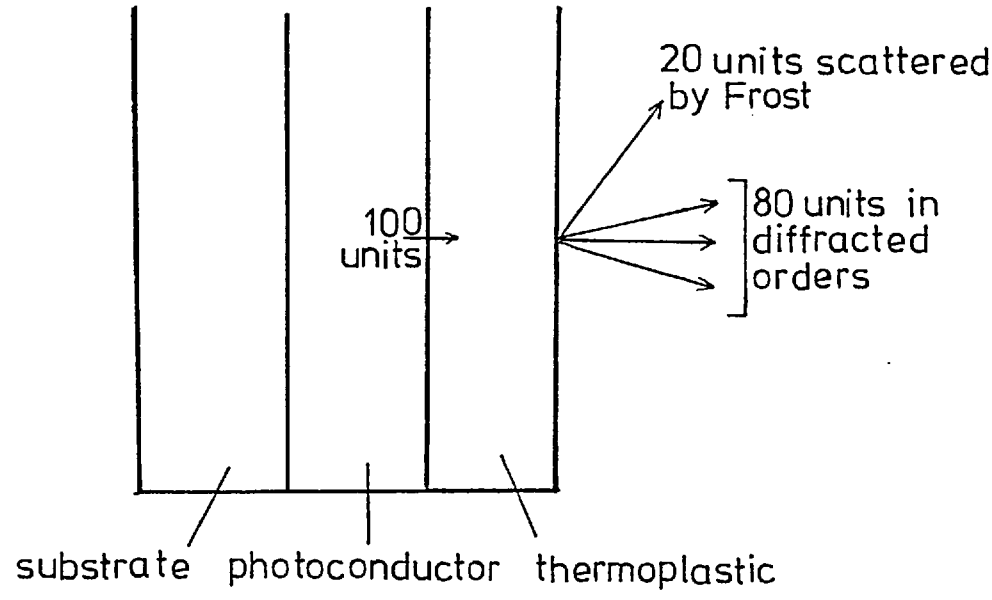

Fig. 24b

Figure 24. Schematic representations of the proportions of intensity lost from the thermoplastic hologram at each of its layers.

lost by reflection from the glass surface.

To gain a better idea of how strong a diffraction grating the thermoplastic layer is forming here, we should consider the percentage of the total transmitted intensity which falls in each diffracted order. This is shown in Table 1b. We see that around 16% of the total intensity transmitted (scattered by Frost as well as that in the diffracted orders) by the hologram lies in each of the first orders. These figures are based on the observation that a hologram plate without any Frost or holographic signal recorded on it transmitted about 50% of the incident light. The proportions of the light present at each stage are roughly as in Fig. 24a for the hologram as a whole, and in Fig. 24b for the thermoplastic layer alone. Here, absorption in the thermoplastic layer is neglected.

We can see that our diffracting phase structure (the thermoplastic layer alone) is producing first order images which are about half as bright as the maximum that may be expected for a sinusoidal grating from theoretical considerations (34%). However, if this grating had been recorded linearly so that it had a sinusoidal form then we would expect from the theory of phase gratings that where each first order held 16% of the transmitted light intensity the second orders would each hold either 0.9% or 23% of the transmitted intensity, according as the wavefront deformation introduced by the grating is less or greater respectively than that required to produce maximum intensity in the first orders.

Neither of these figures is very close to the 11% observed in the second orders so the holographic recording

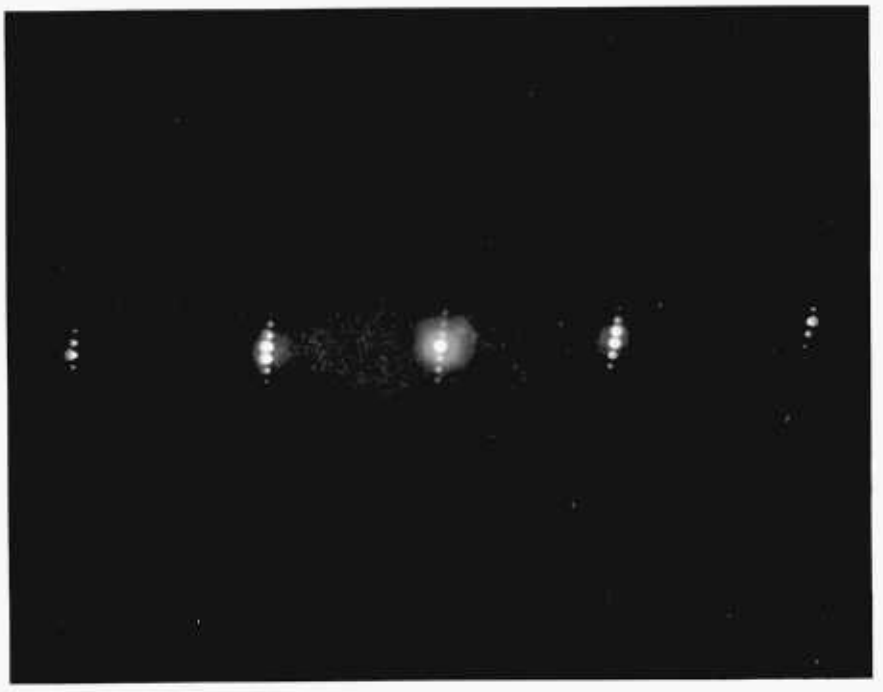

Figure 25. Diffraction pattern observed from a thermoplastic hologram when a second grating was recorded after an earlier one had been supposedly erased.

device we are dealing with is considerably non linear in this case.

6.3 Image Erasure Problems and a Consequent Effect

Attempts to erase the holograms produced so far were only partially successful. The method used was to reheat the substrate to a temperature above its normal development temperature and to hold it there until the image disappeared. This took only a few seconds. However, when another image was recorded on the plate the previous image would often reappear. This happened in spite of various erasure procedures such as erasing at different temperatures, ranging up to those which damaged the thermoplastic film, and erasing in the presence of high ambient lighting levels and corona charging.

An interesting effect was observed at this time which was attributed to the return of an apparently erased image. Fig. 25 is a photograph of the diffracted orders displayed by a thermoplastic hologram on which a holographic grating had been recorded, erased and recorded again. The undiffracted light (zero order) forms the central spot.

Each of the diffracted orders (and the zero order) is accompanied by a number of diffraction spots on a line running roughly vertically through it. The separation of the vertically aligned orders is about $\frac{1}{20}$ of that of those horizontally aligned, suggesting that the former are caused by a grating on the hologram plate whose element spacing was about twenty times that of the normal holographic grating which caused the horizontal diffraction.

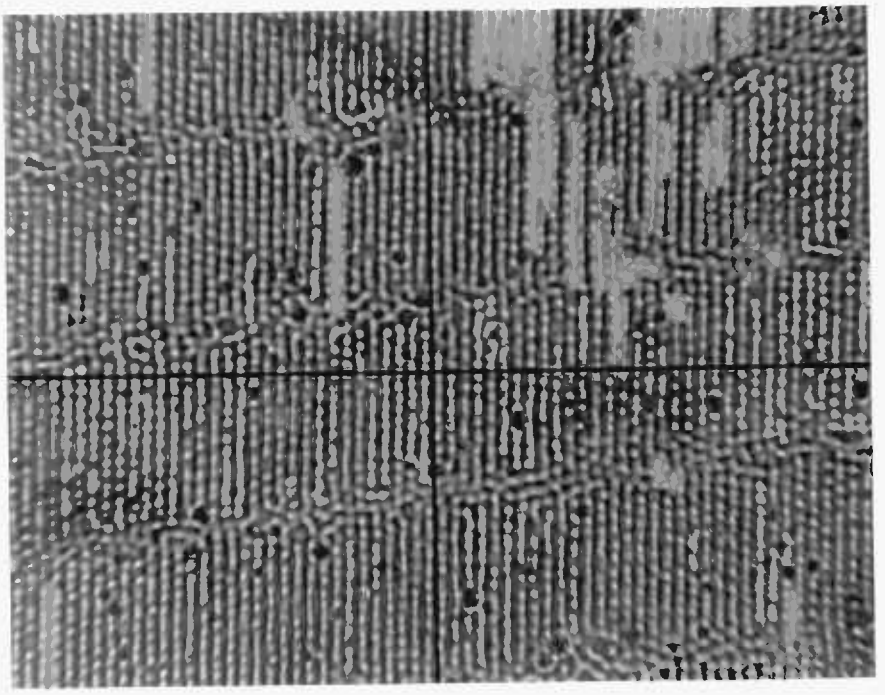

50 μm.

Figure 26. Photomicrograph of thermoplastic surface showing "Moiré" bands in the material. (Seen from the opposite side from that which was towards the camera for Fig. 25)

Furthermore, the orientation of the gratings causing the horizontal and vertical diffraction spectra must have been almost perpendicular to each other.

These conclusions are unexpected, as the hologram plate had at no time been exposed to a grating intensity pattern which had the orientation or spacing necessary to cause this vertically aligned diffraction spectrum. The two holographic grating patterns which had been recorded on this plate each had the orientation and periodicity which would be expected to cause the observed horizontal diffraction spectrum alone.

Fig. 26 is a photomicrograph of the surface of the thermoplastic hologram responsible for these spectra. The close vertical lines are the ridges of thermoplastic caused by the holographic grating exposures and have the correct orientation and spacing to cause the horizontally spread diffraction spots of Fig. 25. Additionally, there are a few roughly horizontal bands running across the surface. These appear to form a periodic modulation of the depth of the holographic fringes. Where the holographic fringe modulation is suppressed there remains only the Frost deformations, randomly oriented.

The separation and orientation of these horizontal bands is consistent with their having produced the vertical diffraction orders of Fig. 25 and they seem virtually certain to be their physical cause; it remains only to account for the existence of these horizontal bands.

The most likely explanation is that when the holographic grating pattern was recorded for the second

time, after the apparent erasure of the first recording, the previously recorded grating returned. If the two holographic gratings now present in the thermoplastic lay at a very small angle (about 3° in this case) to each other, because of the handling of the optical bench components between the two exposures, then Moiré fringes may be expected to form in the thermoplastic surface, whose orientation would be roughly perpendicular to the two gratings.

That the broad horizontal bands of Fig. 26 are Moiré fringes is borne out by the observation that these bands never formed on a hologram unless at least two gratings at closely similar orientations had been recorded on it (with an intermediate erasure, since otherwise after one grating had been formed the thermoplastic would not be able to redistribute itself to form the second grating pattern). Also, deliberate attempts to produce the horizontal bands by recording two vertical gratings with a slight rotation between them (and an intermediate erasure) were generally successful and yielded horizontal bands of roughly the separation expected from Moiré theory.

CHAPTER 7

MODIFICATIONS TO THE FABRICATION TECHNIQUES

7.1 Reconsideration of the Materials for the Conductive Layer

The development of a suitable conductive layer for the substrate had earlier been suspended (Section 5.1) in order to assess the other difficulties involved in producing a working device. Now that it had become possible to produce thermoplastic holograms fairly repeatably it was apparent that the two organic layers of the plates were relatively straightforward to produce to the required thickness and uniformity by dip-coating.

Attention returned to the conductive layer, made hitherto of tin oxide. In the plates produced so far, this layer was considerably uneven in thickness because of the lack of a satisfactory means of heating all parts of the substrate to equal temperatures during deposition of the film. (The use of an oven had been discarded earlier because of the inferior optical quality of the films made this way). Also, the process for producing the tin oxide film involved poisonous and corrosive compounds and fumes, which were not attractive. An alternative was sought which was more suitable for our purpose in these respects.

Vacuum deposition and sputtering are techniques which have a greater potential for uniformity and which are accompanied by more acceptable working conditions for the operator than is the more violent NESA process. Likely

sources of non uniformity in the former methods are purely the arrangement of the vacuum chamber furniture. For example, it is to be expected that the truncation of the electrical discharge at the edge of an electrode in a sputtering operation will lead to irregularities in the film sputtered on to a nearby substrate.

Vacuum evaporation is a technique which is commonly used in the deposition of metal films and with dielectric materials, but these two types of substance are not generally suitable as the conductive layer of a hologram plate, metals because of their opacity and dielectrics their electrical non conductivity.

Sputtering, however, is capable (ref. 9 page 464) of producing metal oxide films which are both transparent and conductive. Reactive sputtering is often used in this connection. A cathode of the respective metal is formed and sputtering carried out in an atmosphere containing some oxygen. The film deposited on a nearby substrate contains the metal oxide, oxidation of the cathode material having taken place at the cathode itself, at the substrate or in the intervening space, as a result of the discharge.

Holland (ref. 9 page 498) tells us that cadmium oxide deposited by reactively sputtering cadmium in a mixture of argon or nitrogen with oxygen has good transparency (around 85% transmission for white light through a film of thickness about half a wavelength) and high conductivity (a resistivity of, say, 50 ohms per square for the same film). This conductivity is in marked contrast to the high resistivity exhibited by cadmium oxide in the bulk, and is said by Preston (38) to be due to a lack of stoichiometry in the

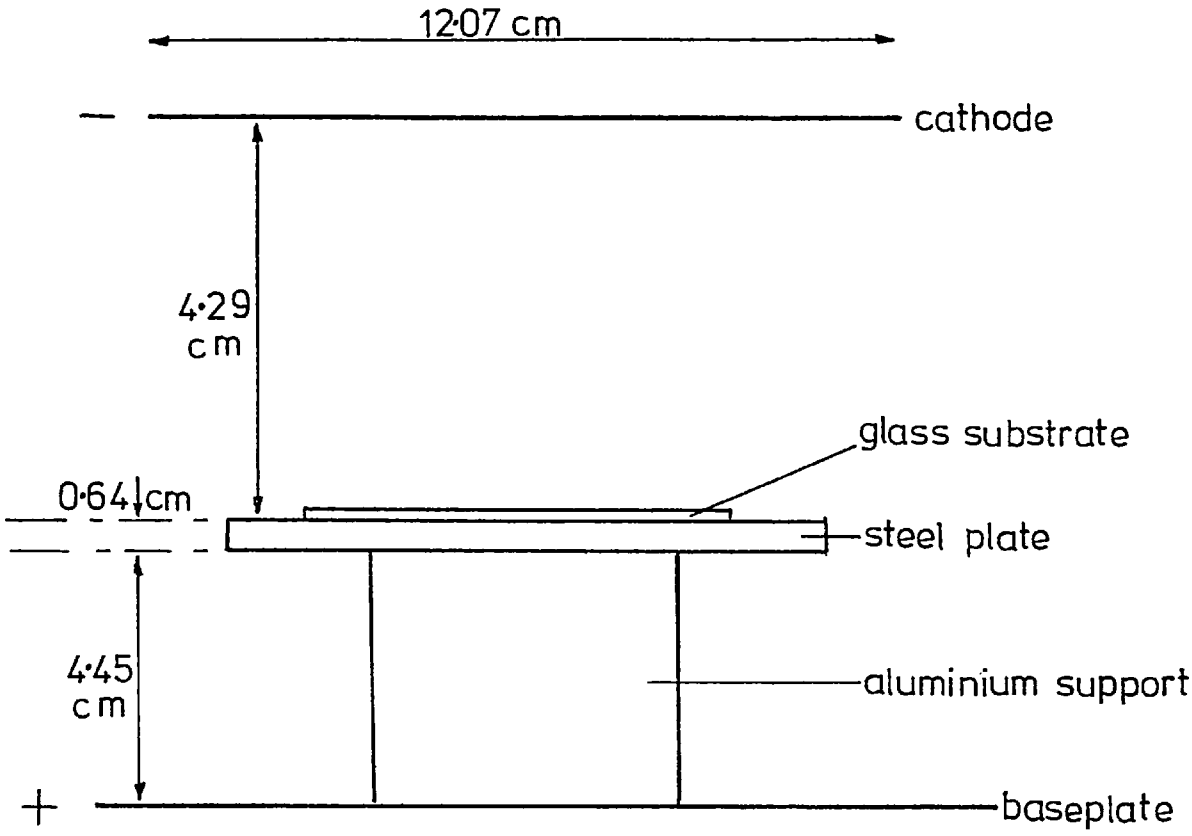

Figure 27. Furniture of the sputtering chamber used to produce preliminary cadmium oxide films.

composition of the film. Preston has determined the charge carriers in these films to be N type suggesting that a slight excess of cadmium ions is necessary for conduction, although chemical analysis of these films carried out by him indicates that less than 2% excess cadmium is necessary.

As Preston points out, the proposal of this conduction mechanism is entirely consistent with the experimental observation that cadmium oxide films sputtered in pure oxygen have low conductivity, as they would be highly oxidised.

In order to assess this type of film for our application a vacuum system was arranged for sputtering. The cathode was formed by evaporating cadmium on to a copper disc about $4\frac{3}{4}$ inches in diameter. This was placed at the top of the sputtering chamber as shown in Fig. 27. The glass substrate to be coated was placed (after cleaning with potassium hydroxide solution, distilled water and alcohol) on a steel plate supported by an aluminium block. The metal substrate supports were intended as a heat sink for the glass plate, but also acted as part of the anode being electrically at ground potential. The cathode potential was -3 KV.

Several plates were coated in this arrangement using various atmospheres. These were produced by bleeding oxygen-free nitrogen (OFN) in various ratios with oxygen into the chamber while pumping continuously in order to maintain a constant pressure. The proportions of oxygen were in all cases low (around $\frac{1}{100}$ of the OFN quantity), and in one case no oxygen was admitted, nitrogen alone being used. The chamber was pumped down to a pressure of

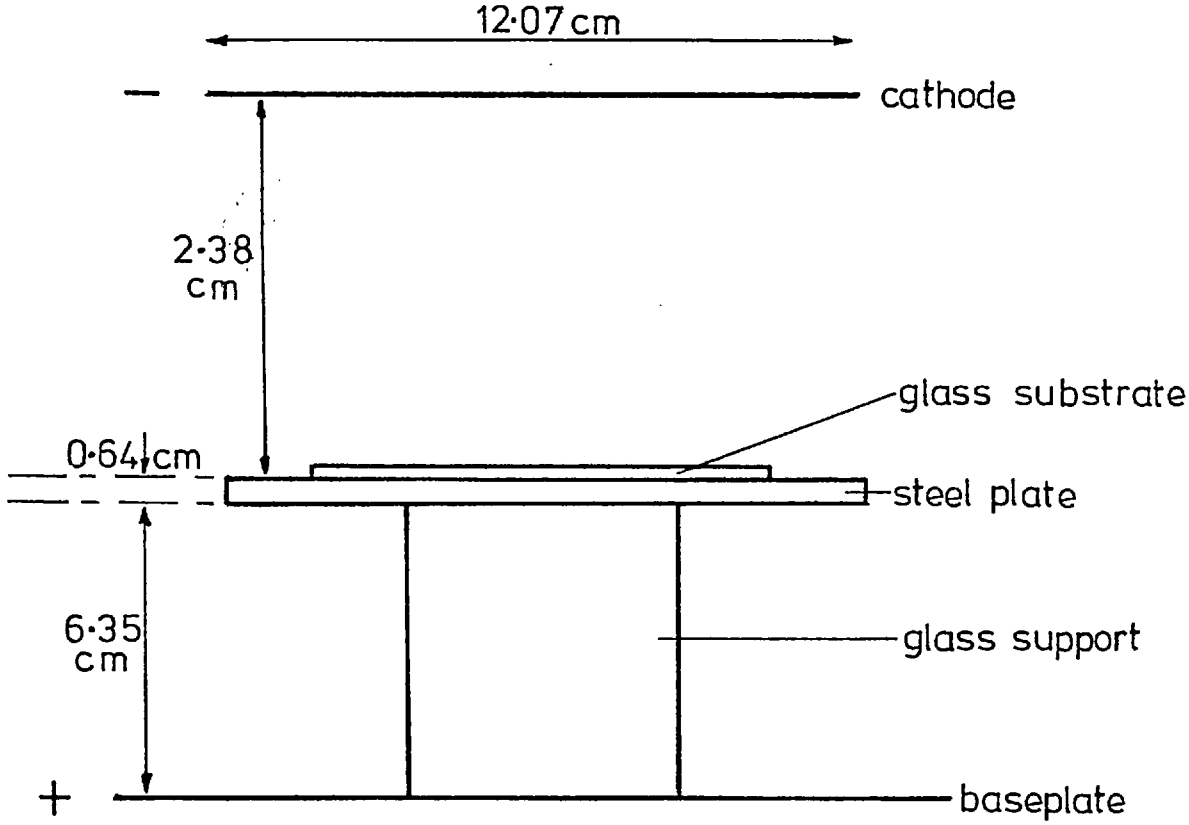

Figure 28. Modified furniture for sputtering chamber.

2×10^{-5} torr before each sputtering run, in an attempt to ensure that only the bled-in gas was present during sputtering, pressures of the bled-in gas being just above 10^{-2} torr for the sputtering operation.

To summarise the results of these attempts, in all cases some sputtered film was found. It could be detected as a faint brown colouration when a sheet of white paper was placed under the glass substrate, and by the squeaking made by a steel pin drawn across its surface, the glass side yielding no sound. Also, all the films were to some extent conductive. The first plate was sputtered for 5 minutes and exhibited a resistivity around 800 KΩ per square. It had a rather non-uniform coating, judging by the distribution of the brown colouration and this was attributed to deformations of the electric field pattern in the discharge caused by the presence of the earthed metal supports close beneath the substrate surface. A more uniform field pattern was expected from an arrangement where the substrate was supported on an insulator between two plane electrodes. This was contrived by the use of a glass block as substrate support (Fig. 28). The steel heat sink was retained for convenience as it closely matched the substrate dimensions but it was now insulated from the anode and, if the surfaces of equipotential in the discharge could now be considered (to a practical approximation) to be planes parallel with the steel plate and the two electrodes, then this plate should have caused little disturbance to the field pattern.

Subsequent plates were coated in this arrangement, using rather longer sputtering times to obtain thicker

films. 15 minutes yielded coatings of about 5 KΩ per square but also the uniformity was much improved.

The substrate which was sputtered while bleeding only oxygen-free nitrogen into the chamber also displayed resistivity of this order: the presence of oxygen in the mixture admitted, at least in the proportions used here, seemed to be having no detectable effect on the conductivity of the films, either for the better or the worse. This was probably due to the presence of oxygen in the vacuum system from other sources in larger quantities than were being bled in deliberately. Possible sources would be leaks, the residual atmosphere remaining after the preparatory pump-down to 2×10^{-5} torr and gases adsorbed on the surfaces of the chamber walls and furniture.

Of these sources, the last is particularly likely to have an influence on the nature of the sputtered deposit as it includes oxygen adsorbed on the surface of the cathode and substrate. Cadmium ions leaving the cathode and arriving at the substrate would be particularly susceptible to oxidation by oxygen held in these surfaces (see, for example, Holland (9) page 458).

As a result of this observation oxygen was no longer bled into the chamber during sputtering in this work, nitrogen alone being used, and for oxidation of the sputtered cadmium reliance was placed upon residual oxygen in the vacuum system. It was not thought worth the effort to investigate the effect on the conductivity of the sputtered films of reducing the amount of oxygen in the system by stopping some of the remaining leaks (a laborious practical process) or using an even longer initial pump-

down (a significant pressure reduction below 2×10^{-5} torr could only have been achieved by lengthening the pump-down to many hours). Instead, it was recognised that the residual oxygen in the system must be accepted, and some study was made of the variation which could be brought about in its effect on film conductivity by altering the position of the substrate within the discharge. This parameter would be expected to act upon film conductivity by virtue of the change which it causes in the path length travelled by a sputtered ion through the sputtering atmosphere before reaching the substrate. A long path would increase the likelihood of oxidation of the ion by increasing the number of its collisions with gas atoms.

Before the investigation could be extended in this direction, however, some modifications to the sputtering plant were necessary.

7.2 Electrical and Mechanical Modifications to the Sputtering Plant

The vacuum equipment used up to now was suitable for initial trials only, as it was regularly used for other work, which required different chamber furniture and limited the amount of time available on it. Also, by this stage the cadmium on the copper cathode disc was beginning to wear thin, the copper showing through in some small areas. For these reasons, an arrangement was sought which would conveniently allow a longer study of the sputtering of cadmium oxide.

An elderly disused vacuum system was located and

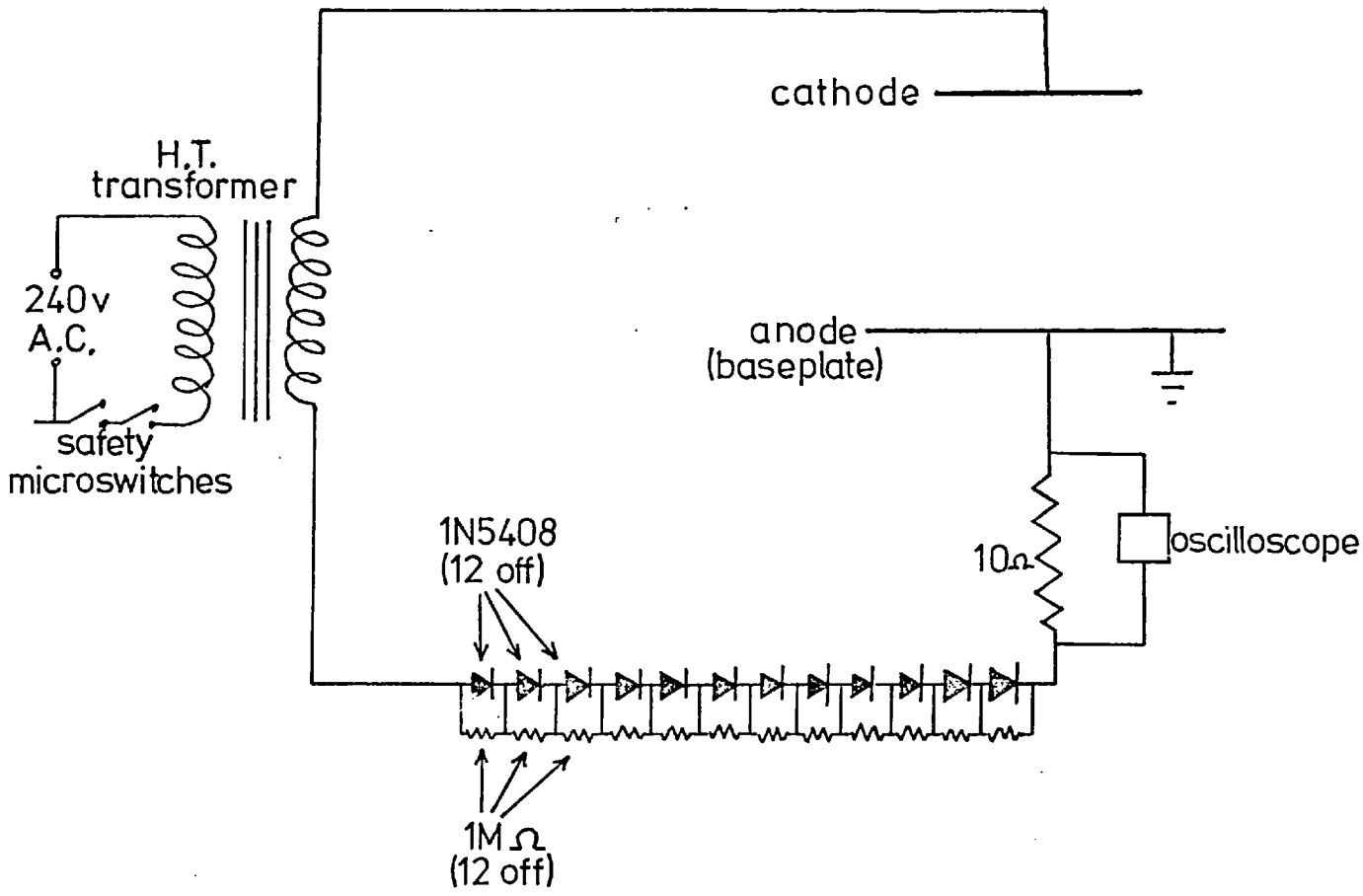

Figure 29. Diagram of the high tension circuit used for sputtering.

renovated for exclusive use on this project. On first examination this plant was found incapable even of producing a low enough pressure to permit any kind of high tension glow discharge. Although sputtering generally takes place at much higher pressures than are used for evaporation, the performance of this particular plant was not considered at all satisfactory.

The main troubles to be rectified were the presence of cracked insulators on the high tension lead-through terminals on the baseplate. Also, all 'O' rings in the system were replaced, both those sealing baseplate fittings and those in the pumping system. Valve diaphragms were replaced, oil was cleaned from the pipes and pumps and fresh oil was placed in the pumps.

After this, the plant behaved much better, achieving a pressure of around 10^{-5} torr within about 4 hours.

The high tension power supply in the plant also needed some modification. It was designed to produce an A.C. discharge for, say, the ionic cleaning of substrates prior to thin film evaporation. A voltage of about 5.6 KV R.M.S. was delivered by the supply off load, falling to 700 v. R.M.S. when producing a discharge in a partial vacuum with the electrodes supplied with the plant.

For sputtering a D.C. discharge is required so half wave rectification was arranged using twelve solid state diodes connected as in Fig. 29. The diodes used were type 1N5408 which can withstand a peak inverse voltage of 1000 v. each and a maximum forward current of 2.4 A. Twelve were needed as the greatest (i.e. open circuit) voltage which the transformer appeared capable of producing

was 8 KV peak (5.6 KV R.M.S.). A safety margin allowing the voltage to rise by a factor of 1.5 above its expected value was thus incorporated. A chain of 1 MΩ resistors was connected in parallel with the diodes to produce a small by-pass current during reverse half cycles of the voltage. This ensured that the inverse voltage was divided equally between the diodes. Otherwise the very high nominal reverse resistance of each of the diodes would have caused considerable uncertainty as to the proportions of the reverse voltage that would have appeared across each diode. In the event of highly unequal voltages, the diode carrying the largest reverse voltage could have been destroyed and its reverse resistance reduced to near zero. This would have put a greater reverse voltage across each of the others leading to the sequential destruction of each within a very short period. For these reasons the resistor chain and a fairly large voltage overload factor were thought highly desirable.

The 10Ω resistor and oscilloscope were included in the circuit during the early stages of the operation of this equipment to monitor the current waveform and measure the current in the discharge.

The primary coil of the H.T. transformer was supplied by a Variac variable ratio mains transformer to allow control of the current in the H.T. circuit.

After these modifications had been completed, two microswitch safety devices on the plant were repaired also. These were designed to disconnect the mains supply from the plant in the event of its front access panel being removed or the pressure in the vacuum chamber rising to near

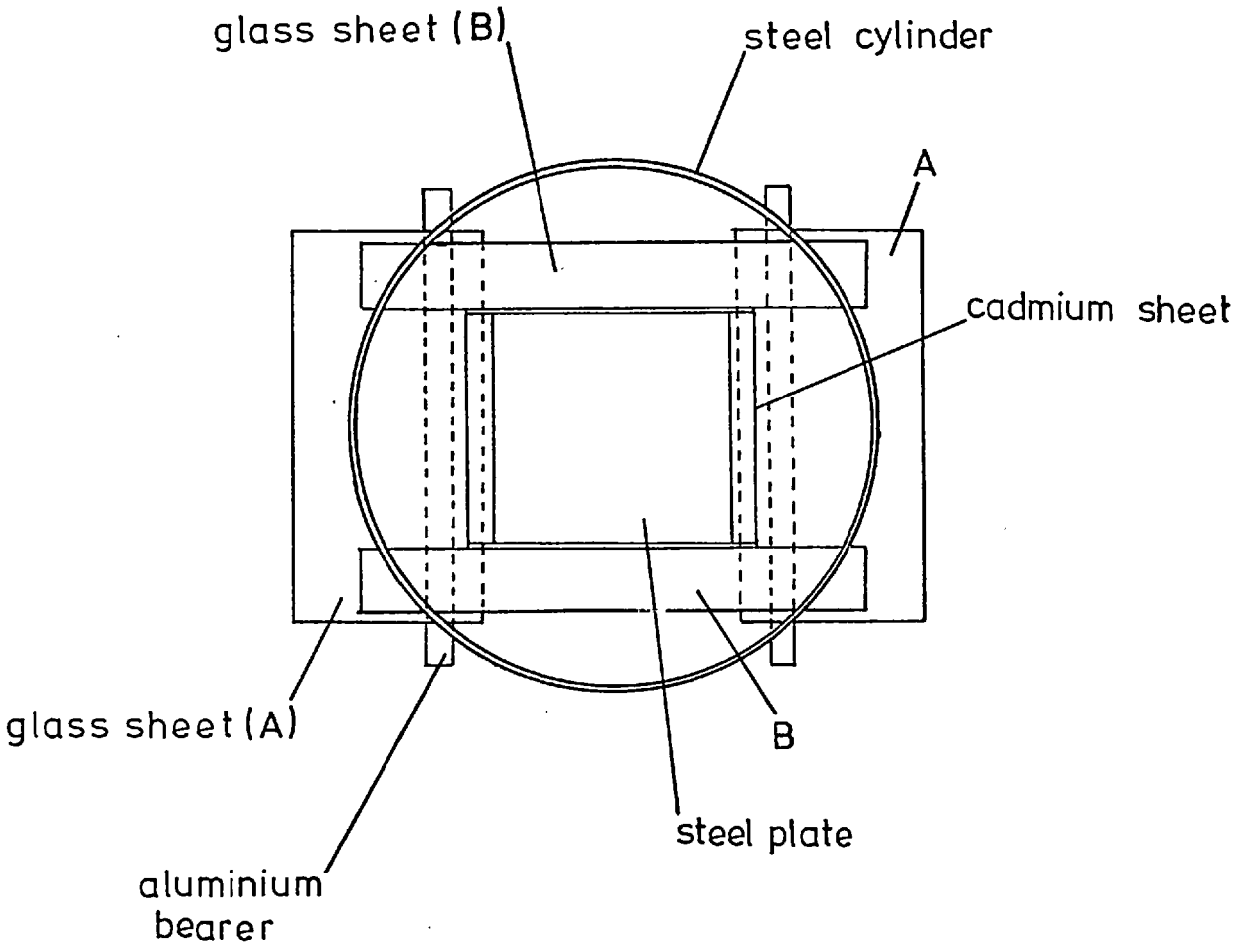

Figure 30. Diagram showing cathode details. Seen from above. Scale ½ real size.

atmospheric. The latter ensured there would be no high tension voltages on the chamber electrodes unless the bell jar was covering them.

These safety switches had either been deliberately disabled for convenience by previous operators, or had slipped so far out of adjustment through lack of maintenance that they would not operate until they were repaired at this time.

A cathode was constructed to the design shown in Fig.30. Two sheets of glass (marked A in Fig. 30) were laid on aluminium bearers and another two pieces of glass (marked B) were placed on top of these at right angles to the bearers. A sheet of cadmium (99.9999% purity, weight 10 grams, thickness 0.25 mm.) was placed on the sheets A, its edges being turned upwards where it met the sheets B. A steel plate was placed on the cadmium to act as an electrical contact and heat sink. The turned up edges of the cadmium sheet ensured that no part of the steel plate was visible from below the cathode. Electrical contact was made to the steel plate via a bolt, the head of which was on the bottom (cadmium sheet side) of the plate. The head was countersunk to give a flat surface on that side.

The aluminium bearers were supported by wires from a steel cylinder which stood on three steel legs. This cylinder and the legs were insulated from the baseplate to suppress strong discharges which would otherwise form between the cylinder and the steel heat sink.

Electrical connection was made to the bolt in the heat sink by H.T. cable of the type used in car ignition circuits.

From below the cathode the only metal part which was at

high potential and which was visible was the cadmium sheet. The only other parts visible from below were metal at a floating potential or glass.

The discharges attainable using this cathode in combination with the half wave rectified power supply consumed only up to a few milliamps (peak) which seemed rather low.

7.3 Summary of Results obtained with Modified Sputtering Plant

Preston (38) found that to produce conductive films using a little oxygen in argon it was necessary for the substrate to lie about 3 mm. outside the cathode dark space of the sputtering discharge. However, it was found in the present work with residual atmospheric oxygen mixed with oxygen-free nitrogen that the sputtered film would be virtually non conducting if the substrate lay outside the cathode dark space during sputtering. A point of agreement between our two experiences of sputtering conductive films of cadmium oxide was that it was much more accurate and yielded more repeatable results if the pressure in the chamber was monitored by observing the location of the lower (movable) edge of the cathode dark space than by using a pressure gauge.

The best results were obtained by adjusting the pressure so that the lower edge of the cathode dark space lay just below the substrate surface. If this edge lay above the surface a non conducting film was obtained. Also the lower it lay the smaller was the current in the

discharge, so that sputtering times were increased for a given film thickness and, for a given film conductivity.

The probable reason for the low conductivity of films sputtered on to substrates lying outside the cathode dark space is the increased oxidation suffered by cadmium ions in the higher pressure atmosphere as a result of the greater number of collisions between cadmium ions and oxygen atoms, causing the proportion of metallic cadmium in the sputtered film to be too low.

The decrease in film conductivity seemed quite abrupt as the edge of the dark space rose above the substrate, suggesting that a different oxidation mechanism was involved within the dark space from that acting in the adjacent glow region.

The cathode seemed to be too small to produce a uniform film on the substrates in use, which were 3¼ inches square. The sputtered material was thicker in the centre than at the edges, so enlargement of the cathode was necessary.

Sputtering times of about ½ hour using a current of 1 mA. peak (half wave rectified) produced a film of about 1000Ω per square which was a suitable resistivity. The sputtering time was rather long but this was not a serious matter as it could easily be shortened if necessary by changing to a full wave bridge rectifier so that sputtering would take place during both half cycles of the voltage waveform.

The greatest difficulty was the non uniformity of the film arising from the smallness of the cathode, although uniformity (in terms of resistivity) was now better than achieved earlier by the NESA process with tin oxide.

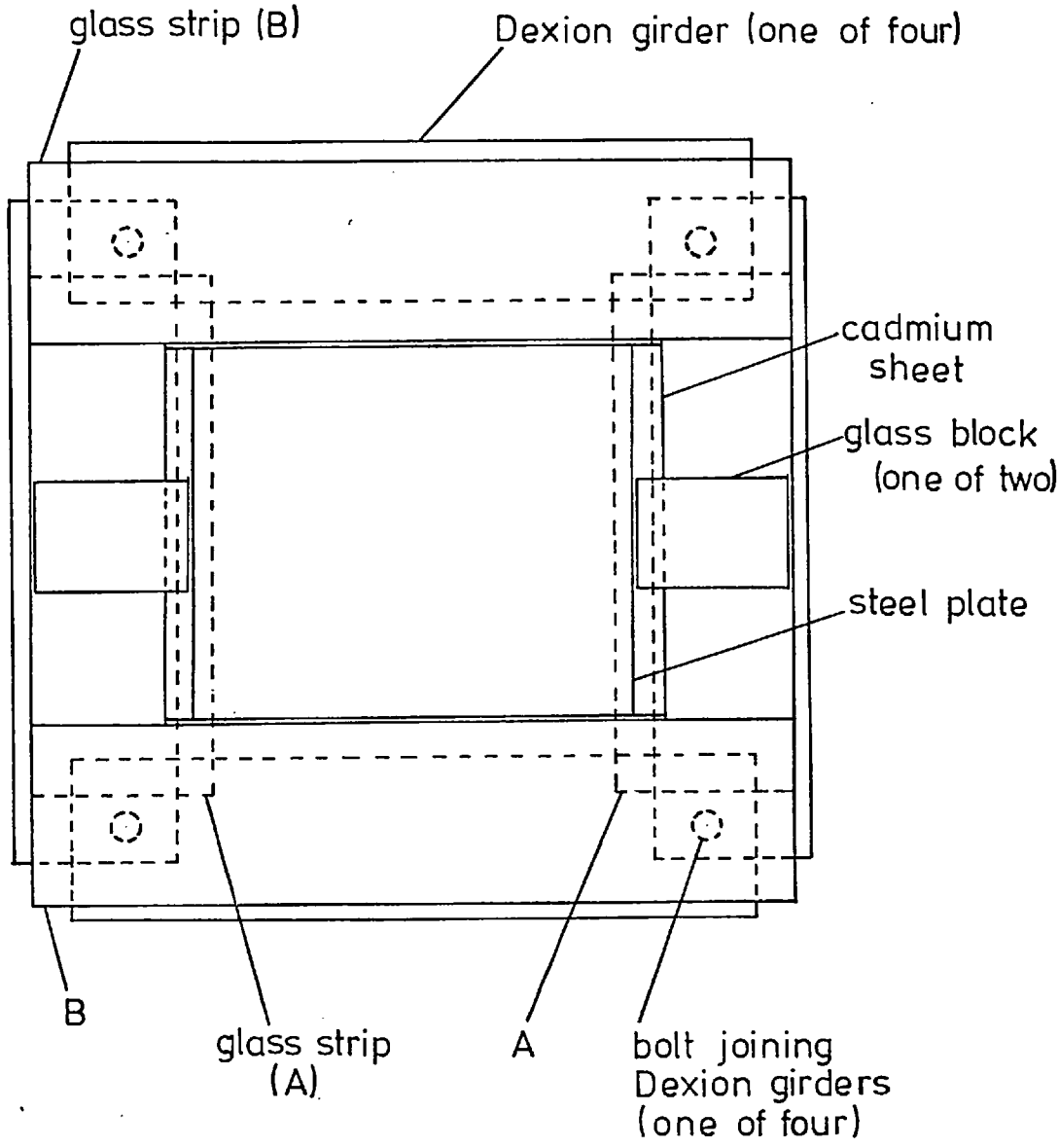

Figure 31. Diagram showing details of enlarged cathode. Seen from above. Scale ½ real size.

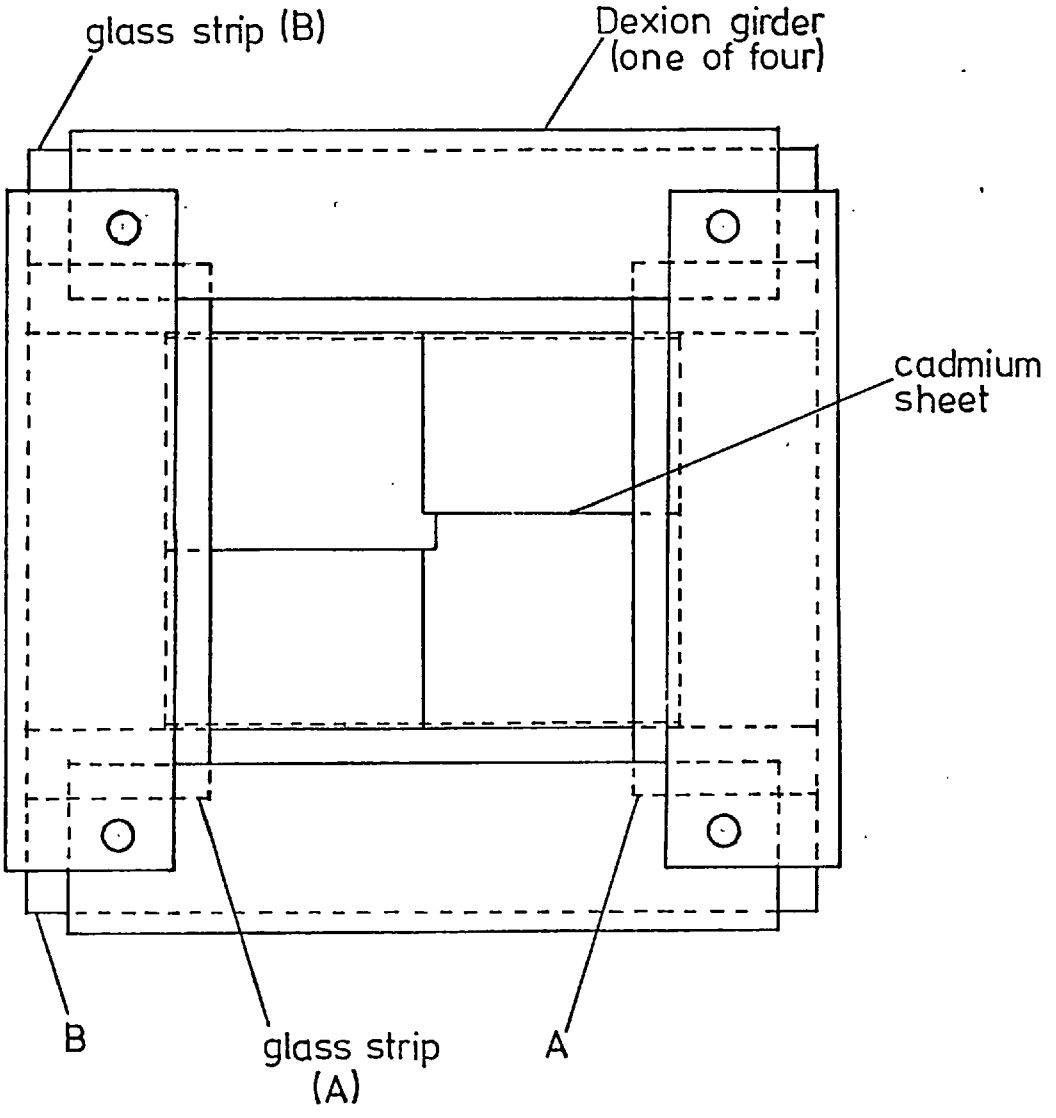

Figure 32. Diagram showing enlarged cathode construction. Seen from below. Scale ½ real size.

7.4 Construction of an Enlarged Cathode

For the construction of a larger cathode three more squares of cadmium sheet (10 gm. each) were joined to the existing sheet by folding their edges together and beating them gently with a small hammer.

A new support frame for the enlarged area of cadmium was built to the design shown in Figs. 31 & 32. The frame consisted of a "Dexion" steel surround on which were laid two strips of glass (marked A in Fig. 31). Across these were laid two similar strips of glass (marked B). The cadmium sheet was placed on the strips A, its edges being turned upward where it met the strips B so that the latter prevented lateral movement of the sheet in one direction.

A steel plate was placed upon the cadmium sheet to act as an electrical contact and heat sink. The weight of the steel was borne entirely by the strips A, so that the cadmium did not sag downwards and was trapped between the glass and the steel along two edges to hold it in place.

A glass block was placed on each of the strips A beside the steel plate to prevent movement of the plate. Had such movement been able to occur as a result, say, of vibration from the pump motor then the weight of the steel would no longer have been borne by the glass and the cadmium sheet, which is quite malleable, would have collapsed under the weight.

This arrangement formed a very suitable design. Only the steel plate and the cadmium sheet were connected to the power supply, the "Dexion" frame being at a floating potential. The steel plate was not exposed at all to the

substrate so that only cadmium would be sputtered on to the substrate. Also, although the glass and cadmium components and the steel plate were not clamped together in any way, they nevertheless interlocked so that the arrangement was quite stable mechanically, even under quite severe vibration, and there was no danger of high tension components falling out of place during sputtering through any foreseeable mechanical disturbance.

The cathode was supported on four glass legs so that the steel frame was not at the anode (earth) potential.

7.5 Initial Results from the Enlarged Cathode

Using the enlarged cathode it was quickly confirmed that the substrate surface should lie within the cathode dark space if the sputtered film was to be conductive.

With regard to uniformity of the film it seemed best for the substrate to be at 3 cm. from the cathode. If it lay closer the film was thinner at the centre than the edges and if it lay farther from the cathode it was thicker at the centre than the edges.

This is likely to be a result of two separate and opposing geometrical effects. As the distance between cathode and substrate is increased the cathode subtends a smaller angle at the substrate and it is to be expected that edge effects of the electric field will become more significant. The electric field will be weaker in the gas towards the edge of the cathode as the field lines are not parallel there so that the accelerating force on gas ions will be less, and material will be sputtered more slowly

from here. The substrate is not far enough from the cathode for the latter to act as a point source of sputtered material so some correspondence may be expected between the rates of sputtering from various parts of the cathode and the distribution of the sputtered deposit on the substrate.

However, if the substrate is placed too close to the cathode then most of the ions produced in the discharge are not liberated in the space between cathode and substrate. For these ions to reach the cathode and sputter its material it is necessary for them to pass through the now rather small gap between cathode and substrate and it is more likely that they will be attracted to the edges of the cathode than that they will penetrate to its centre. This would account for the lower thickness of the central area of the sputtered film in comparison with its edges when the substrate is close to the cathode.

Probably, these two mechanisms operate, and do so in opposition so that the distance of 3 cm. from substrate to cathode represents the situation where the mechanisms balance out to give a uniform film over most of the substrate.

If the current in the discharge was allowed to rise too high the uniformity of the film again decreased, the fall off in thickness towards the edges becoming more noticeable. Also, patches of discoloured, cracked and non conducting film appeared around the edges of the substrate. This was probably the phenomenon known as "frosting" (which has no connection with thermoplastic Frosting except in name) which can be due (39) to sputtering with the substrate surface inside the cathode dark space, or to water vapour

or gases occluded in the sputtered film.

Remedies for this are said (39) to be arranging the substrate to be outside the cathode dark space or using lower discharge currents. The first of these was not available as a solution, as it led to non conductive films, so the second alone was adopted. Discharge currents were kept to around 2 mA. peak.

In sputtering times of about 30 minutes, film resistivities of about 1000Ω per square were obtained.

The technique developed above gave films which had good uniformity of optical absorption and of temperature when used as a heating layer. This method of producing the conductive film was used for the work from this stage onward, until the usefulness of thermoplastic holography in the present application had been better established, after which conductively coated glass was bought from commercial suppliers.

7.6 Establishment of a Satisfactory Technique for Organic Film Coating

As mentioned in Section 5.2, the technique used by previous workers for controlling the thickness of the organic photoconductor and thermoplastic films was to vary the speed of withdrawal of the substrate during the dip coating. However, in the present work this was not found to produce usefully large variations in film thickness. Most probably, this technique would succeed only if a wide range of withdrawal speeds could be arranged, wider indeed than that available in practice by changing the sleeve

diameter on the final drive from the gearbox of the synchronous electric motor presently in use.

Rather than investigating means of varying the speed more widely it seemed simpler and probably cheaper to see whether the organic film thicknesses could be modified at will by changing the concentrations of the solutions. This would in any case be a useful parameter over which to have control, as natural evaporation of solvents from storage containers would certainly cause slow changes in solution concentration and would probably lead to increasing film thicknesses unless the correct concentration was deliberately restored.

The withdrawal speed was standardised at 8 cm. per min. for both solutions. Collier (34) used speeds of 7.5 cm. per min. and 3.25 cm. per min. for the photoconductor and thermoplastic respectively.

Solution concentration was found to give sensitive control over the thickness of the resulting films. For example, a change in the concentration of the thermoplastic solution from 0.25 gm. of resin per cc. of naphtha to 0.10 gm. per cc. caused the thermoplastic film thickness to change from 1 μm. to 0.25 μm. As before, the film thicknesses were measured by examining a scratch in the film through the Linnik interference microscope. Similarly sensitive control was available over the photoconductor film, it requiring even smaller changes in concentration to produce a given change in photoconductor film thickness.

Conversely, this sensitivity of film thickness to solution concentration indicates that the effects of

solution evaporation during storage on film thickness will be considerable.

As mentioned earlier (Section 4.3) other workers have found that if the photoconductor film was drawn in conditions of fairly high humidity then the film would often become opaque as it dried. This problem had occurred during the present work also, and at this time was confronted. It had been previously noted (ref. 30) that humidity was a factor affecting it and that some photoconductor solvents seemed more susceptible than others, but little discussion of the mechanism involved appears in the literature.

From observing the onset of opacity in these films, it appears that this occurs only if condensation also forms on the plate. The condensation is caused by the lowering of the temperature of the plate below the dew point as a result of the evaporation of solvent while the film dries. This is consistent with the observation that humidity plays a rôle, as that affects the dew point temperature, and consistent with the variation in the effect caused by changing the solvent, as these evaporate at different rates and cause various rates of cooling.

The simplest means of avoiding the trouble was to warm the substrate gently over a hotplate while the film dried to prevent its temperature falling. This was completely effective providing there was no delay after drawing the film before reaching the hotplate, and this technique was used in the production of all further thermoplastic plates.

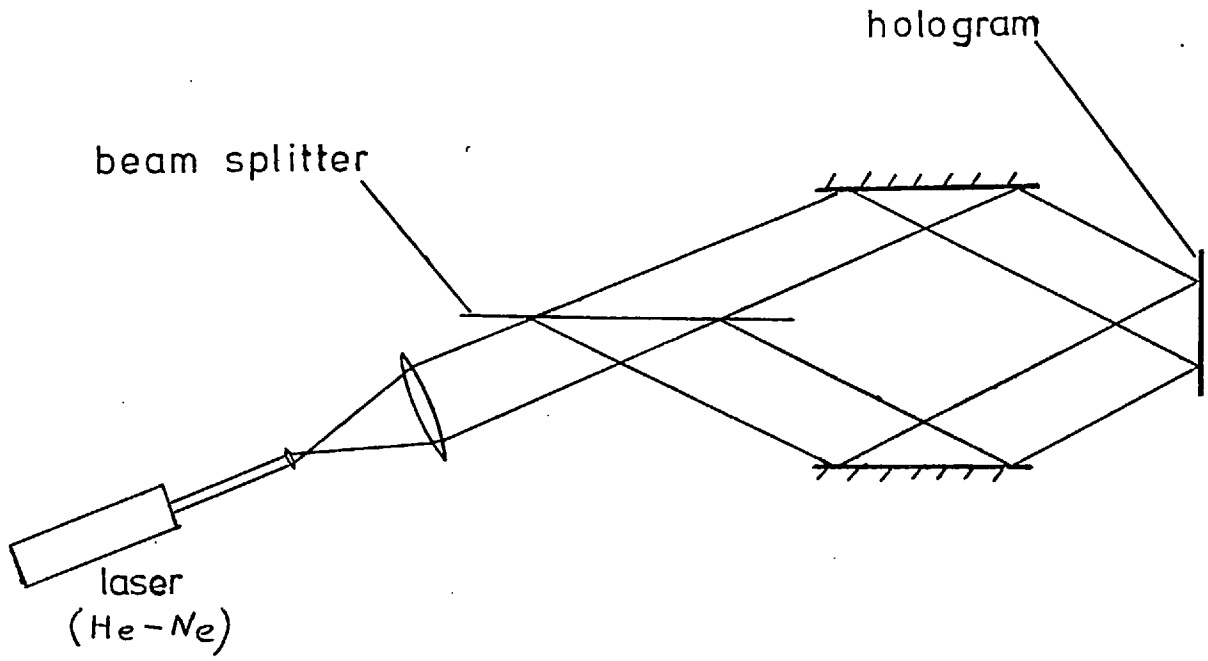

Figure 33. Arrangement used for recording holographic gratings of uniform spatial frequency.

7.7 Response of Recording Plates as a Function of Spatial Frequency

A particular reason for needing control of the film thicknesses, is that, in the case of the thermoplastic film, there is a strong dependence of the spatial frequency of maximum holographic response of the material upon thickness.

Consequently, a series of trials was now made to determine the behaviour of our recording plates in this respect and to see whether the organic films were of sufficiently consistent thickness to give reproducible results in holography. A summary of this work can be found in reference 40.

The behaviour of a holographic recording plate when recording a non-periodic wavefront such as generally exists in the Fourier plane during a spatial filtering operation is likely to be rather different from that when it is recording a wavefront of sinusoidal amplitude such as is used in the formation of holographic gratings. This is especially true where the recording mechanism, as at present, involves a chain of physical events of different characters, because of the large number of parameters involved and their interrelation.

Nevertheless, it is only by making some simplifying assumptions that practical results can be achieved in such situations so the response of the material to pure sinusoidal deformations was investigated a little.

Fig. 33 depicts the arrangement of optical components used here. It is similar to the equipment used earlier (Fig. 20) for the initial trials, but this time the beams

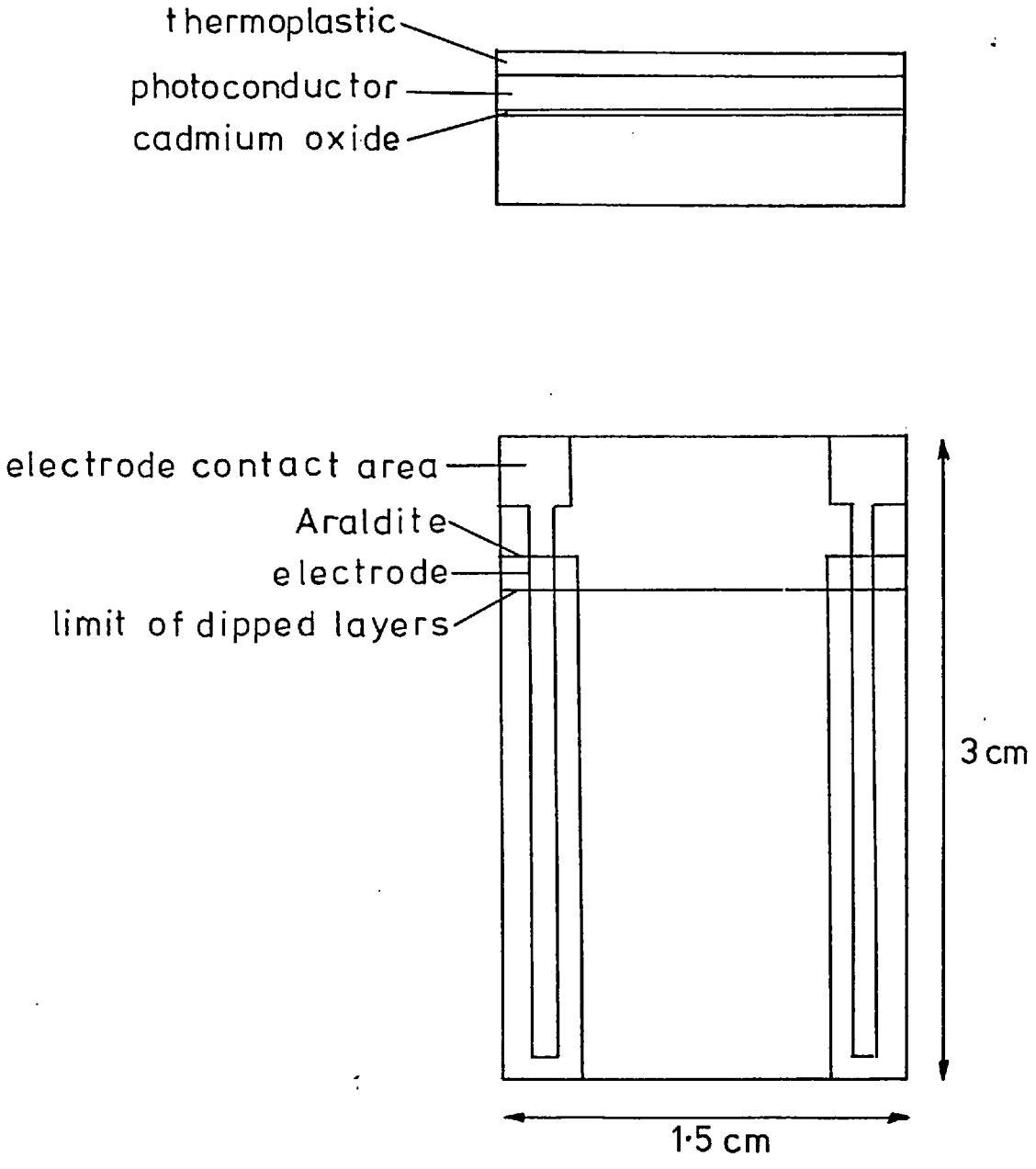

Figure 34. Details of thermoplastic plate.

arriving at the recording plate were collimated so that the spatial frequency of the interference fringes they formed was uniform.

A series of holographic gratings was then recorded. Three thermoplastic film thicknesses were used: 0.2μm., 0.3μm. and 0.4μm. For each of these, gratings were recorded for a range of spatial frequencies, the range chosen in each case being roughly centred on the frequency at which the material appeared to give the greatest response.

The substrates used here were smaller than those used so far, being 3 cm.$\times$1.5 cm. These were coated on one side with the reactively sputtered cadmium oxide conductive layer. Contact electrodes were formed on this layer by lines of paint drawn down each of the long sides of the substrate. The paint used this time (and for all future substrates) was DAG 915 produced by Acheson Colloids. This is a high conductivity silver paint, the resistance between the ends of a single electrode on the substrate being around 1Ω only.

The only disadvantage of this material is that it is instantly removed by the solvents used in the photoconductor solution. To protect it during the dipping process it was therefore covered with a layer of Araldite which, when hard, is scarcely affected by short periods of contact with dichloromethane.

In order to make electrical connections to the contact electrodes a small area of the paint was left uncovered at one end of the substrate, and this end was kept clear of the solution when dipping. The design of the substrate was, thus, as shown in Fig. 34, and the same design was used for

all further work until larger, more uniform substrates were needed.

The photoconductor layer was given a thickness of 2.5μm., the thickness being measured again with the Linnik microscope. The thermoplastic thickness was measured by noting the increase in thickness of the organic layer caused by dipping in the thermoplastic solution. In both cases the thickness was controlled by altering the solution concentration.

A single substrate was used for all the diffraction efficiency measurements made at each thermoplastic thickness, as variations in the resistivity of the conductive film between one substrate and another seemed to cause the recording plates to have different absolute maximum levels of diffraction efficiency. Generally, the films of lowest resistivity led to the highest diffraction efficiencies, but it was necessary to avoid any such variation if results were to be obtained in which the only significant variable was spatial frequency.

In order to avoid any change in the properties ("ageing") of the organic films arising from their being used many times, fresh films were coated on top of the same cadmium oxide layer for each of the measurements at a single thermoplastic thickness.

In order to avoid any ageing of the cadmium oxide film through its repeated use a fresh oxide film and substrate were used for each of the three sets of measurements at different thermoplastic thicknesses.

It seemed likely that the inorganic conductive (CdO) layer would age more slowly than the organic layers and this

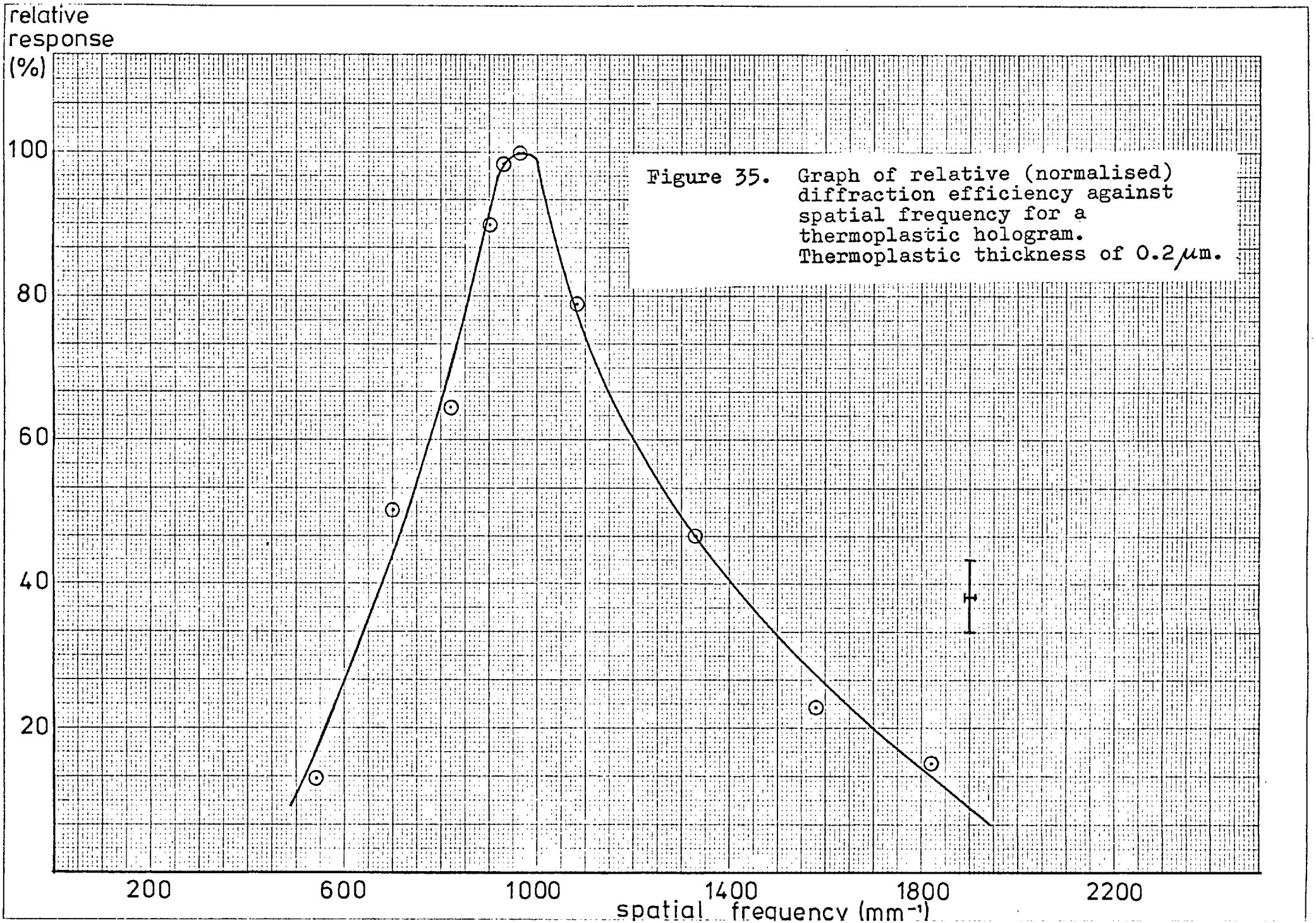

Figure 35. Graph of relative (normalised) diffraction efficiency against spatial frequency for a thermoplastic hologram. Thermoplastic thickness of 0.2μm.

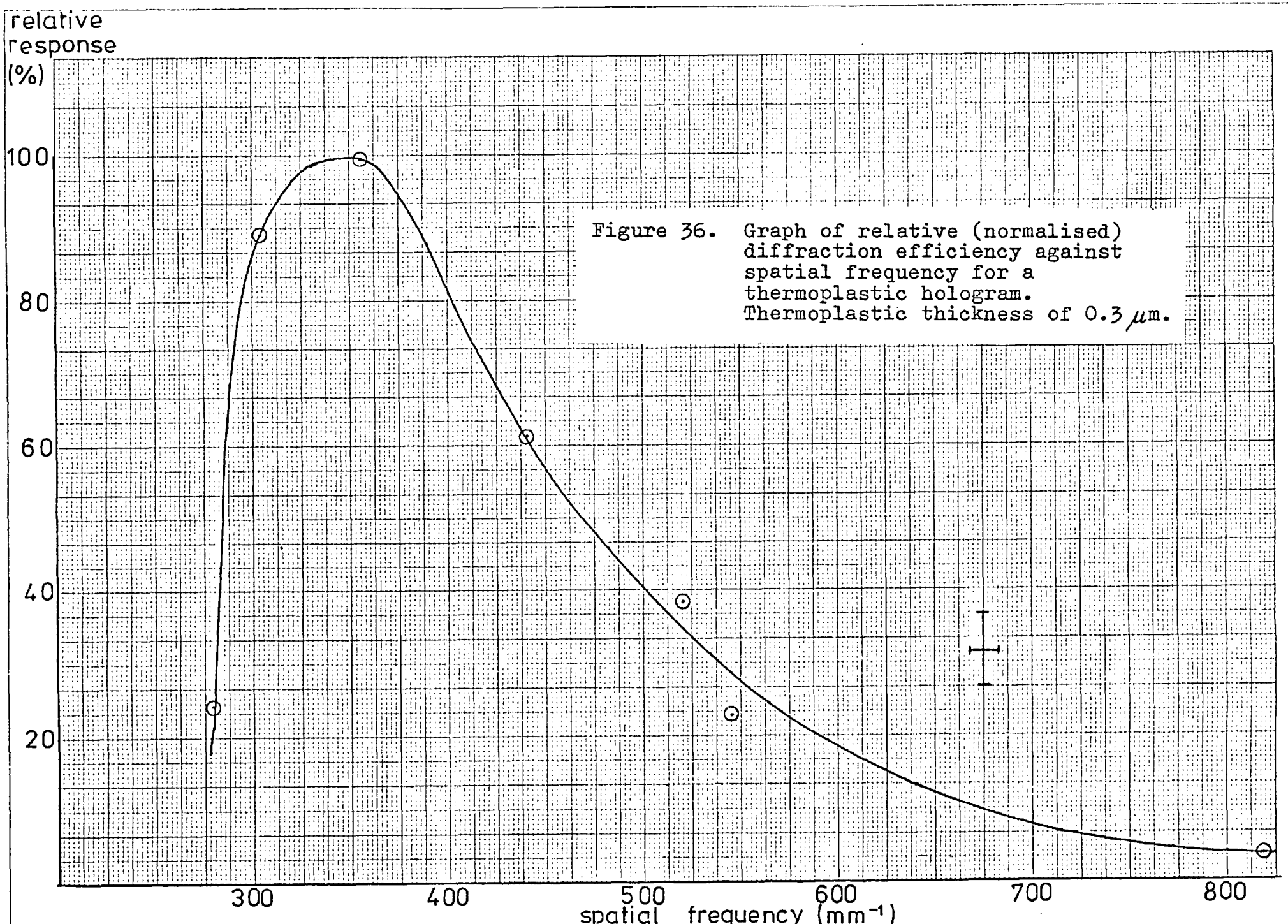

Figure 36. Graph of relative (normalised) diffraction efficiency against spatial frequency for a thermoplastic hologram. Thermoplastic thickness of 0.3 μm.

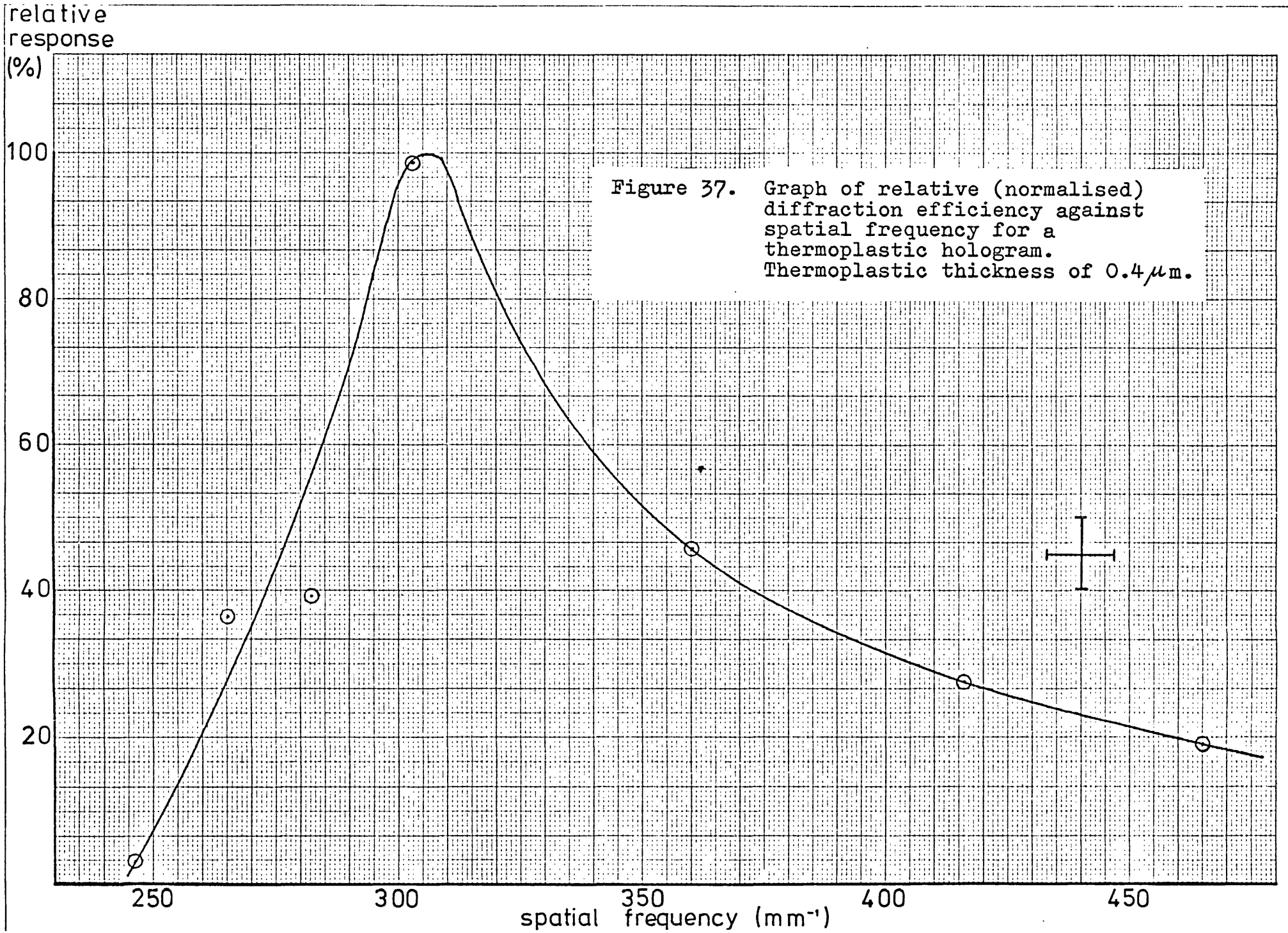

Figure 37. Graph of relative (normalised) diffraction efficiency against spatial frequency for a thermoplastic hologram. Thermoplastic thickness of 0.4μm.

was borne out by the observation that no detectable change in its resistivity occurred during repeated use. This enabled a single specimen of this film to be used for a number of measurements at a single thermoplastic thickness. Nevertheless, it was deemed prudent to change the conductive film after each of these sets of measurements had been completed in case ageing was taking place. The whole series of measurements occupied several weeks, and apart from any effect the dichloromethane may have on cadmium oxide films, it is known (9) that atmospheric humidity attacks these films eventually, as do finger marks.

Naturally, a change in the substrate and oxide layer between each of the three sets of measurements meant that, although the functional dependence of diffraction efficiency upon spatial frequency should be properly displayed by the resulting data, it would not be possible to compare absolute diffraction efficiencies between the different thermoplastic thicknesses at a single spatial frequency. Normalisation would permit the shapes of the curves to be compared but comparison of absolute magnitudes would be meaningless.

However, it was anticipated that spatial frequency variations at a single thickness would have a much greater effect on diffraction efficiency than would variations in film thickness at a single spatial frequency, so for practical purposes the investigation of the spatial frequency dependence was the more urgent requirement.

The results, shown in Figs. 35 to 37 take the form of normalised diffraction efficiency for the first diffraction orders only. These were obtained from photomultiplier measurements of the intensities incident on the grating

t	$\Delta\nu$ at 50% max	$\Delta\nu$ at 80% max	$\left\{\frac{\Delta\nu}{\nu_{max}}\right\}$ at 50% max	$\left\{\frac{\Delta\nu}{\nu_{max}}\right\}$ at 80% max
0.2 μm	570 mm^{-1}	210 mm^{-1}	0.58	0.22
0.3 μm	200 mm^{-1}	127 mm^{-1}	0.57	0.36
0.4 μm	60 mm^{-1}	28 mm^{-1}	0.20	0.09

Table 2. Comparison of widths ($\Delta\nu$) of the frequency response curves of thermoplastic holograms for three thicknesses (t) of the thermoplastic layer.

and diffracted into the first orders, for gratings recorded at different spatial frequencies (inter-beam angles). 632.8 n.m. wavelength was used. The corona charging device was operated at a distance of 2.2 cm. from the recording plate, the simultaneous recording mode being used.

The tendency, noted by other authors, for the peak of response to occur at lower spatial frequencies as the thermoplastic thickness is increased is clearly seen here. The peaks lie at about 975 mm^{-1}, 350 mm^{-1} and 305 mm^{-1} for the 0.2, 0.3 and 0.4 μm films respectively. These spatial frequencies corresponded to inter-beam angles of 35.9°, 12.7° and 11.1° respectively.

The location of the response peak is of primary practical importance to us as it tells us the thermoplastic thickness which is needed to obtain maximum holographic response in a given beam geometry. However, also of interest is the width of the response peak. as this gives an indication of the range of inter-beam angles that can be recorded on one plate.

Table 2 shows a comparison between the widths of the peaks of the three graphs. The widths, $\Delta\nu$ are given for each curve at 50% and 80% of peak response and their ratios to the frequency of maximum response (ν_{max}) are also given.

The values for $\frac{\Delta\nu}{\nu_{MAX}}$ suggest a similarity between the shapes of the curves for 0.2 and 0.3 μm thermoplastic films (0.58 and 0.57 at 50% response and 0.22 and 0.36 at 80% response). Both at 50% and 80%, however, the response peak for the 0.4 μm film seems narrower than for either of the two thinner films ($\frac{\Delta\nu}{\nu_{MAX}}$ = 0.20 and 0.09 respectively).

A least squares fit was attempted between the curves on

	Film thickness (t)		
	0.2 μm	0.3 μm	0.4 μm
Left of peak	log		log
Right of peak	exp	exp	power

Table 3. Comparison of the forms of curve approximating most closely to each side of the frequency response curves for three thermoplastic thicknesses (t).

each side of the response peak for each of the graphs. Fitting to an exponential ($y = a.e^{bx}$), a logarithmic ($y = a + b.\ln x$) and a power curve ($y = a.x^{b}$) was carried out for each side of the response peak in each case except one, the curve to the left of the peak for the 0.3μm film where too little data was available for even an attempt to be made.

The form of curve giving the best fit in each case is shown in Table 3. The amount of data available is very small for such an exercise and the results should be used cautiously, but again, as far as we can tell, the 0.2 and 0.3μm thermoplastic films show similar behaviour (at least to the right of the peak where both display exponential characteristics the most strongly) and the 0.4μm film seems to behave differently (following, rather, a power curve).

This analysis of the graphs is only rudimentary, owing to the small amount of data, but the tentative conclusion to be drawn from the peak widths and curve shapes is that some different physical process was at work in the recordings made with the thickest films from those operating when recording on the thinner ones.

Considerably more work along these lines would be necessary for these conclusions to be made firm.

More definitely, it was confirmed from repeated observations at this time that the first order diffracted light was brightest when it fell at the same distance from the zero order as did the annular ring of light diffracted by the Frost.

7.8 Response of Recording Plates as a Function of Development Temperature

To investigate the relationship between diffraction efficiency and development temperature a further series of measurements was carried out upon holographic gratings recorded on thermoplastic plates of the same design as used in the spatial frequency investigation (Section 7.7).

To measure the temperature of a hologram plate during the development of the image poses the practical problem of how to make good thermal contact between the hologram surface and, say, a thermocouple without damaging the organic layers on the plate. This is particularly true if one attempts to measure the temperature at the particular point on the plate which is to be used for the measurement of diffraction efficiency.

To avoid this difficulty the temperatures attained by each substrate slide over a range of electrical power dissipation were plotted before the organic films were applied. The temperatures were measured using a thermocouple attached to the plate by silicone grease.

Power dissipation was then used as the indicator of substrate temperature during development.

By this means fourteen substrates were calibrated and each was used to record a thermoplastic holographic grating. Various power dissipations and, hence, development temperatures were used for these, and the diffraction efficiencies they exhibited were again measured using a photomultiplier.

It was noted in Section 7.7 that substrates having

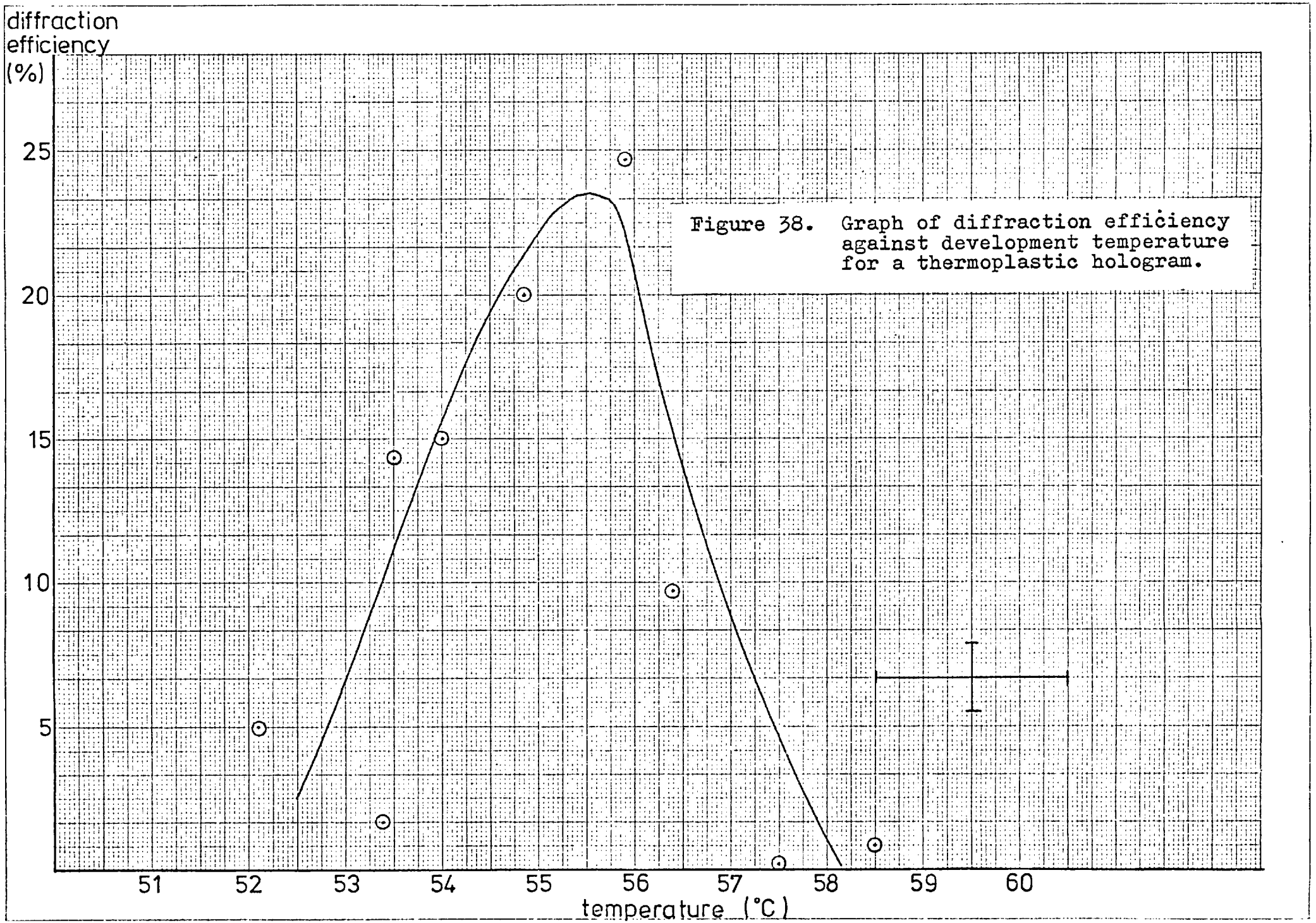

Figure 38. Graph of diffraction efficiency against development temperature for a thermoplastic hologram.

different resistivities of their conductive film displayed differing properties with regard to their maximum obtainable diffraction efficiencies. Although no explanation of this has been found it seemed that, before attempting to draw conclusions from the present data, some account should be taken of this observation.

Consequently, only the data obtained from substrates whose resistivities fell within a 10% band on each side of 400Ω per square (i.e. between 360 and 440Ω per square) were used. The figure of 400Ω per square was chosen as it was roughly central in the range of resistivities exhibited by the substrates. Thus, it was likely to be a figure readily reproduced in later substrates and it would permit the largest number of substrates of the present set to be used in forming conclusions.

The data selected by this method is displayed in Fig. 38. From this it appears that the highest diffraction efficiencies were obtained using development at a temperature of 55°C and that the temperature should be kept to within ±1°C of this for diffraction efficiencies above 15%.

The error bars on the graph indicate only the uncertainty in the temperature measurements. That the curve does not cut each of the error bars arises from the drifting of parameters other than temperature, concerned with, for example, corona charging and organic film thicknesses, even though these were held as constant as possible.

7.9 Towards a More Practical Determination of Development Temperature

Although the results of Section 7.8 give us some insight into the behaviour of these plates with respect to development temperature, the information is not in a form particularly suitable for mundane use in the recording of thermoplastic holograms on a routine basis. To be able to use electrical power dissipation as a means of measuring temperature is a step in the right direction as the former is much the more accessible parameter, but experience with the thermoplastic plates reveals that there is another parameter which is even more suitable in practice.

If a thermoplastic plate is raised to a temperature which is just too high for any recording to be made and is allowed to cool very slowly through the vicinity of 55°C by gradually decreasing the heater current whilst it is being charged and exposed to the holographic pattern, then the heater voltage value at which Frost just begins to appear in the thermoplastic film can be sensitively determined. It seems that the highest temperature at which the Frost just appears, under these conditions is also that which gives the holographic recording its greatest diffraction efficiency.

On the first occasion that a particular substrate is used, the hologram can be recorded by allowing the plate to cool slowly until the onset of Frost. If the voltage is noted at this point then, after recoating the substrate with fresh organic films, further recordings can be made by setting the heater voltage to that value, allowing two minutes for the temperature to stabilise, and then

proceeding with the corona charging.

The use of the Frost-onset voltage as an indicator of temperature is convenient in use as it requires no procedure other than those normally carried out in recording holograms, merely an additional observation. Also, unlike the use of electrical power dissipation as an indicator of temperature, the Frost-onset voltage is even more directly associated with the hologram recording properties of the thermoplastic film than is the temperature of the film. For example, unwanted fluctuations in parameters such as the thickness and composition of the organic films and changes in humidity and ambient temperature which may affect the corona charging should not have such a severe effect upon the final diffraction efficiency of the hologram if Frost onset is used for the development criterion as they would if temperature measurements or power dissipation is used.

CHAPTER 8

THE PRACTICAL ASPECT OF HOLOGRAPHIC (VANDER LUGT) FILTERING

8.1 An Introduction to some Practical Problems in Holographic Filtering

By this stage it was to be hoped that, having produced a practical thermoplastic hologram plate, problems regarding the accurate repositioning of the holographic filter during Vander Lugt filtering would no longer exist, because of the in situ processing which these plates allow.

However, there remains one particular difficulty which is often encountered in this type of filtering. This concerns the very high range of intensities present in the Fourier transform plane during optical spatial filtering when normal photographic images are used as the input data. For example, Keyte (41) has considered the limitations imposed upon holographic filtering by the inability of photographic emulsions linearly to record the large range of amplitudes present in the Fourier plane.

Actually, Keyte distinguishes between effects arising from the limited dynamic recording range and those arising from the deviations from linearity of the available dynamic range. Although this may appear an arbitrary distinction, the first case simply being an extreme example of the second, it is nevertheless a useful viewpoint as it corresponds with a particular simplification of the photographic curves of amplitude transmission against exposure which is convenient when using computer simulation to explore the consequences

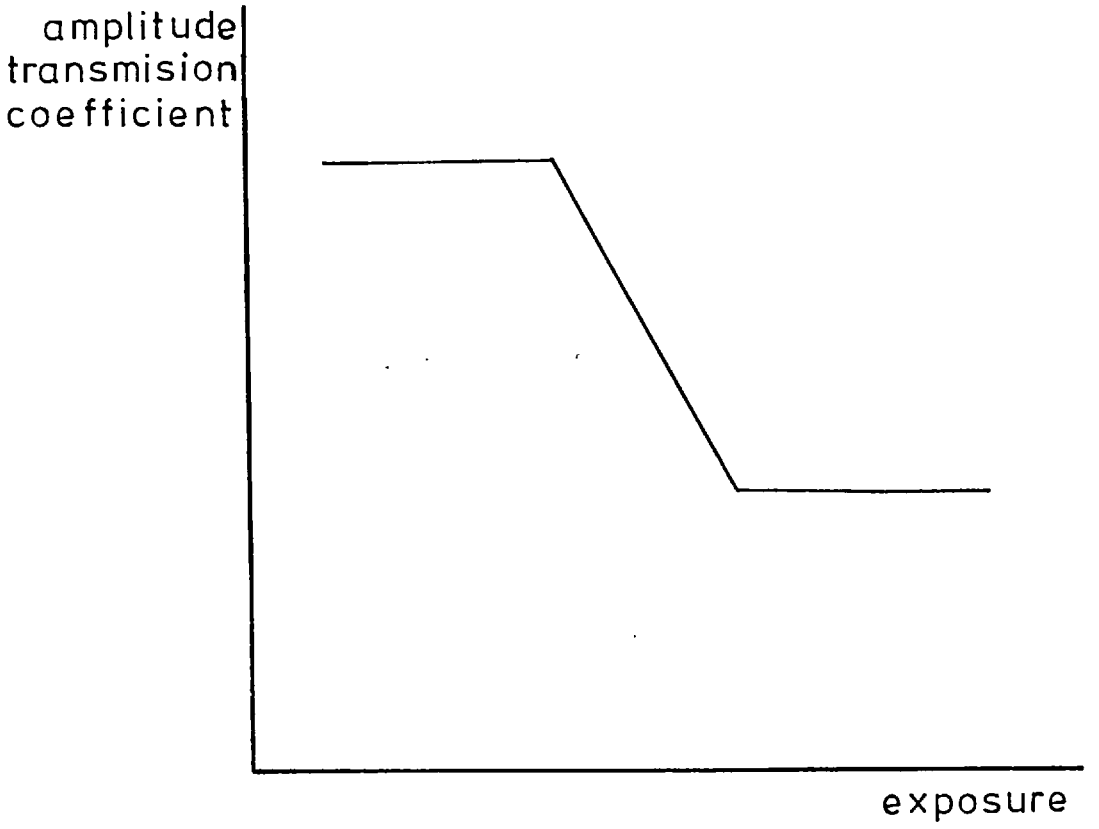

Figure 39. Simplified form of exposure characteristic for a photographic material.

of these photographic limitations upon holographic filter response. This simplification is to assume that the curve can be approximated by three straight lines (Fig.39). It presumes that the consequences of non-linearities within the usable exposure range are negligible compared with those arising from the severe non-linearities (amounting, virtually, to its truncation) at the ends of this range.

The principal result of these deviations of the filter recording material from the ideal is likely to be some degree of high pass spatial filtering of the image information whose transform is recorded on the filter hologram (42). This arises from the failure of the hologram to record the very bright central area of the optical Fourier transform.

This effect, in connection with photographic emulsions, is described, for example, by Collier et al (ref.34 p405).

They point out that with an absorption hologram formed in the Fourier plane the central area, corresponding to the lowest spatial frequencies, will normally be overexposed to the extent that it becomes highly absorbing and the holographic fringes recorded there will have very low modulation.

With a phase hologram such as the thermoplastic kind, although the central area will not become absorbing, it will probably nevertheless have very low modulation and diffraction efficiency because of the saturation of the recording mechanism here by the high intensity levels.

In practice, there will not be a sharp cut-off frequency below which no information is recorded in the Fourier plane, but rather a progressive decrease in the

holographic response of the recording material towards the low frequency (central) region of the Fourier plane. A special case of this effect, suppression of the spatial frequencies according to a parabolic radial function in the Fourier plane, would lead (ref.34 p.406) to differentiation, spatially, of the input data. The image reconstructed from such a Fourier transform hologram would show the derivative of the original object transparency.

The effects of this inadvertent high-pass spatial filtering are likely to be apparent mostly when the object plane contains relatively large areas of uniform tone. Only the higher frequency components of such areas will tend to be recorded on the holographic filter so that a reconstruction of the image from such a filter hologram would show only the edges of the areas. An attempt at autocorrelating such an area would, in fact, yield the cross correlation between the original scene and the high pass filtered version of it, if such a filter were used in Vander Lugt filtering.

Several methods have been used to overcome the difficulty of the high intensity range in the Fourier plane. For example, the ratio of reference to object beam intensities can be made very high. The central bright part of the Fourier transform can then be recorded linearly. However, the higher frequencies, containing information about shapes and detailed structures in the object transparency will be so weak as to be completely immersed in noise, and lost. This is likely to be troublesome in, say, the recognition of shapes by cross correlation.

Another way of meeting the problem is to displace the hologram slightly from the Fourier plane, towards or away from the transform lens. As this is done the central peak in the light intensity distribution falling on the hologram plate broadens and becomes diffuse quite rapidly so that the range of intensities to be recorded is lower. The hologram need not be moved very far and for some purposes this may be satisfactory, but if it is required accurately to locate in the object transparency a structure whose impulse response is seen in the correlation plane of the filter, then it is necessary to assume that there is good correspondence between displacements in the object and correlation planes. The level of confidence in this assumption will be low if the filter hologram is not recorded as closely as possible to the Fourier plane.

In addition to modifications to the filter hologram recording arrangements it is possible in some cases to make the original data more suitable for presentation to a filter recording material of limited dynamic range. For example, if the original transparency contains large transparent areas and little opaque area than photographic reversal of the tones will reduce the amount of light reaching the centre of the Fourier plane in comparison with that reaching the outer areas. For this reason, whenever the recognition of alphanumeric characters is being attempted the character set comprises transparent letters upon an opaque background, rather than the converse. The characters themselves occupy far less of the area of the input scene than does the background, so the use of an opaque background greatly reduces the amount of light reaching the low spatial

frequency areas of the Fourier plane, (see ref. 42 for example).

This procedure can be useful for binary input data, containing only black and white areas, but where the original transparency is a continuous tone photograph, say an aerial or satellite photograph of the Earth's surface, the areas of light and dark tone are roughly equal and little, if any, reduction in the intensity of the transmitted low frequency components can be achieved by tone reversal.

A further method which may be considered for improving the ratio of high frequency to low frequency intensities is to combine the object transparency with a diffuser, say a ground glass screen. This has the effect of breaking up large uniform areas of the transparency into fine detail. Phase modulations rather than amplitude ones are being used to do this, but the effect is the same: light which would otherwise have contributed to the bright central area of the Fourier plane is scattered into outlying regions.

A disadvantage of using this technique is that the autocorrelation of the transparency will be considerably modified by the autocorrelation of the diffusing screen. Correlations between areas which in the original transparency were uniform would be much more strongly peaked in the centre when the diffuser is present.

8.2 The Power Spectra of Continuous Tone Photographic Data

In order to assess the size of the problem involved in attempting linearly to record the Fourier transform of a

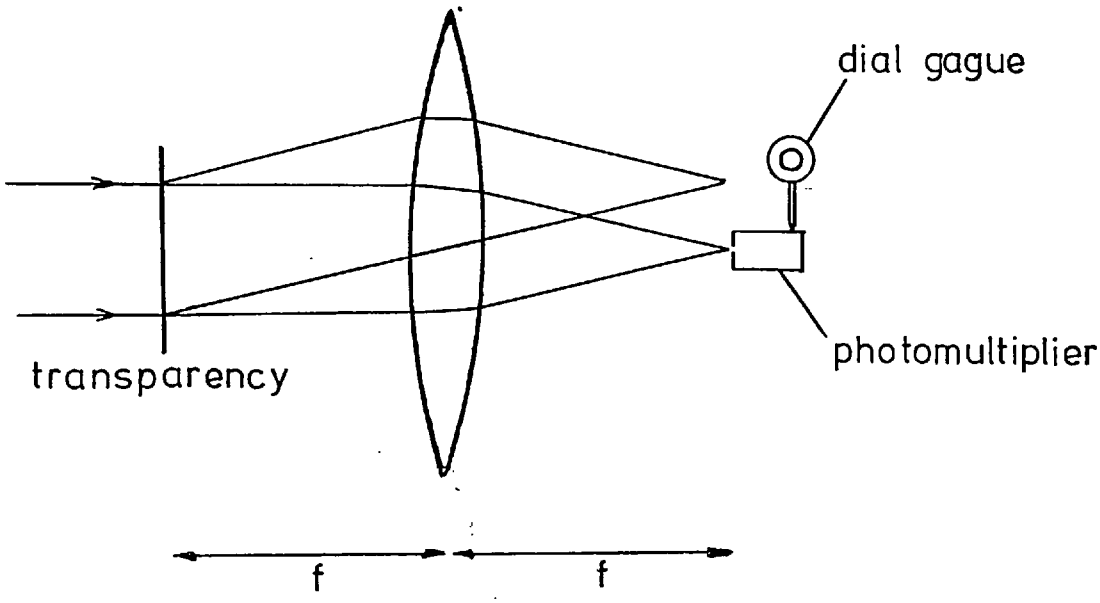

Figure 40. Arrangement for investigating the power spectrum of a transparency.

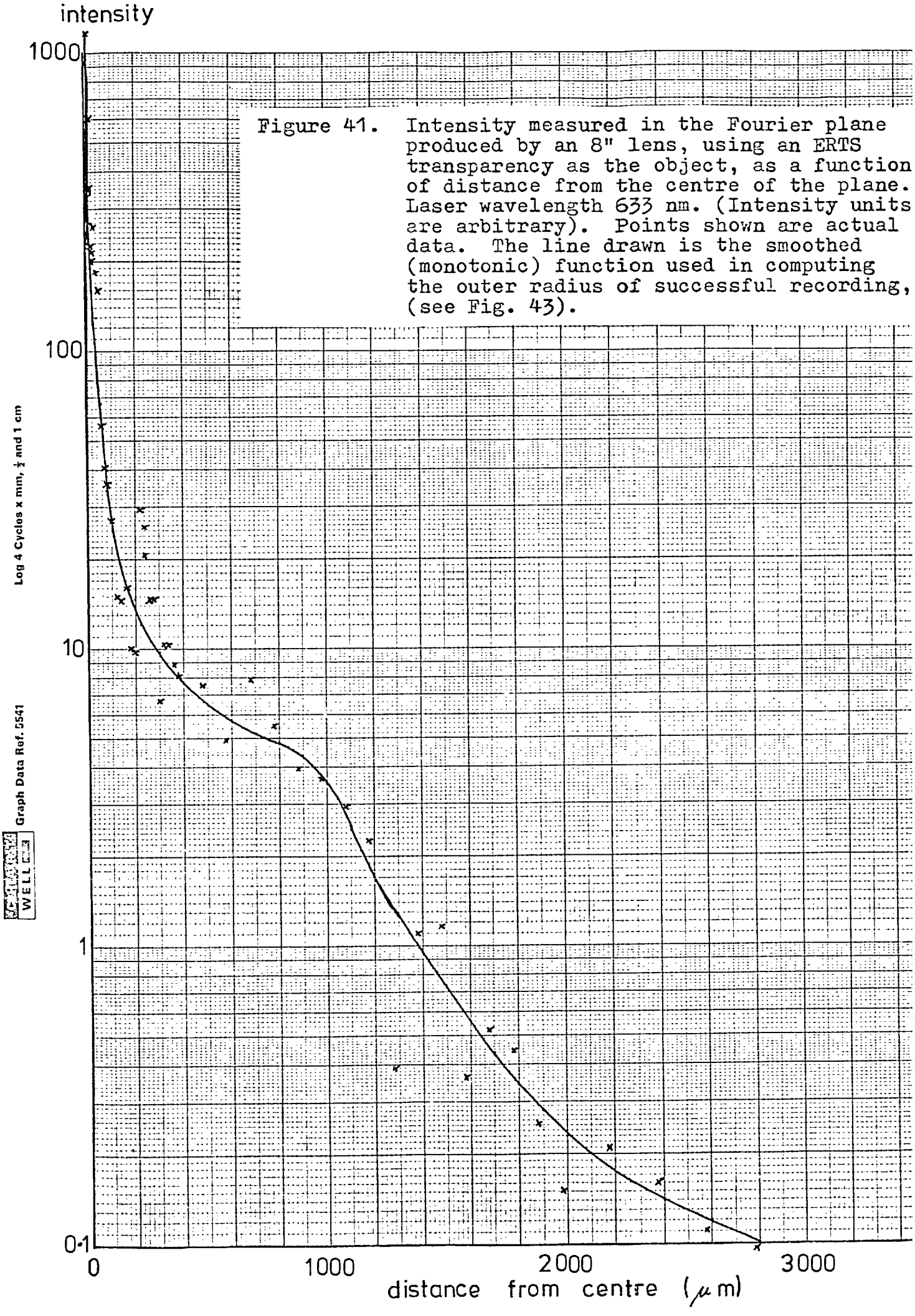

Figure 41. Intensity measured in the Fourier plane produced by an 8" lens, using an ERTS transparency as the object, as a function of distance from the centre of the plane. Laser wavelength 633 nm. (Intensity units are arbitrary). Points shown are actual data. The line drawn is the smoothed (monotonic) function used in computing the outer radius of successful recording, (see Fig. 43).

continuous tone photograph on a holographic plate, preparatory to carrying out correlation operations, some measurements were made of the intensity profiles likely to be encountered. This was done using an ERTS satellite transparency showing an area of Scotland involving a mountainous region, but broadly similar intensity profiles were observed with other frames of ERTS imagery.

The Fourier transformation was performed by an 8 inch focal length Dallmeyer Serrac lens.

The intensity was measured (Fig. 40) by a photomultiplier in front of which was placed a 5 μm. diameter pinhole. The centre of the Fourier transform was assumed to be the position of the pinhole at which the greatest intensity level was found and displacements of the photomultiplier from this position were measured with a dial gauge.

Two absorbing filters (having a combined absorption factor of 350) were included in the system for measuring the brightest parts of the profile. These were removed one at a time as the fainter regions were reached. This was necessary to keep the intensity within the working range of the photomultiplier tube.

The results of these measurements are shown in Fig. 41. The data here is somewhat smoothed, detailed structure (of the order of 10 μm.) constituting the relatively small speckle contribution present in the transform plane not being revealed, as the labour involved in recording and plotting the large number of data points which would be needed was not thought justifiable for this preliminary work. Similarly, automated recording of the data was not

worth the setting up for this work. Only the broad profile was needed, for assessing the practical situation.

It can be seen that the range of intensities encountered in the transform is around 20000 : 1. This is considering only the central 8mm. diameter region of the transform (corresponding to spatial frequencies up to about 10 mm^{-1}). A ratio of about 100 : 1 is encountered within 60 μm. of the centre (corresponding to spatial frequencies up to 0.14 mm^{-1} in the original transparency).

There is clearly a very strong low frequency contribution to the Fourier transform, and even approximately linear recording of the entire intensity range is out of the question with photographic materials; it is unlikely to be possible with the thermoplastic plates.

8.3 Computations of the Effects of Limited Dynamic Range upon Filter Behaviour

If it is accepted that recording the whole of the Fourier transform is not possible we can, at least, investigate some of the consequences of recording only a part of it. The resulting autocorrelations can, for example, be explored by computation.

The section of the transform which can be successfully recorded will generally be an annular ring centred on the zero frequency point of the transform plane. The width of the recorded ring will always be such that the intensity incident upon the inner circumference of the annular ring will bear a ratio to the intensity incident on the outer circumference which is fixed for a particular holographic

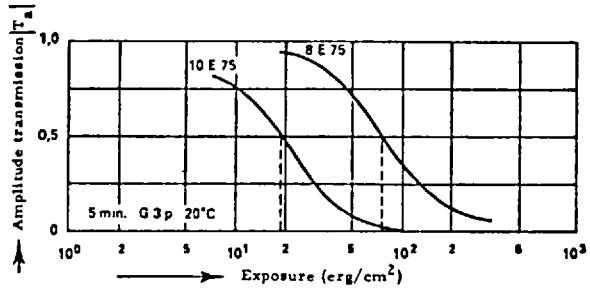

Figure 42. Amplitude transmission characteristic of Agfa 10E75 and 8E75 holographic plates. (Developed for 4 minutes in G3p at 20°C).

recording material and development process.

For example, using Agfa 10E75 holographic plates in the Fourier plane, Fig. 42 suggests that the usable range of exposure is from 10 to 30 ergs cm^{-2}. The successfully recorded section of the Fourier plane will be wherever the energy received by the plate lies in this range. Assuming that we are free to choose the exposure time as we wish, we can, therefore, successfully record any region of the Fourier plane across which region the intensity varies by a ratio no greater than 3 : 1 (i.e. 30 : 10).

As mentioned above, the region concerned will generally be an annular ring as the intensity distribution in this plane is roughly symmetrical about its central point. The intensities at the inner and outer circumferences of the annulus will therefore be in the ratio 3 : 1 for this recording medium.

This analysis makes several assumptions, such as the emulsion characteristic's being of shape shown in Fig. 39, the dynamic range being roughly defined by Fig. 42. However, at least we now have a means of investigating the more gross effects of the photographic limitations, even though these assumptions may not be precisely valid.

The intensities recorded in Fig. 41 plot out in effect, the power spectrum of the amplitude transmittance of the original transparency, for one particular direction in the image. According to the Autocorrelation Theorem (see, for example, ref. 43, p.115), the autocorrelation of a function is identical with the Fourier transform of its power spectrum.

Assuming, again, that the data of Fig. 41 is a description of the intensity distribution for any azimuth in

the Fourier plane (i.e. circular symmetry), then the autocorrelation of the original scene transparency can be obtained by Fourier transforming the function shown in Fig. 41.

Circular symmetry is, here, a convenient assumption as the process of measuring the intensity point by point over a two-dimensional Fourier transform is very lengthy. The amount of information we have about the image is, of course, no greater than in the one-dimensional data of Fig. 41 as a result of making the assumption, and this is reflected in our ability to reduce the two-dimensional Fourier transformation of a circularly symmetrical function to a one-dimensional form of transformation which involves only the radial co-ordinate. This one-dimensional transform is known as the Hankel transform (see, for example, ref. 43, p. 244).

As the Fourier plane of the optical system will only be recorded by the hologram for a restricted range of the radial co-ordinate, to find the correlation response of a Vander Lugt filtering operation with realistic materials we should (Hankel) transform only that part of the Fourier plane intensity (i.e. power spectrum) which lies in this restricted range.

Our computer programme should, therefore, first establish the range limits of the radial co-ordinate for which the function of Fig. 41 can successfully be recorded on the hologram plate (subject, of course, to some initial constraints which correspond, physically, with the exposure duration and brightness of the illuminating laser). The programme should then carry out the Hankel transformation of

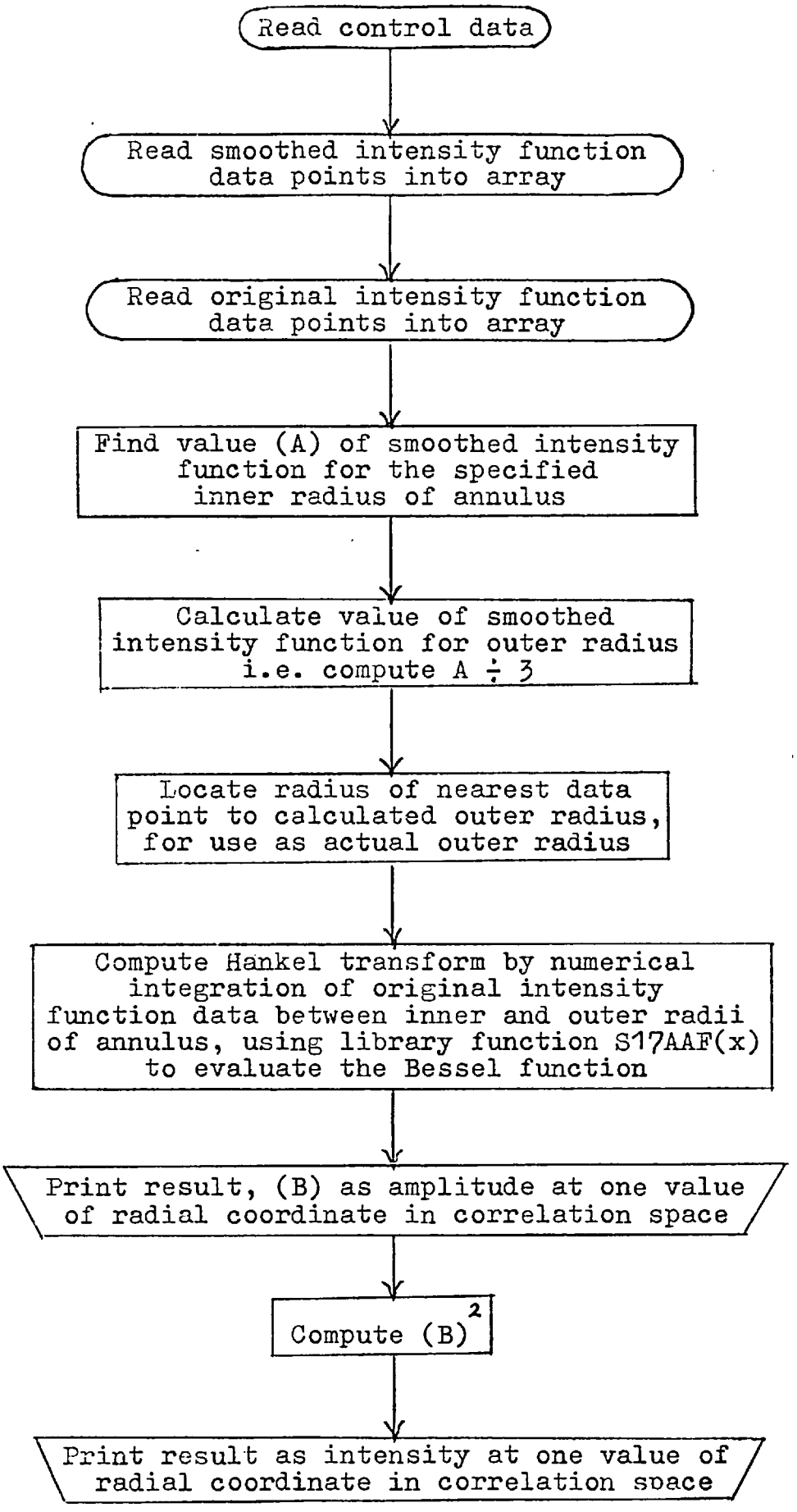

Figure 43. Flowchart of autocorrelation programme. Smoothed (monotonic) data (See Fig. 41) were used for convenience in finding the size of the successfully recorded annulus. The actual data were used in computing the autocorrelation.

```
      PROGRAM THJORSA(INPUT,OUTPUT,DATA,TAPE5=DATA,TAPE6=TAPE6)
      DIMENSION F(2000),R(2000),FUNC(2000),RUFR(2000),RUFF(2000)
      READ(5,100) SSTEP,SMAX,ATA,N1MIN,N1STEP,N1MAX
  100 FORMAT(3F10.4,3I10)
      WRITE(6,102)SSTEP,SMAX,ATA,N1MIN,N1STEP,N1MAX
  102 FORMAT(5H 102=,3F10.4,3I10)
      LDATA=IFIX(ATA)
      DO 311 I=1,2000
      F(I)=0.0
  311 R(I)=0.0
      READ(5,110)(R(I),F(I),I=1,LDATA)
  110 FORMAT(8F10.4)
      DO 312 I=1,2000
      RUFF(I)=0.0
  312 RUFR(I)=0.0
      READ(5,120)(RUFR(I),RUFF(I),I=1,LDATA)
  120 FORMAT(F10.4)
      N1=N1MIN
   25 WRITE(6,252)R(N1),F(N1)
  252 FORMAT(7H R(N1)=,1PE16.4,12X,7H F(N1)=,1PE16.4)
      F2=F(N1)/3.0
      M=0
    5 M=M+1
      IF(F(M).LT.0.000001) GO TO 10
      IF(F(M).GT.F2) GO TO 5
    4 FDIFF=F(M-1)-F(M)
      FMID=F(M)+(FDIFF/2.0)
      IF(F2.LE.FMID) GO TO 6
   10 N2=M-1
    9 WRITE(6,300)R(N2),F(N2)
  300 FORMAT(7H R(N2)=,1PE16.4,12X,7H F(N2)=,1PE16.4)
      S=-SSTEP
   17 S=S+SSTEP
      N=1
   11 EX=S*RUFR(N)*4.8048604E-5
      BESS1=S17AAF(EX)
      IF(RUFR(N+1).LT.0.000001) GO TO 12
      EX=S*RUFR(N+1)*4.8804604E-5
      BESS2=S17AAF(EX)
      FUNC(N)=(RUFF(N)*RUFR(N)*BESS1+RUFF(N+1)*RUFR(N+1)*BESS2)/2.0
  450 N=N+1
      GO TO 11
   15 N=N1-1
      SUM=0.0
   16 N=N+1
      SUM=SUM+(FUNC(N)*(RUFR(N+1)-RUFR(N)))
      IF(N+1.LT.N2) GO TO 16
      SUMSQ=SUM**2
      WRITE(6,105) S,SUM,SUMSQ
  105 FORMAT(4H S= ,1PE10.3,12X,6H SUM= ,1PE10.3,12X,8H SUMSQ= ,1PE10.3)
      IF(S.LT.SMAX) GO TO 17
      N1=N1+N1STEP
      IF(N1.LE.N1MAX)GO TO 25
      STOP
    6 N2=M
      GO TO 9
   12 FUNC(N)=RUFF(N)*RUFR(N)*BESS1
      GO TO 15
      END
```

Figure 44. Autocorrelation programme.

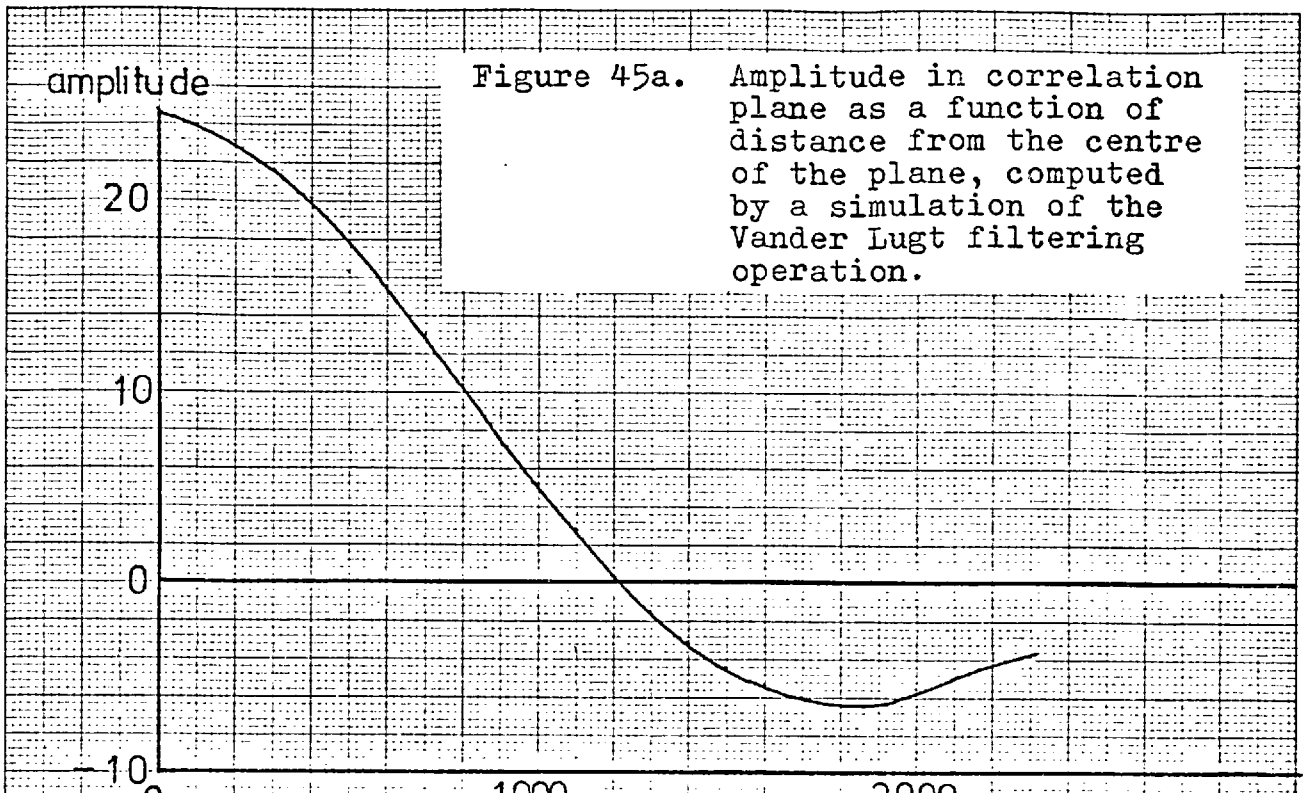

Figure 45a. Amplitude in correlation plane as a function of distance from the centre of the plane, computed by a simulation of the Vander Lugt filtering operation.

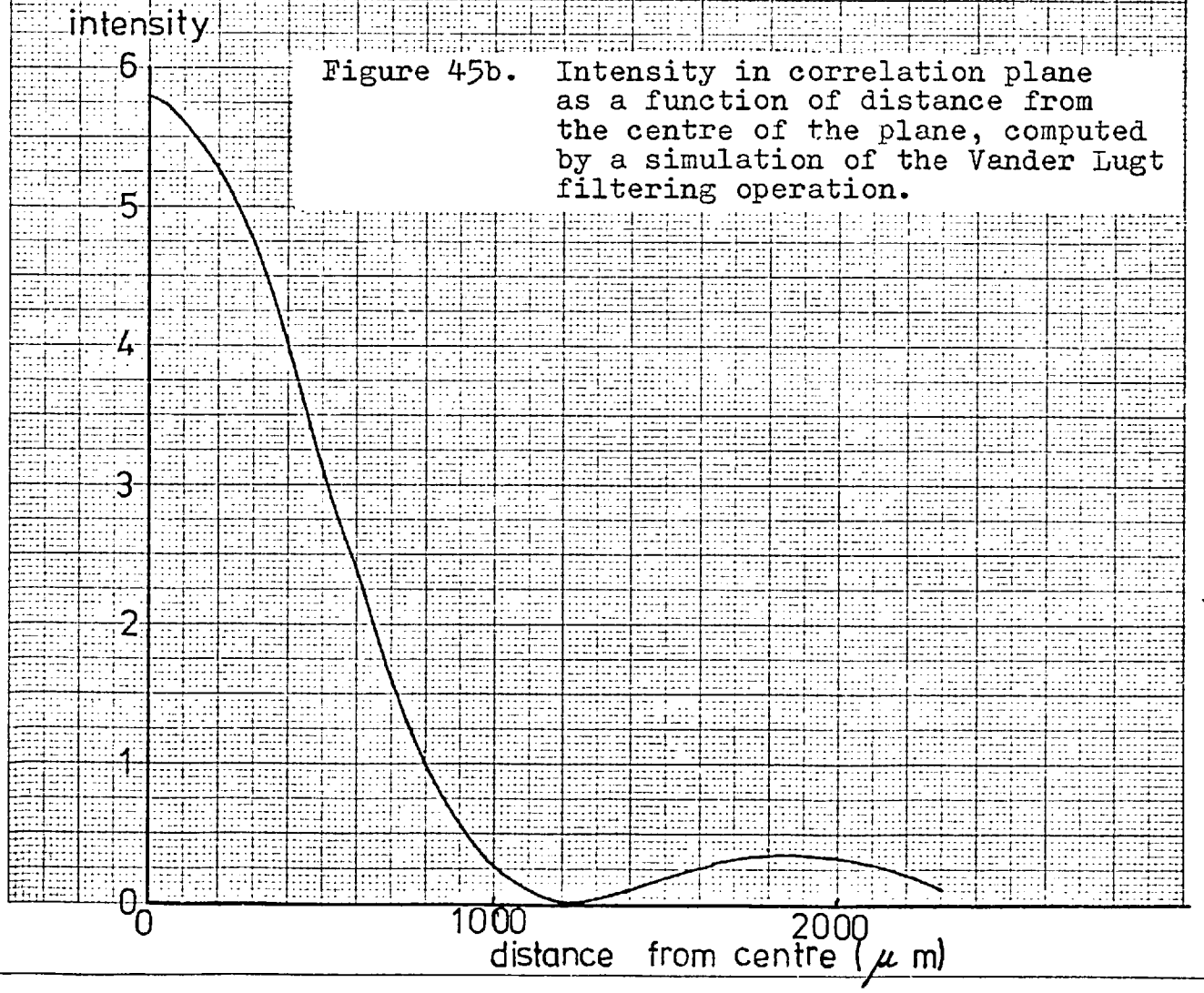

Figure 45b. Intensity in correlation plane as a function of distance from the centre of the plane, computed by a simulation of the Vander Lugt filtering operation.

the data of Fig. 41 over this range of the radial co-ordinate. The result will be the radial profile of the circularly symmetrical correlation response that would arise from attempting to carry out the autocorrelation operation by Vander Lugt filtering using recording materials having this particular dynamic range.

The flow charts and listing of a programme designed to do this are shown in Figs. 43 and 44.

It is interesting to note that if we had desired to compute the image which would be reconstructed from the information stored on the hologram then we should have needed to transform both the amplitude and phase information present in the Fourier plane with our programme. However, what we actually require is the autocorrelation of the original transparency, not the image of it. We can accomplish this by transforming the intensity present in the Fourier plane (i.e. the power spectrum of the original transparency) rather than the amplitude and phase.

Clearly, ours is the simpler task, both in the collection of the data from the Fourier plane and in the computation.

Figs. 45a and 45b show the functions produced by the programme of Fig. 44 when run using the data collected previously (Fig. 41).

As may be expected, the general form of the intensity distributions is in all cases a central bright peak surrounded by bright and dark rings. Fig. 45 shows, in effect, a section through these structures.

Fig. 19 depicts schematically the optical realisation of the Vander Lugt filtering process. We can see that the

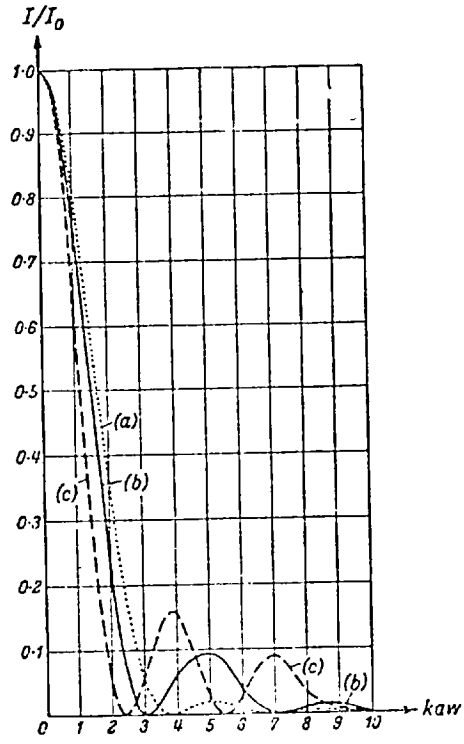

Figure 47. Normalized intensity found in the far field when annular aperture stops having various values of ε (the ratio of the inner radius to the outer radius of the annulus) are used. (a) $\varepsilon = 0$ (circular aperture). (b) $\varepsilon = \frac{1}{2}$. (c) $\varepsilon \to 1$. (From Born and Wolf). (On the horizontal axis, $k = \frac{2\pi}{\lambda}$, a is the outer radius of the annular aperture and w is the angular subtense of points in the diffraction pattern at the centre of the diffracting aperture.

region of the hologram within which the Fourier plane intensity is successfully recorded can be considered as the aperture stop for the two stage optical system. (It is a two stage system in the sense that the transformation from the object transparency to its Fourier spectrum takes place on a separate occasion from the transformation from the Fourier spectrum to the correlation plane. The hologram's recorded area forms the aperture stop for the entire two stage process). It is, of course, generally an annular stop across which the intensity is not uniform.

The presence of this "stop" is the cause of the autocorrelation's ring pattern, broadly speaking. However, it is the distribution of intensity within the area of the aperture which, generally, is characteristic of the particular object transparency and which modifies the shape and scale of the rings and central peak in a manner determined by the true autocorrelation of the amplitude transmittance of the object transparency. (To be more specific, it is the amplitude in the output, or correlation, plane of the system rather than the intensity which corresponds in theory with the autocorrelation).

That the existence of a ring pattern is a consequence of the annular form of the recorded area on the hologram rather than the detailed form of the power spectrum of the transparency recorded within that area can be supported by comparison with the diffraction pattern produced by uniformly illuminated annular apertures.

Born and Wolf (44, p. 417) provide data on such diffraction patterns, some of which is shown in Fig. 47. This curve shows the Fraunhofer diffraction pattern obtained

from an annular aperture whose inner perimeter has half the radius of its outer one.

Fig. 45 shows that the first dark ring of the pattern computed for an annular aperture of 60 μm outside radius and 25 μm inside (using the data of Fig. 41 for the intensity distribution within the aperture) had a radius of about 1.22 mm.

From Fig. 47 we find that, using an 8 inch lens and a diffracting aperture of the same dimensions as above but uniformly illuminated, the radius of the first dark ring would be 1.02 mm.

Similarly the radii of the first bright ring are 1.85 mm. and 1.70 mm. from the power spectrum computations and the uniform annular aperture respectively.

The radii of the rings are slightly smaller with the uniform aperture illumination than with the aperture illuminated by the transparency power spectrum. This is probably due to the general tendency of the power spectrum to be brighter towards the centre than the edges.

The size of the ring pattern can, therefore, be accounted for by considering only the dimensions of the recorded area on the hologram plate and the general form of the intensity distribution in the power spectrum recorded within that area of the plate. This general form of the intensity distribution is likely to be the same with almost all normal continuous tone object transparencies and it has not been necessary to make any use of the detailed structure or form of the power spectrum data in accounting for the ring pattern. It seems, therefore, that the rings predicted by the computation are likely to be a result of the dynamic

range restriction in the hologram material, rather than to be a feature of the true autocorrelation of the object transparency.

The situation that we face is an example of the common matter of diffraction limited resolution, even though it is a correlation plane we are considering rather than an image plane, and despite ours being a two stage optical system rather than the more normal single stage.

An alternative view of our computations is that we have been investigating the frequency response of our optical system (from object plane to correlation plane), with an annular aperture stop in it. Normally, one does this by using a point source (a "delta function" of intensity) in the object plane so that the aperture stop is illuminated by a plane wavefront of uniform intensity, and the output plane (the correlation plane) contains the Fraunhofer diffraction pattern.

In our computations, we have been considering using a continuous tone photographic transparency as the input. Whereas the point source contains all spatial frequencies to equal degrees, the transparency contains far more of the low frequencies than the high ones although all frequencies are present to some extent. This has considerably modified the intensity distribution across the aperture stop and has had some effect upon the diffraction pattern in the output (correlation) plane, but we have seen that the latter is not great.

It has, however, been necessary to use the actual object transparency in the input plane, as the dimensions of the annular "aperture stop" and, hence, the frequency

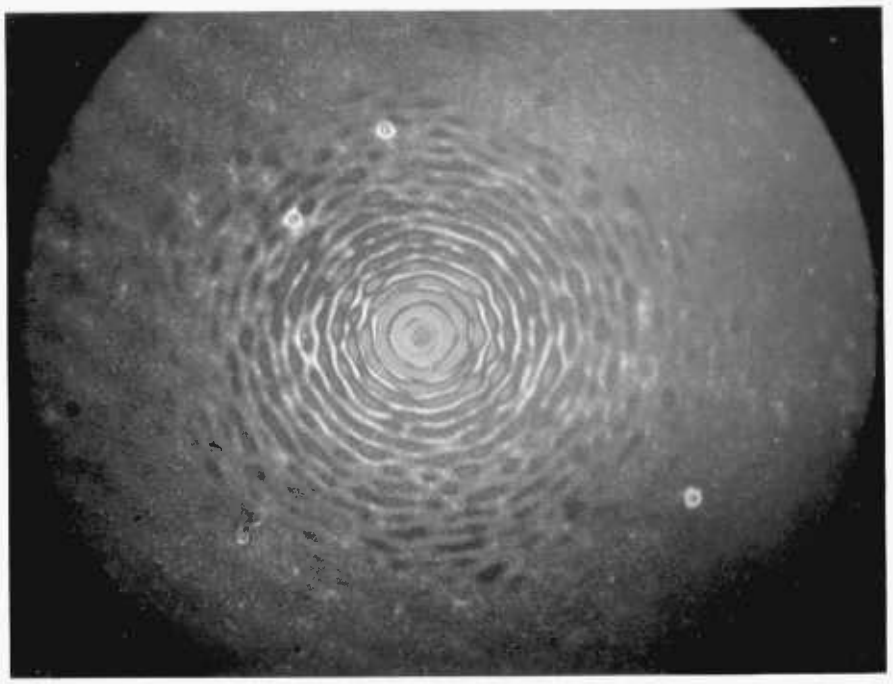

0·5 mm.

Figure 48. Photomicrograph of central area of a thermoplastic Fourier transform hologram.

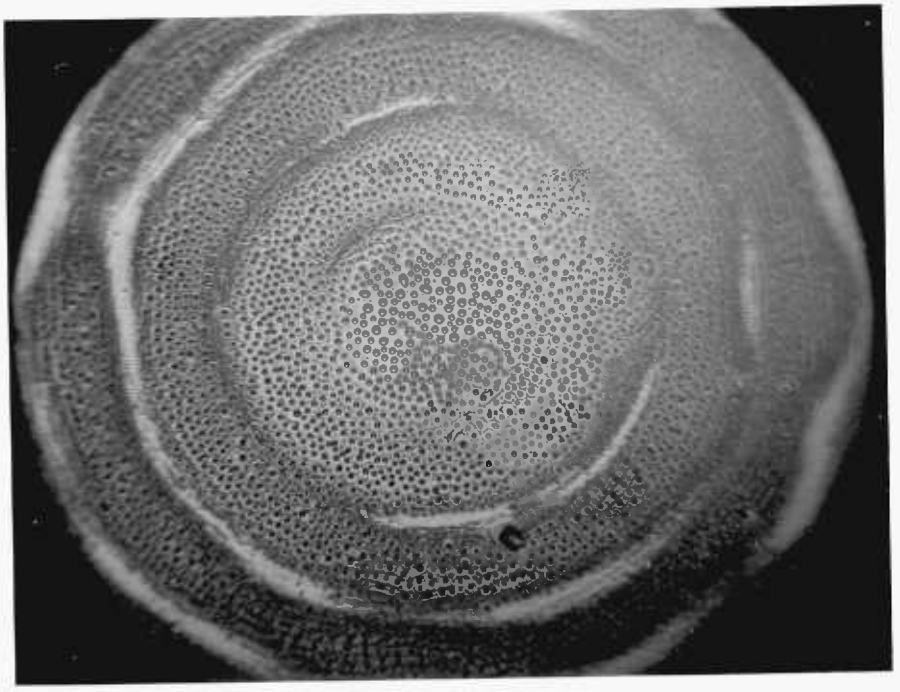

Figure 49. Photomicrograph of central area of a thermoplastic Fourier transform hologram.

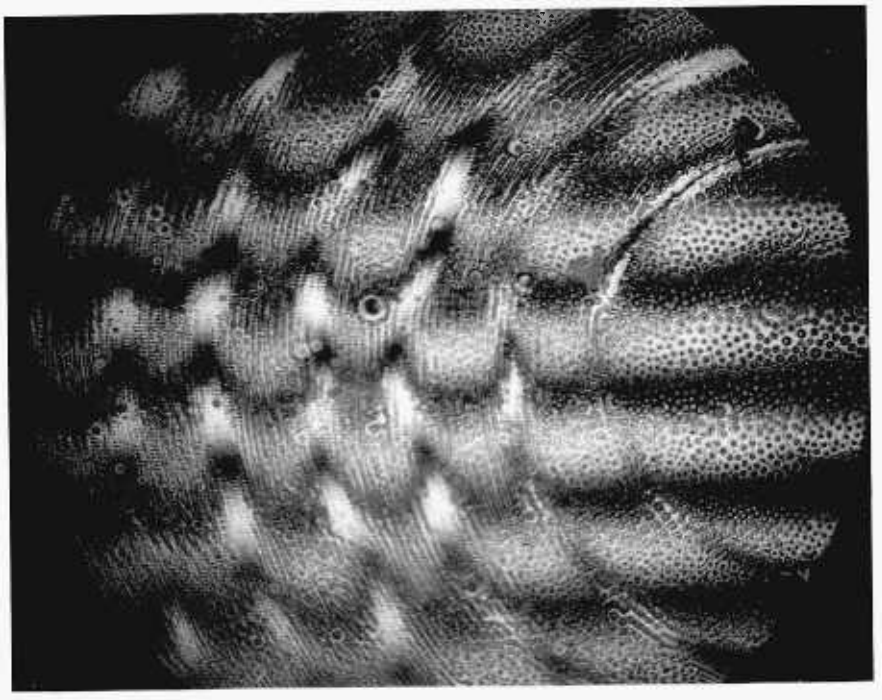

Figure 50. Photomicrograph of a thermoplastic Fourier transform hologram, with interference fringes formed in reflection to show surface profile.

response of the system, are dependent upon the form of this transparency's power spectrum and upon the exposure given to the hologram recording it.

Clearly, a major factor to be taken into consideration when exposing the holographic material in the Fourier plane is the size of the region of the Fourier plane which is successfully recorded within the dynamic range of the material as this is likely to limit the resolution of the system.

These computations were carried out using a photographic material as an example, and the results should not be applied in detail to, say, a thermoplastic recording material as it will probably have different exposure characteristics. However, the above results do serve to draw attention to the nature of the problems which may be expected from restriction of the dynamic range in the recording material during holographic correlation filtering.

8.4 Microscopic Appearance of Thermoplastic Surface in use as a Fourier Transform Hologram

We can gain some insight into the behaviour of the thermoplastic recording material in Fourier transform hologram recording by photomicrography of the deformed surface. Figs. 48 to 50 show typical results. Here, a thermoplastic recording plate, constructed as developed in Chapter 7, has been exposed to the holographic pattern formed by interference between a plane reference beam and the optical Fourier transform of a small area of an ERTS transparency.

The lens used to carry out the Fourier transformation was purpose-built†. It was of six elements and 70 cm. focal length.

Fig. 48 shows the central area of one of these holograms. The thermoplastic thickness was 0.2 μm. and the thickness of the underlying photoconductor was 2.5 μm.

The area within about 1 mm. of the centre of the transform shows a strong ring pattern, each ring being modulated in width. The modulations of each ring show some tendency to be symmetrical on opposite sides of the centre. The order of size of these rings and the symmetry of their modulations respectively makes it probable that the rings are a recording of the diffraction pattern of the aperture defining the area of the object transparency, and the modulations are the consequence of the convolution of that diffraction pattern with the Fourier transform of the object transparency itself.

However, we should not have expected the ring pattern directly to modulate the thermoplastic, as the spatial frequency of the rings is around 20 mm^{-1} whereas the frequency of peak response for our 0.2 μm thermoplastic film was found, earlier, to be at 1000 mm^{-1}. Fig. 35 shows that very little modulation would be expected at 20 mm^{-1} according to our previous results. Rather, we should have expected the high frequency (about 1000 mm^{-1}) interference pattern between the Fourier transform and the reference beam to have appeared. The rings would then only have been present as a modulation of the straight holographic fringes.

Fig. 49 shows the absence of holographic fringes in the central area of this recorded transform. The random

† SEE FOOTNOTE AT END OF CHAPTER.

Frost deformations can be seen there, but there is no systematic modulation other than the ring pattern.

Fig. 50, where the centre of the transform is to the side of the field of view, was taken using reflection interference microscopy. The broad horizontal fringes therefore record the profile of the surface. The displacement of these fringes by an amount equal to their separation corresponds to a surface deformation equal to half the wavelength of the microscope illumination, or 0.27μm in this case.

We can see that the circular ring pattern has an overall depth of about 0.1μm from top to bottom of the ring deformations.

The holographic ridges are, in fact, visible in this photograph, as fine horizontal lines starting at about 0.2 mm. from the centre of the ring pattern.

Fig. 50 probably gives us some indication of the mechanism by which the ring pattern is being recorded by the thermoplastic even though its frequency is far from the peak response frequency. Each of the rings is seen to be made up of a number of finer circular rings which are of about the same spatial frequency as the holographic fringes and the Frost. In the absence of a holographic interference pattern, the thermoplastic will deform into a Frost pattern of random orientation (i.e. no alignment) but more or less uniform spatial frequency, if charged and softened. If a holographic fringe pattern is present the Frost tends to align itself to this, giving in effect, a recorded hologram. It seems that where the material has been exposed to a strong circular fringe pattern during development the Frost

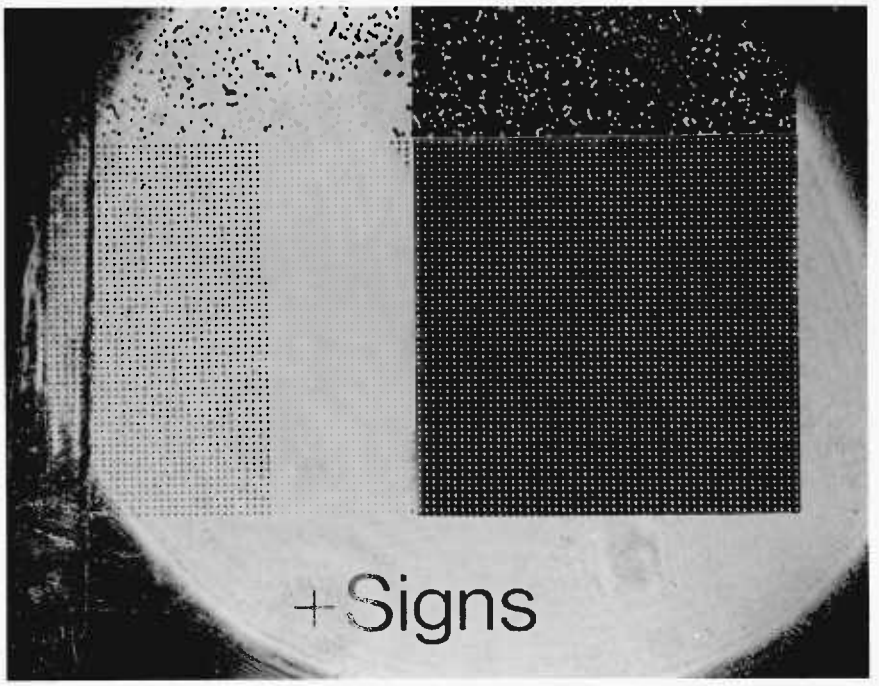

Figure 51. Test transparency, imaged by laser light through Fourier transform and inverse transform lenses.

tends to align itself with these fringes, even though the frequency of the fringes is much larger than that of the Frost. The recorded Airy ring pattern is, in fact, still being recorded as a modulation of a higher frequency than its own, but the alignment of this higher frequency is circular rather than the straight holographic fringes which we would have preferred.

Although the Airy ring pattern and the power spectrum combined with it are being recorded on our plate as modulations of a higher frequency, we can expect no contribution from the first few rings to an image reconstructed using the plate, as the high frequency fringes are of this circular form here.

This tendency for the Frost to form ring structures rather than straight lines at the centre is certainly due to the very high intensity here in the Fourier transform; greater by several orders of magnitude than the reference beam intensity so that the ring pattern has greater modulation than the holographic fringes and so tends to win the competition for the compliance of the Frost.

8.5 Thermoplastic Fourier Transform Hologram of a Test Object

Fig. 51 shows an image of a test transparency. The transparency was a binary object, containing only black and white levels. The image has been made by carrying out the Fourier transformation and inverse transformation in laser light (632.8 nm.) using 8 inch Dallmeyer Septac lenses.

To investigate the ability of the thermoplastic plates to record in the Fourier plane, such a plate was placed in

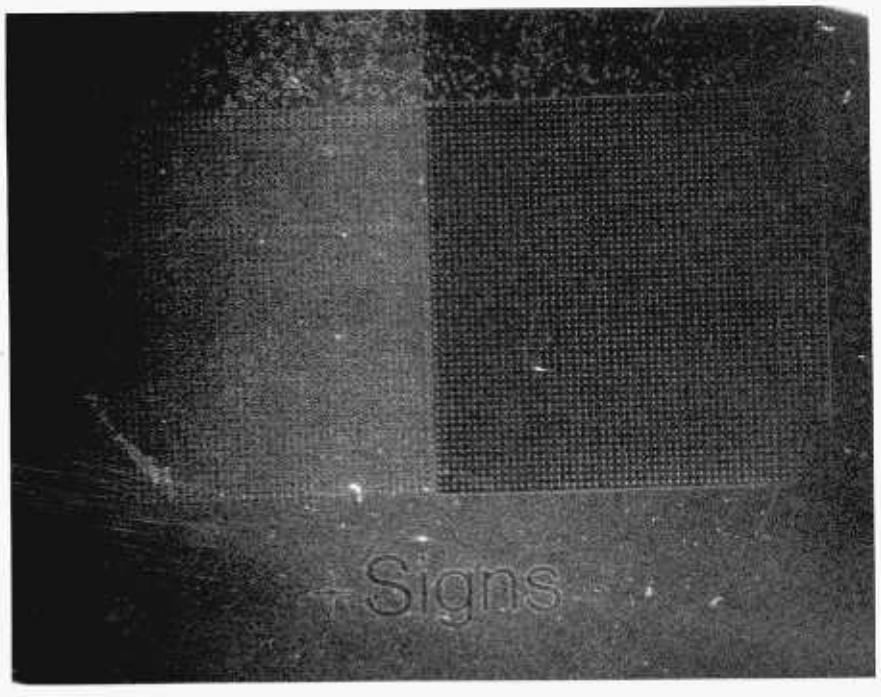

Figure 52. Image of test transparency reconstructed from a thermoplastic Fourier transform holographic recording of the original transparency.

this position and used to record the transform, a plane reference beam being brought in at 30° to the axis of the bench. The total laser power was about 1 mW, this being divided into two roughly equal parts to provide the reference beam and the transparency illumination. The thermoplastic and photoconductor thicknesses were 0.2μm and 2.5μm respectively in this case, as in all future work, and a green dye (brilliant green) was used as the photoconductor sensitiser. The simultaneous recording mode was adopted from here on as the only one capable of giving usefully high diffraction efficiencies.

An image reconstructed from this hologram is shown in Fig. 52.

The low contrast between areas of low spatial frequency, such as the backgrounds to the upper two large panels, is immediately apparent. This is to be expected, because of the very high central intensity in the Fourier plane; the recording of low spatial frequencies on the hologram is likely to be severely attenuated by saturation of the recording process. This saturation may result from a physical cause such as saturation of the photoconductor, but certainly a contributory factor is simply the low modulation which must exist in the holographic interference pattern at the centre of the transform because of the great inequality of intensity between the reference and object beams in this region.

Another factor, whose effect upon the image is more difficult to predict, is that the object beam would have been brighter than the reference beam in this central area of the Fourier plane. The modulation of the holographic

fringes and, hence, the diffraction efficiency of the hologram, would therefore be inversely related to the brightness in the Fourier plane here: the higher the Fourier plane intensity during the Fourier transformation stage, the lower it would be during the inverse transformation (reconstruction) stage. Such meddling with the Fourier components will have a complicated effect upon the image and would probably be best investigated at first by computation.

Another consequence of the removal of low frequencies from the image can also be seen in this photograph. This is the occurrence of narrow bright lines at the boundaries between large areas of uniform brightness. This is an effect similar to differentiation. Precise differentiation would require the Fourier plane amplitudes to be attenuated according to a parabolic radial function (ref. 34, p. 406). The function in our case is unlikely to be this particular one, but is, at least generally similar, the attenuation being greatest in the centre and decreasing radially, with decreasing rapidity.

The holographic recording in the Fourier plane could probably be improved by the obstruction of the large uniform bright areas of this transparency. If the bright surround was obstructed, the amount of light reaching the centre of the Fourier plane would be considerably reduced and the recording of the remaining areas would be more accurate. This expedient has often been used in practical Vander Lugt filtering, but is not pursued here as we are more concerned with the ability of our material to record the transforms of continuous tone images, where we shall have little control

5 mm.

Figure 53. ERTS transparency, imaged by laser light through Fourier transform and inverse transform lenses.

Figure 54. Image of ERTS transparency reconstructed from thermoplastic Fourier transform holographic recording.

over the proportions of power in the lower and higher frequencies.

8.6 An Image Reconstructed from a Thermoplastic Fourier Transform Hologram of a Continuous Tone Transparency

Fig. 53 shows part of an ERTS satellite frame, imaged through the same 8 inch transform and inverse transform lenses as before in laser light. The particular transparency used for this was, in fact, a copy of the ERTS product, at a smaller scale than the original.

A holographic recording of the Fourier transform of this was made on a thermoplastic plate using the same film thicknesses, reference beam angle and beam intensity ratio as before.

A reconstruction of this hologram is shown in Fig. 54. Here again, there is some occurrence of edge differentiation of uniform tone areas, although less than in Fig. 52. Presumably, this reduction of the effect reflects the smaller proportion of very low frequencies present in the present transparency compared with the binary test object.

Indeed, the various grey levels of the step wedge show no edge enhancement at their mutual boundaries, and only a little at their boundaries with the surrounding black region.

The steps of the wedge appear, in the reconstructed image, to be composed of speckle, the elements of which have more or less uniform size but various degrees of compactness within the different steps. In this way an appearance of grey level steps is given visually by the image, although there are in fact no very low frequencies present.

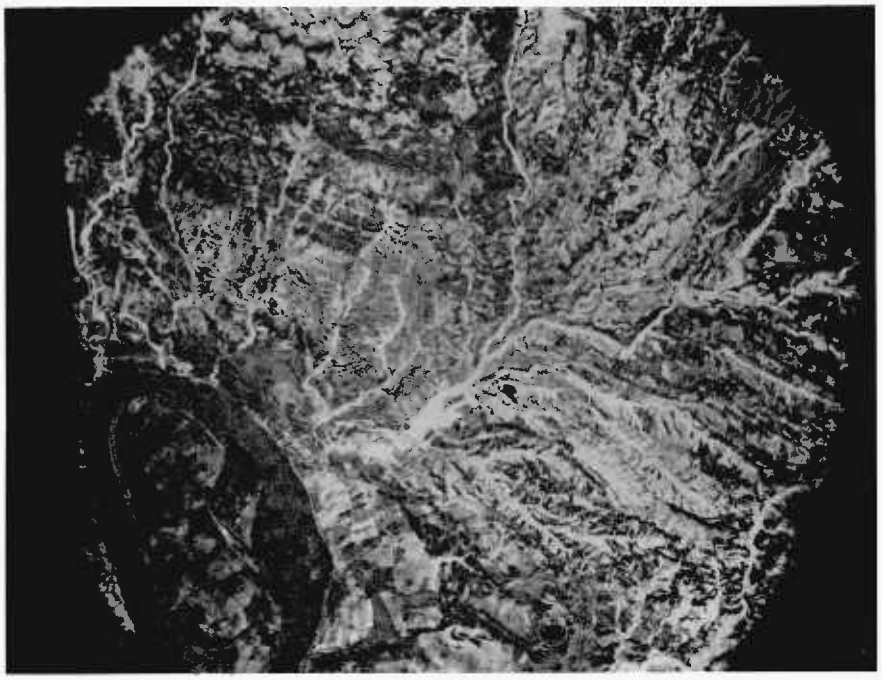

5 mm.

Figure 55. ERTS transparency imaged by laser light through Fourier transform and inverse transform lenses.

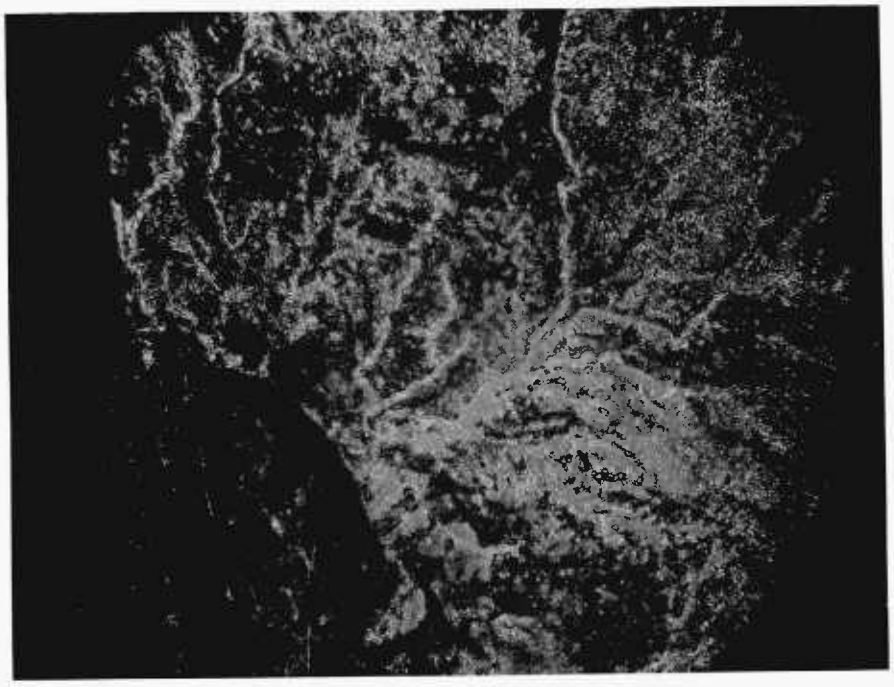

5 mm.

Figure 56. ERTS transparency imaged by laser light through Fourier transform and inverse transform lenses, but spatially filtered.

The lettering below the satellite image itself is recorded, at least in the central area, fairly well. This is, no doubt, because it corresponds to high frequencies in Fourier terms and is therefore largely recorded on a region of the hologram away from the saturated central area.

The satellite image area is found, on close inspection, to contain many elongated, vermicular structures, in addition to the background speckle. Processed images having this type of composition have been formed by Rotz and Greer (45) as a consequence of band pass spatial filtering (not using a holographic recording) with continuous tone images.

An example of the production of this type of image is shown in Figs. 55 and 56. Fig. 55 shows a satellite frame imaged through 8 inch transform and inverse transform lenses. Fig. 56 shows the result of inserting a central obstruction of 630 μm diameter into the Fourier plane. This spatial filter was formed as a dot of DAG915 silver paint on a glass microscope slide, and was positioned by screw adjusters.

The elongated formations are clearly apparent and seem to be associated with areas of high frequency detail in the original.

This suggests that the appearance of these structures in Fig. 54 is yet another consequence of the high pass filtering effect of the restricted dynamic recording range.

8.7 The Detailed Characteristics of an Image from a Thermoplastic Fourier Transform Hologram

An image recorded holographically on a thermoplastic recording plate, especially if recorded in the Fourier plane,

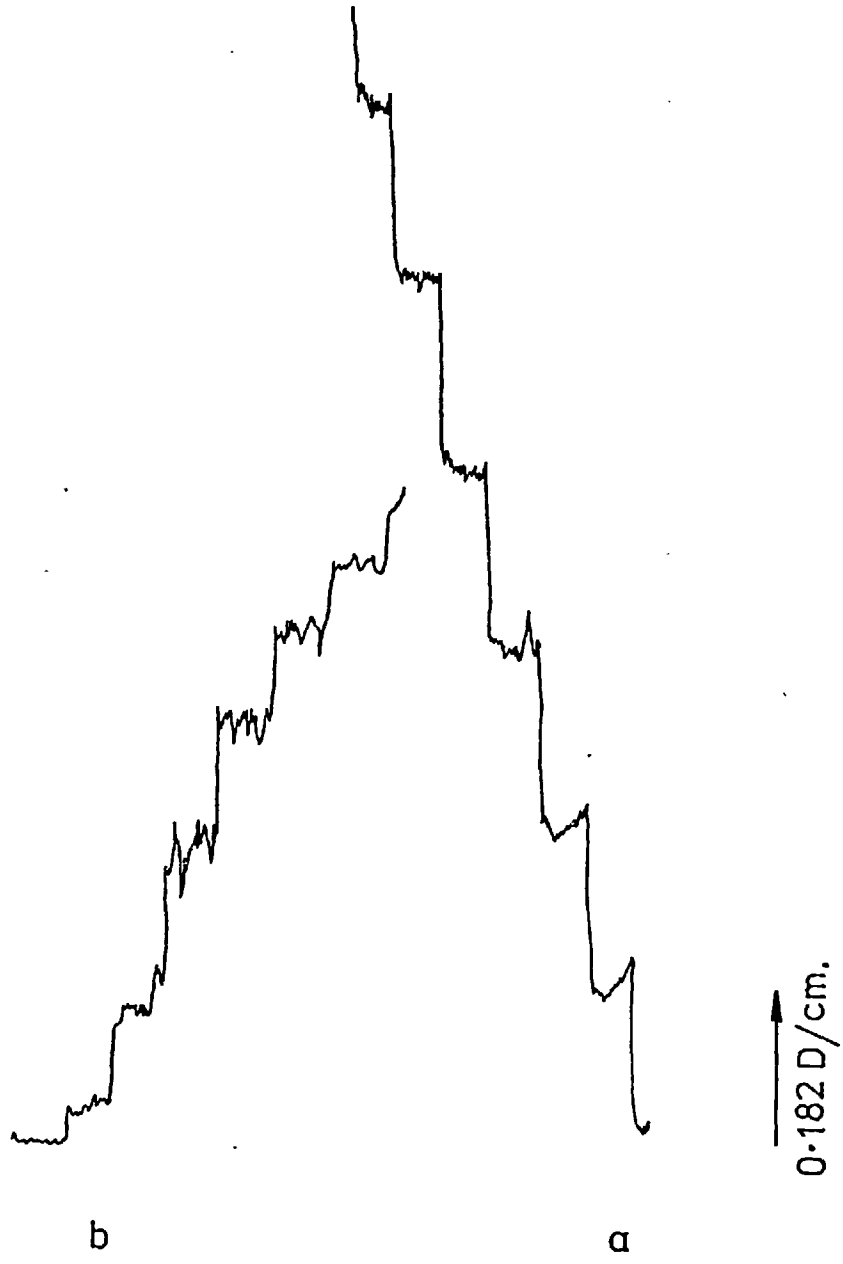

Figure 57 (Part 1). Microdensitometer traces of
a) original density step wedge, and
b) the photograph of the step wedge.

Figure 57 (Part 2). Microdensitometer traces of
b) the photograph of the step wedge, and
c) a photograph of the reconstructed image from a thermoplastic Fourier transform hologram of the step wedge.

is considerably more difficult to describe quantitatively than, say, a photographic image. The behaviour of photographic film can be specified fairly well by its characteristic curve. With a little additional information concerning its modulation transfer function, development time and temperature characteristics and reciprocity failure a useful and fairly complete record of the film's behaviour under a wide range of conditions can be made.

The holographic images with which we are dealing, however, involve more parameters in their specification, and it will be difficult to describe the behaviour of the material for more than a limited range of conditions.

A function similar to the characteristic curve of photographic emulsions can be used to describe the Fourier transform hologram image. As the final image is an aerial light distribution rather than a hard copy on film the function we need, to characterise the hologram plate, will show the relation between input intensity and output (reconstructed) intensity rather than exposure and density.

Intensity rather than exposure (i.e. the product of intensity and time) is used here to describe the input because the simultaneous mode of hologram recording was employed. In this, the exposure is allowed to proceed until a steady state condition is reached by the recording. The time of exposure is, then, of little consequence, intensity being the determining factor.

To measure the relative intensities in the input and output planes, photographic film offers a convenient method. Fig. 57 shows microdensitometer recordings made, (a) of a density step wedge, (b) of the recording of the wedge on

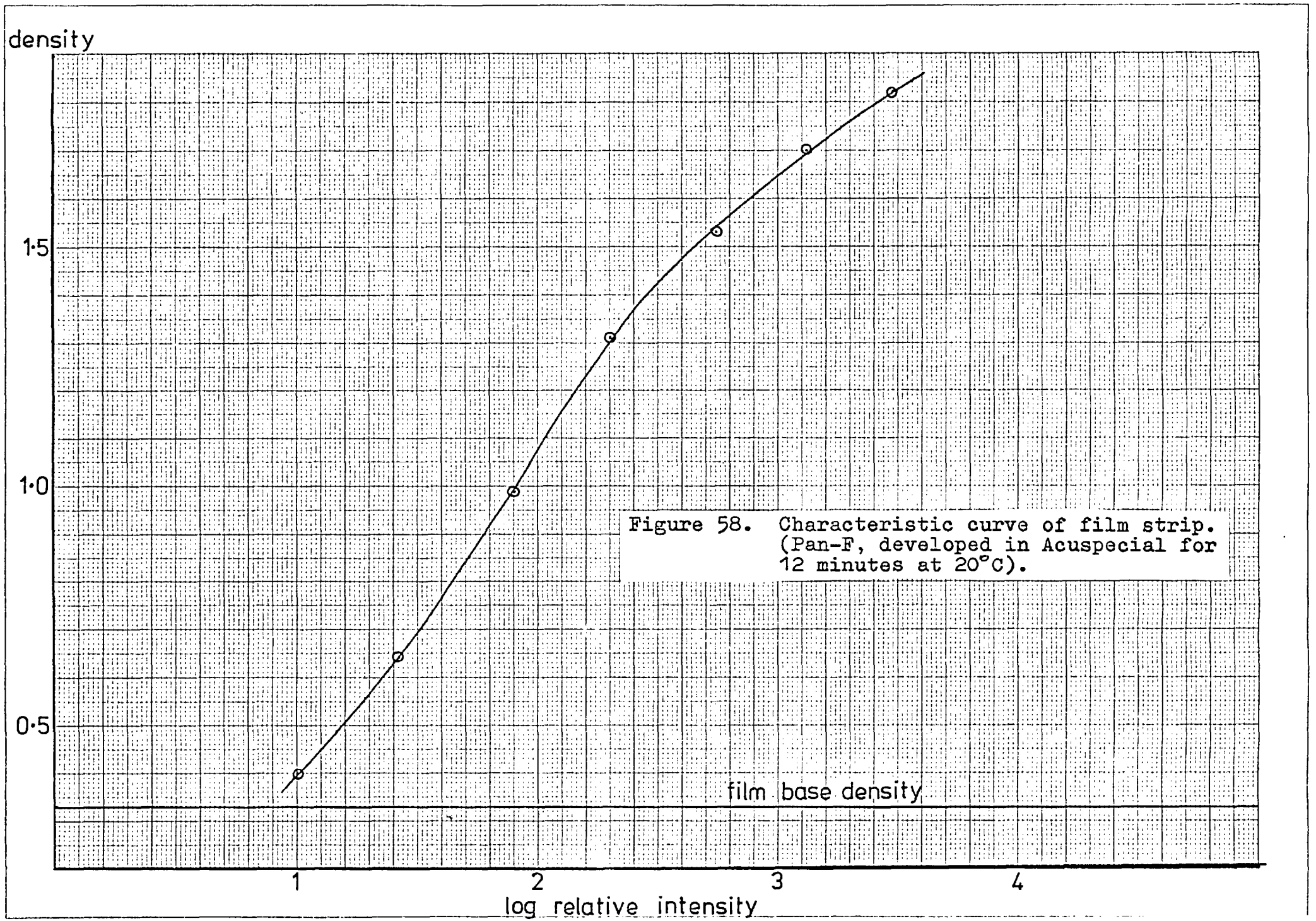

Figure 58. Characteristic curve of film strip. (Pan-F, developed in Acuspecial for 12 minutes at 20°C).

photographic film and (c) of a photograph of the reconstruction of a thermoplastic Fourier transform hologram of the step wedge. (b) and (c) were recorded on the same strip of film. The wedge used was the one along the edge of the frame shown in Fig. 53. The traces in Figs. 57b and 57c were taken from the negatives used to print Figs. 53 and 54 respectively.

The traces of Figs. 57a and 57b were used to plot the characteristic curve for the strip of film. This is shown in Fig. 58.

The intensities which were present in the aerial image of the step wedge reconstructed from the hologram were those incident on the film whose density steps are shown in Fig. 57c. If we assume that the characteristic curve we have plotted applies to these density steps too, (the two exposures were made close together on the same film strip and should have received very similar processing) then we can find the intensities in the reconstructed holographic image of the wedge by referring from the density steps they caused on the film (Fig. 57c) to the characteristic curve of the film (Fig. 58). In doing this, allowance must be made for the different exposure times used when photographing the original step wedge and its reconstructed image. In our case the reconstructed image required sixteen times the exposure required by the original wedge if both were to be recorded within the dynamic range of the film. A correction by a factor of 1.5 was also needed for reciprocity failure (see ref. 46).

The intensities of the reconstructed image deduced in this way were used to plot a graph of input intensity

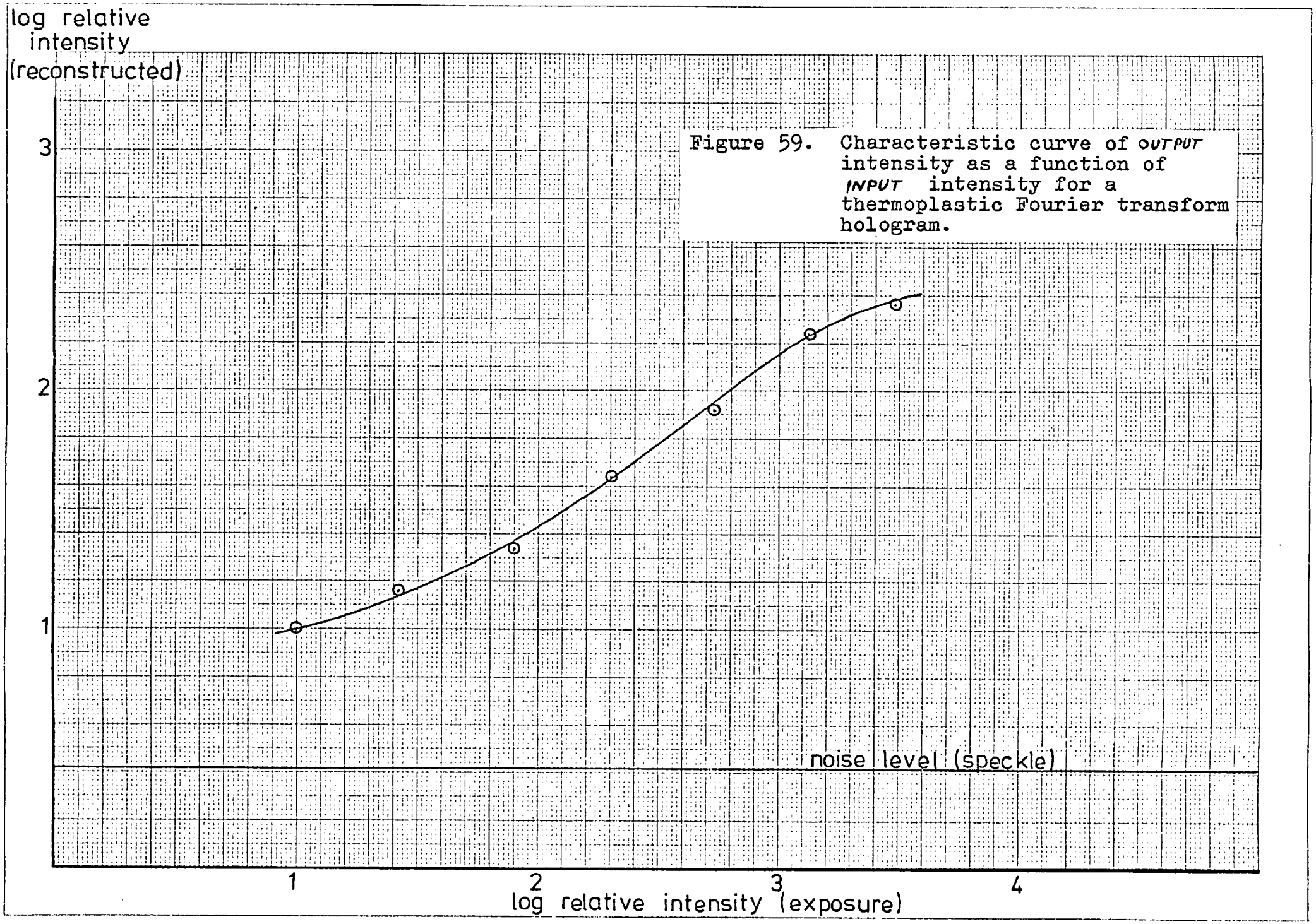

Figure 59. Characteristic curve of OUTPUT intensity as a function of INPUT intensity for a thermoplastic Fourier transform hologram.

against output intensity (Fig. 59). The relative logarithmic units used on the two axes are identical, numerically equal values corresponding to equal values of intensity. Logarithmic scales are used here because, as with photographic characteristic curves, the aim is to describe the relationship between the visual appearance of an original object and the visual appearance of an image of it. The eye responds roughly logarithmically to brightness so scales of this type probably give the best impression of image appearance.

The shape of the curve in Fig. 59 depends on many factors. Some of these such as laser intensity, beam ratio and the construction of the recording plates can be standardised for as many holographic recordings as we wish. However, other factors by their very nature cannot be standardised in practice.

For example, light corresponding to different spatial frequencies of the image from those involved in recording the steps will be recorded on another area of the hologram plate in a region where the mean intensity is probably different, the actual intensity here being determined by the power spectrum of the whole area of the original object transparency. The shape of the intensity transfer characteristic for any given object transparency will depend upon the spatial frequency which is being considered. Also, for other object transparencies with different power spectra the shape of the characteristic at each spatial frequency will, in general, be different.

Also, regions of the object transparency lying at different distances from the side of the transparency will

be recorded on the hologram plate at different holographic frequencies. Thus a step wedge which is extended in the plane containing the object and reference beams will have its various steps recorded at various holographic frequencies whereas one which is extended perpendicularly to this plane will be recorded at a single holographic frequency. The curve of Fig. 35 shows us the amount of variation of the recording plate response with spatial frequency: we must also therefore be prepared for the shape of our transfer characteristic to be dependent upon the position and orientation of information in the object transparency. This should be a fairly small effect if small transparencies and long focal length transform lenses are used.

The characteristic we have plotted (Fig. 59) is by no means a complete description of the behaviour of the recording plate, but it does, nevertheless, provide us with some measure of the extent to which the visual appearance of the low spatial frequencies of this image is being modified by recording the thermoplastic Fourier transform hologram.

that time (July 1975). An argon laser was used, at a wavelength of 488nm. and a power of~100mW. The holographic reference beam was collimated by that mirror which collimated the light used for illuminating the object transparency, rather than by the Fourier Transform lens. (cf. Fig. 22 rather than Fig. 19a.) Also, the axis of the inverse Transform lens lay on the axis of the holographic reference beam during correlation operations. These two expedients kept the lens apertures within practical limits.

CHAPTER 9

OPTICAL CORRELATION RESULTS

9.1 The General Situation

It is well known (33) that the technique of Vander Lugt holographic filtering can, in principle, be used to test for the presence of a known spatial structure within an optical field whose form is otherwise unrelated to that structure, (i.e. within "noise").

As was mentioned in Section 8.1 the main practical difficulties in implementing this type of filtering with continuous tone photographs such as are commonly used in disciplines outside optics have been the inability linearly to record the Fourier transform of these photographs holographically on photographic film, and the need for accurate repositioning of the recorded filter after development.

The first of these is likely to be a problem with any recording material which can be envisaged at present. The extent to which it is a drawback to the use of the thermoplastic material in the rôle of the holographic filter can to some extent be assessed from the results of Section 8.6. Attempts to use the material for carrying out a cross correlation between two images would amount to a cross correlation between one of the images and a version of the other which had been band pass filtered to give an appearance similar to that of Fig. 54. It seems that, for the time being, this effect must be tolerated.

In some situations the loss of high frequencies will be the more serious and in others, the low frequencies. For example, in attempting to identify structures of various shapes and sizes by correlation, it is the position and orientation of edges (higher frequencies) which is most necessary rather than the tone of uniform areas (lower frequencies). On the other hand, when attempting to carry out the autocorrelation of an area of uniform tone (low frequency) the absence of information concerning low frequencies would be troublesome.

The original photographic data will, in any event, itself be of restricted bandwith, being limited at the high frequency end by the resolution of the film or optical system used to record it and at the low frequency end by the frame used to surround it or the field stop of the Fourier optical system.

In principle we could choose the frequency range most needed in any given application and adjust the hologram exposure so as to record as much of that range as possible. In practice it would be difficult to do this in the low frequencies as the gradient of intensity is very great in those regions of the Fourier plane and very slight exposure differences would shift the recorded frequency band considerably. This band would also be extremely narrow.

The results which follow generally describe applications where the frequency range of interest is quite high and it is the higher frequencies which are well recorded on the hologram filter rather than the lower.

With regard to the second problem normally encountered in correlation filtering the prospect is brighter. As the

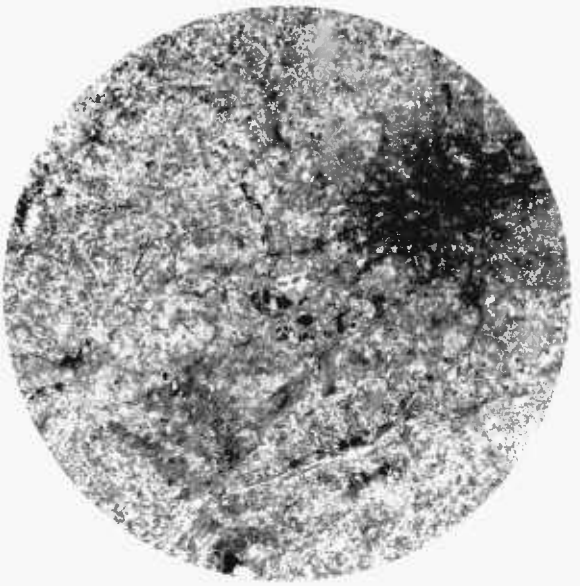

1 cm.

Figure 60. The region of an ERTS transparency used for a trial of cross correlation.

foregoing chapters suggest, the thermoplastic device has been found, in this work, to offer a convenient means of forming a hologram and reconstructing it without mechanical displacement.

Some results of applying the material to optical correlation in conditions which simulate the requirements of workers in other disciplines such as geography and forestry will now be described, some sections of which have been summarised elsewhere (refs. 48 & 49).

9.2 Cross Correlation using Satellite Imagery

As an initial example of optical cross correlation, an area of an ERTS satellite image was selected. The frame used was No. E1228 10293 (band 7) which includes London and South East England. The intention was to test by cross correlation for the presence of the runway pattern of London (Heathrow) Airport within a region of the transparency containing London and a large area of the surrounding country. The region in which the airport was to be sought is shown in Fig. 60.

The optical system used was the Vander Lugt arrangement of Fig. 19. The transform and inverse transform lenses were the purpose-built lenses described in Section 8.4.

The holographic filter was formed by recording a Fourier transform thermoplastic hologram using, in the input plane, a 2 mm. diameter circular aperture which just covered the runway pattern of the airport (seen at the centre of Fig. 60). Once the Fourier transform of this area had been recorded, using the simultaneous mode of operation, the whole area of Fig. 60 (about 2 cm. diameter on the input

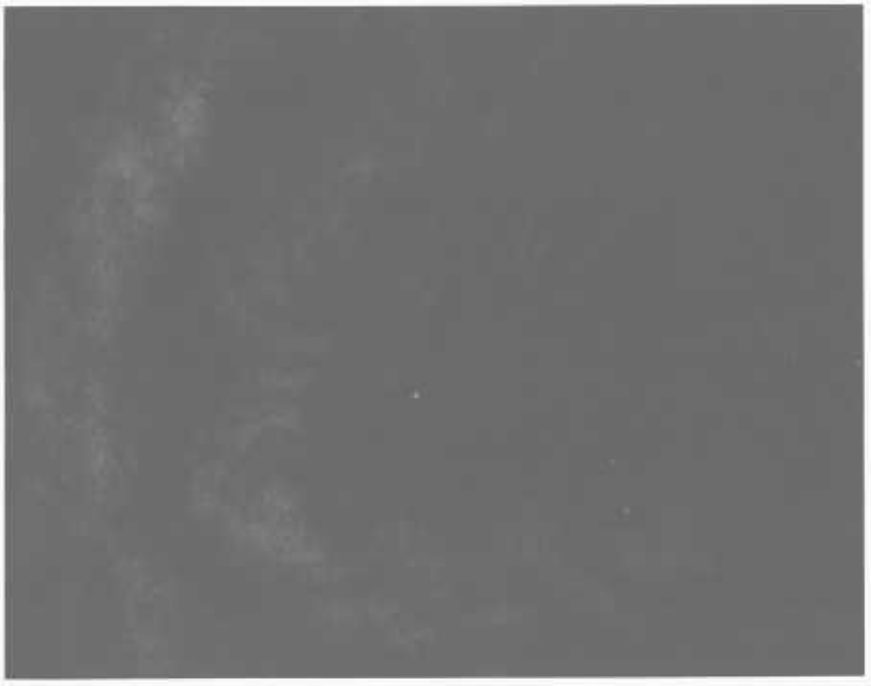

5 mm.

Figure 61. Cross correlation response for airport area within the ERTS transparency.

transparency) was uncovered and the correlation plane was found to contain the response shown in Fig. 61.

This correlation response appears at first sight to be a slightly diffuse circular structure, but on close examination is found to have a bright, roughly elliptical core whose shape presumably contains information concerning the autocorrelation of the area recorded on the matched filter.

In order to investigate the degree of similarity needed between the two scenes for a correlation response to be obtained, a second recognition task was designed. This involved correlating two patterns which, although representing the same physical object, were nevertheless derived from that object by widely different techniques.

The object chosen was again the runway pattern of Heathrow Airport. The task set was again to locate, by cross-correlation, the airport runways within the ERTS frame, but this time the transparency with which the ERTS frame was to be correlated would show a drawing of the runway pattern which had been traced from a map.

The significance of this exercise is that it investigates the amount of information we need concerning the appearance of the object we are seeking when using cross-correlation. Previously we used a single photographic transparency to provide our two scenes for cross-correlation which gave us a fairly high certainty that our runway pattern would be identified by the correlator if it was included in the larger field because its appearance would be identical in the two scenes. This time, however, there is less certainty of recognition as although the two scenes

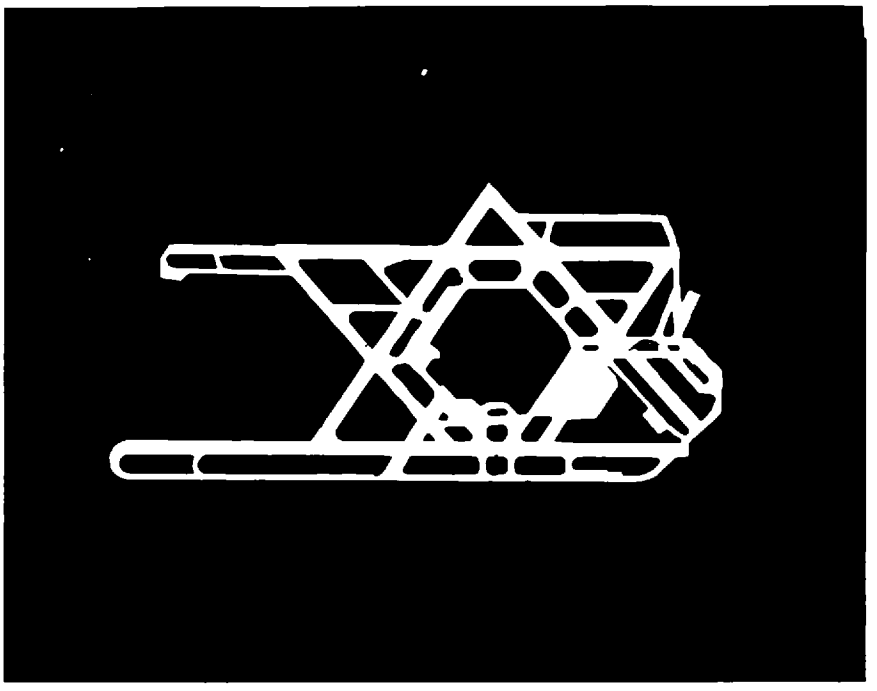

Figure 62. Photograph of a transparency of a drawing of the runway pattern. The transparency, whose scale is indicated, was used in the cross correlation experiment.

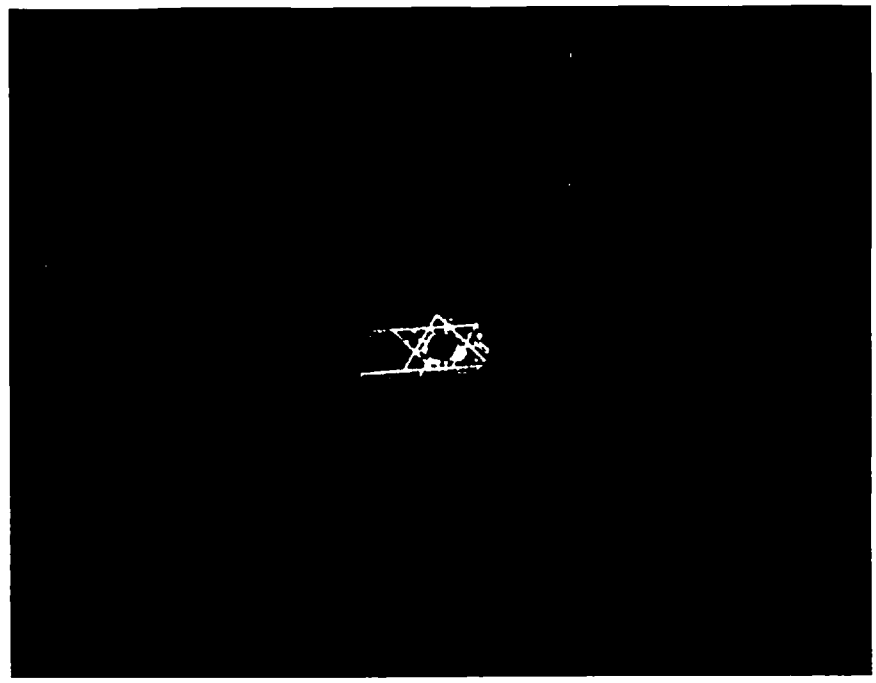

Figure 63. Photograph of the image reconstructed from a thermoplastic Fourier transform hologram of the drawn runway pattern.

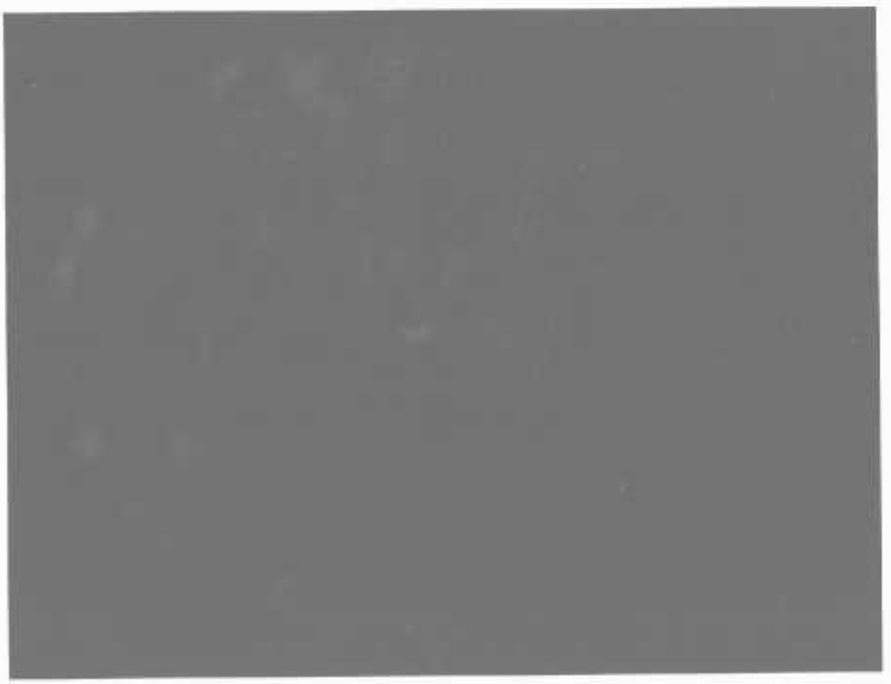

2 mm.

Figure 64. Photograph of the cross correlation response formed between ERTS transparency (Fig. 60) and the transparency of the drawn runway pattern (Fig. 62).

still represent the same airport in the real world, they show different representations of it. One is the ERTS satellite photograph, the other a binary transparency made from a drawing which in turn came from a map which was itself surveyed upon the actual airport site. One must go back to the real airport before one finds any common ground between the channels through which our two transparencies have been obtained: any similarity between the transparencies stems from the real world and does not originate within the laboratory.

The map used was the Ordnance Survey 1 : 10560 scale. The pattern drawn from this is shown in Fig. 62. This was reduced on to Agfa-Gevaert holographic plates (Scientia 8E75) until it was of the same size as the pattern in the ERTS image. The thermoplastic Fourier transform hologram of this was recorded, a reconstruction of this being shown in Fig.63.

This hologram was then used as the matched filter in the second (correlation) stage of a Vander Lugt filtering procedure, the input tc which was the ERTS frame. The result in the correlation plane is shown in Fig. 64.

Again, the airport was located at the centre of the object plane so the correlation response should appear in the centre of the correlation plane. We find that there is in fact a slightly brighter region at the centre, elongated horizontally; although it is much weaker than the response found before it seems a small degree of correlation is indicated.

9.3 Phase Modulated Input Material for Matched Filtering

Although the input material used in our correlator should embody the typical requirement of potential users: to employ non-binary photographic data (aerial and satellite photographs, say), there is no reason why pre-processing of the image should not be considered. These photographs are generally designed for use as absorbing structures in incoherent light; in enlargers and projectors for example. They are commonly recorded so that their density is linearly related to the logarithm of the original scene brightness, which is intended to give the image, when illuminated in that way, a visual appearance which is as closely similar to the appearance of the original scene as possible in a monochrome recording system.

However, the matched filtering process is carried out in coherent illumination and uses the transparency as a diffracting structure. Furthermore, there is no visual interpretation of the image so its appearance to the human eye is immaterial.

There is no reason to suppose that a transparency designed for one function is optimal for the other, so we should consider how best to present the information in the continuous tone photographs to the correlator.

In using the correlator for pattern recognition as described in Section 9.2, it is the information contained in the higher spatial frequencies which is most needed. It is the transparency's ability to diffract light from the illuminating beam which permits a correlation response to be formed.

A possible criterion of a good transparency for the input plane of an optical correlator would therefore be its diffraction efficiency. An input transparency with a higher diffraction efficiency would scatter more of the light towards the edges of the Fourier plane, reducing the range of intensities present in that plane, to some extent.

The diffraction efficiency of an absorbing structure is greatest if it has a binary amplitude transmission coefficient, which takes the value one or zero but not intermediate values. We could produce transparencies of this type from continuous tone images by printing the latter several times on a high contrast photographic emulsion such as the Agfa-Gevaert Scientia 8E75 holographic plate.

However, this would throw away a large amount of information from the continuous tone scene. In any case, the greatest diffraction efficiency which can be hoped for with a binary absorbing structure is 10% (see ref.34, p.224) if the diffraction theory of absorption holograms can be generalised to include diffraction by the correlator input transparency.

On the other hand, a structure which modulates only the phase of the transmitted light can have a higher diffraction efficiency than this, values of 33.9% and 6.25% being the theoretical limits for sinusoidal phase and amplitude structures respectively.

It seems, then, that if we form an input transparency which modulates the phase of the illuminating beam in the same spatial manner that the original photographs modulate

its amplitude, we can expect more of the light to be diffracted away from the centre of the Fourier plane. This will increase the signal to noise ratio in the outer parts of the holographic filter and reduce somewhat the large range of intensities present in the hologram plane. This in turn should allow a larger region of the Fourier plane to be recorded on the matched filter.

Techniques for producing the phase modulated image are the photographic bleaching methods for producing phase holograms. An example of these is the method suggested by Agfa-Gevaert Ltd. (see ref. 50 and Appendix 1). This process removes the silver from a developed but unfixed photographic image. The transparent undeveloped silver bromide is unaffected. The density distribution in the original image has now been mapped into a distribution of refractive index, yielding a spatial distribution of phase modulation when illuminated in transmission.

Although the process is designed for use with the sinusoidal structures of a holographic recording it is equally suited to use with the less symmetrical modulation distributions of photographic images. To investigate the technique, the first of the two correlation exercises of Section 9.2 was repeated using a phase modulated input transparency produced by the photographic bleaching method.

The ERTS frame showing London was contact printed on to an 8E75 plate using a tungsten source. The exposure used was estimated from the information given by Agfa-Gevaert (50) for holographic exposures. They recommend a beam intensity ratio of 4:1 and an average density of about 3 in the plate after development but before bleaching. This

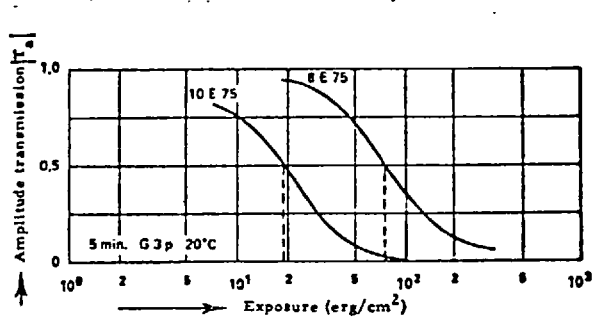

Figure 65. Characteristic curve of amplitude transmission coefficient against exposure for Agfa holographic materials 10E75 and 8E75. (According to Agfa-Gevaert Ltd.).

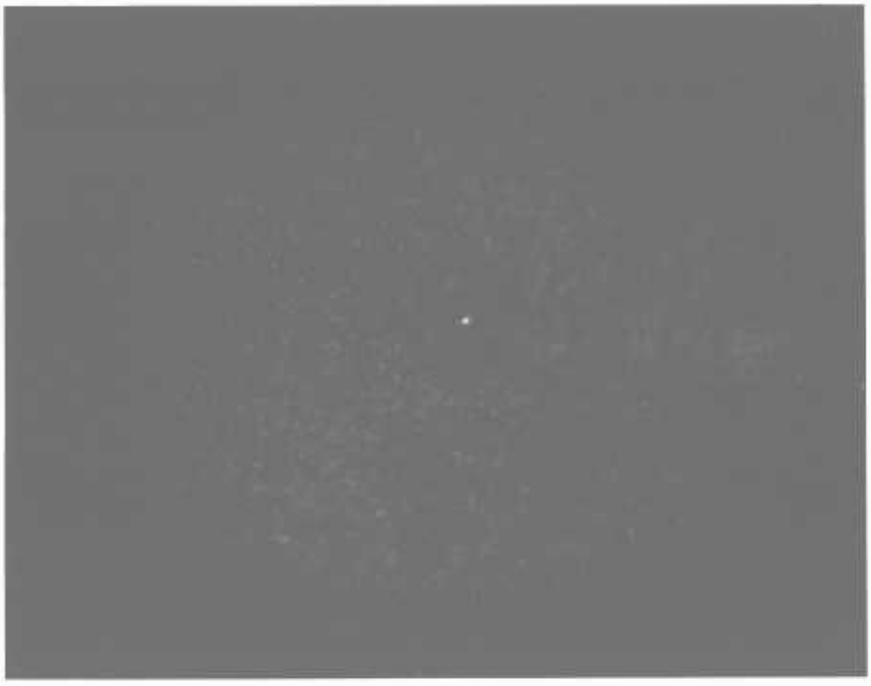

5 mm.

Figure 66. Photograph of cross correlation response obtained between phase-modulated transparencies.

suggests (see Fig. 65) that an exposure range of 9:1 and a mean exposure of 300 erg cm^{-2} at a wavelength of 633 nm. should be presented to the 8E75 plate. This implies that an exposure range of 60 to 540 erg cm^{-2} at 633 nm. would be suitable. As the actual printing exposures were to be carried out with a tungsten white light source it was necessary to determine by trial exposures the degree of exposure to this lamp which gave the plates the same range of densities after development as would be caused by exposure to a range of 60 to 540 ergs cm^{-2} at a single wavelength of 633 nm. It is necessary to hope that the characteristic curve for the material is substantially the same shape at 633 nm. as it is for white light.

The ERTS frame was printed on to the 8E75 plate, the exposure being kept everywhere within the range 60 to 540 erg cm^{-2} by the use of a uniform prefogging exposure to control the contrast. The processing was according to Appendix 1.

The resulting phase modulated image was used in the input plane of a Vander Lugt filtering system using a thermoplastic plate to record the matched filter.

As in Section 9.2, a small area containing the runway pattern was uncovered in the input plane to record the matched filter. Then a larger area was uncovered, within which the smaller area was to be sought. The resulting cross-correlation is shown in Fig. 66. The correlation response for the runway pattern is again seen at the centre of the field, but the difference between the intensity of the correlation signal for the runways and the intensity of the unwanted cross-correlations between the runways and

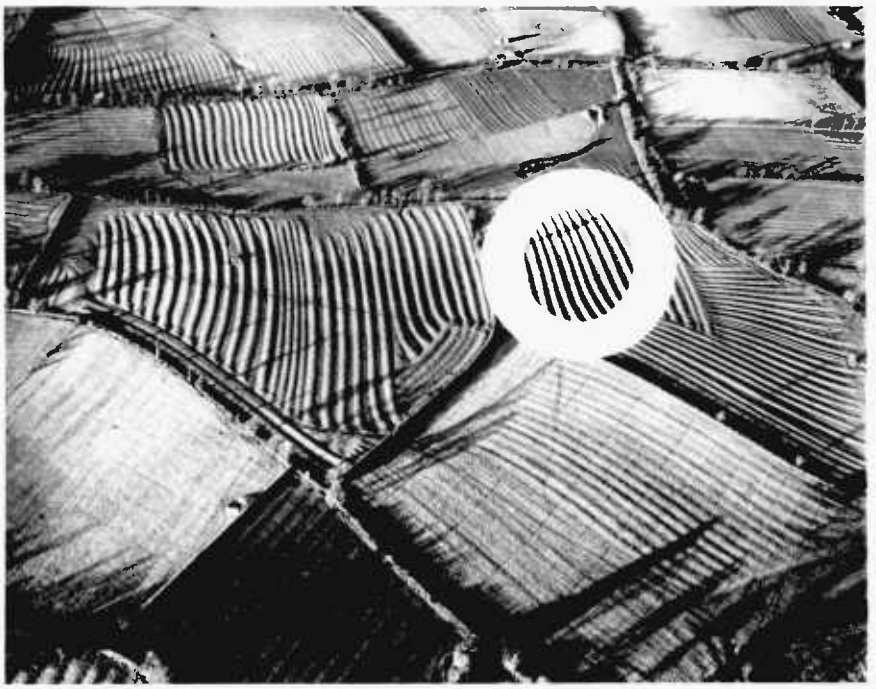

5 mm.

Figure 67. Photograph of a transparency (whose scale is indicated) showing land area in Warwickshire. The ringed area was used in the correlation experiment.

the surrounding area seems greater in this case than with the amplitude modulated input transparencies (see Fig. 61).

In a recognition task it is this difference which yields the signal to noise ratio of the operation, so it is possible that the phase modulated input material may prove useful for tasks of this sort.

9.4 The Optical Autocorrelation of Photographic Data

If the pattern in the object plane during the recording of the matched filter is identical with that present there during the second (correlation) stage then, naturally, it is the autocorrelation of that pattern which appears in the correlation plane.

A relatively simple demonstration of the practical approximation to this was arranged, as a preliminary examination of the application of holographic filtering to geographical continuous tone photographic data through the agency of thermoplastic holography.

Fig. 67 shows an oblique aerial photograph of an area in which the land surface is corrugated in the form known as "ridge and furrow". This surface structure is a direct result of medieval strip farming practices, there being cases where the ridge and furrow pattern corresponds very closely with the arrangement of the strips cultivated by individual peasants as shown on early maps which are still in existence (51). The ridges are up to a few feet in height and are most apparent when, as in Fig. 67, the lighting is across them at a low angle.

This type of area was chosen for the relative simplicity of the structure it presents to the correlator.

Hence there was a reasonable chance that a recognisable autocorrelation would be produced. Nevertheless, the original data was by no means ideal for input material to the correlator, being continuous tone instead of binary, and showing patterns which do not have perfect form, the ridge and furrow being of slightly variable spacing and orientation even within a single furlong. Also, the oblique nature of the view introduces a distortion of any ground pattern, through perspective effects. In these deviations from ideal correlator input material, the image in Fig. 67 is like many photographs of interest in geographical and other similar applications.

For this and all later sections of the work the construction of the hologram plates was slightly different from that used hitherto. Instead of sputtering cadmium oxide on to glass to form the conductive layer upon the substrate material, glass sheets were purchased with a conductive layer of indium oxide already coated upon one side. The resistivity of this film was about 200Ω per square. Contact to it was again made by electrodes of conductive silver paint (DAG 915). The substrates used were about 7 cm. square.

The construction was otherwise much as before, contact electrodes being placed along two opposite edges and being protected for most of their length by Araldite.

A difficulty encountered with the design used previously was concerned with the terminal areas at the ends of the electrodes. Repeated use of these areas by crocodile clips when connecting the heater supply to the hologram plate caused the conductive paint to flake off.

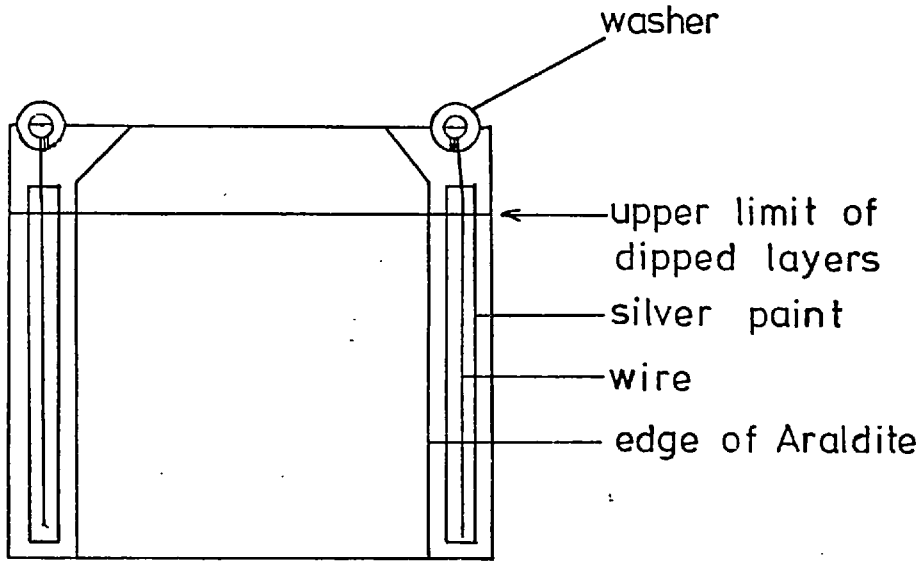

Figure 68. Details of the construction of the final form of thermoplastic holographic plate.

To avoid this, the painted terminal areas were replaced by metal terminals for the crocodile clips to hold.

These terminals were formed from washers of about 8 mm. diameter which were set in the Araldite with about half of their area protruding beyond the glass sheet. Connection between the terminal washer and the painted electrode was made by a thin strand of wire soldered at one end to the washer at a point within the Araldite, and laid for most of its length in the silver paint which formed the electrode. The wire was entirely protected from mechanical damage by the Araldite, only part of the washer being exposed.

The wire extended down the whole length of the painted electrode, ensuring that all parts of a single electrode were at the same potential. This construction is shown in Fig. 68. The organic films were again coated to thicknesses of 2.5μ and 0.2μ for the photoconductor and thermoplastic respectively.

The optical arrangement used for the autocorrelation was as before, using the two 70 cm. transform lenses. An area of the transparency covering a single furlong on the ground was defined in the input plane by an aperture and the holographic filter recorded by the simultaneous mode of operation as described previously. When using these larger hologram plates it was found useful to direct an electric fan at the plate in order to break up convection currents in the air caused by the heat generated by the plate during development. Otherwise the upper part of the hologram plate became markedly hotter than the lower.

The need for earthing one side of the heater supply

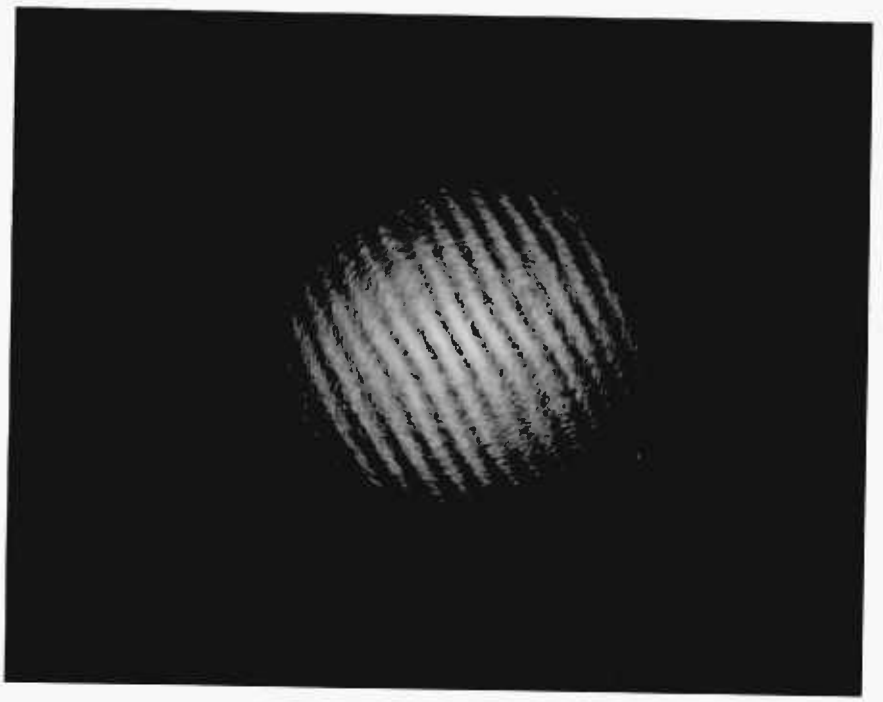

Figure 69. Photograph of the autocorrelation response obtained from ridge and furrow area of the aerial photograph transparency (Fig. 67).

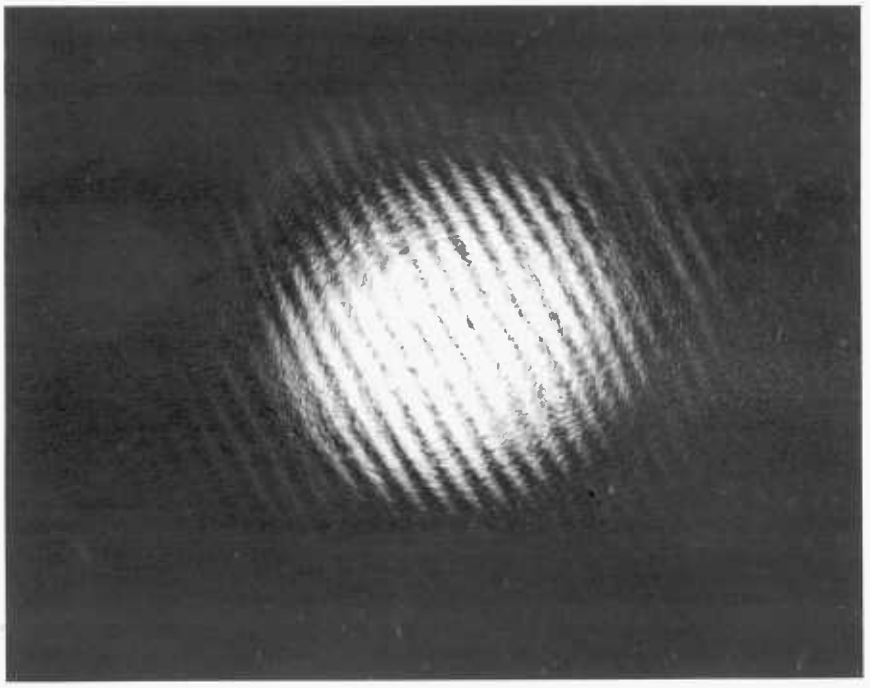

Figure 70. Photograph of the autocorrelation response obtained from ridge and furrow area of the aerial photograph transparency (Fig. 67) (to show detail of outer area).

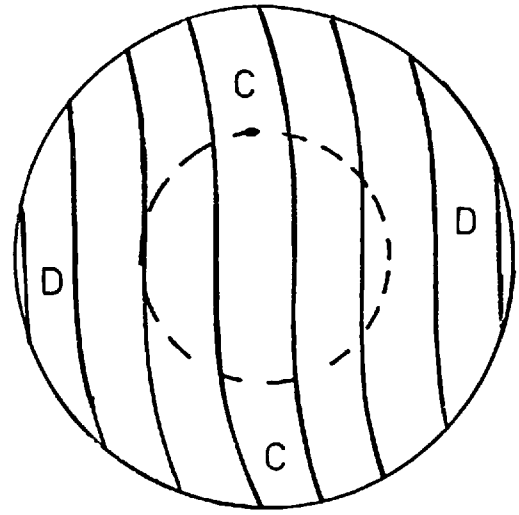

Figure 71a. Diagram of reversed S shaped elements seen through a circular aperture.

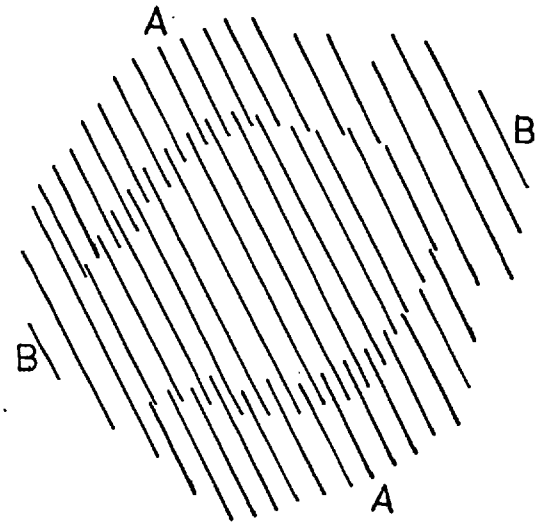

Figure 71b. Form of the fringes traced from the autocorrelation of ridge and furrow (Fig. 69).

was demonstrated at this time. The accidental omission of this earth link on one occasion permitted the D.C. isolated output circuitry of the power supply to float to very high static voltages as the exposed parts of the circuit wiring acquired charge from the corona device during the recording of a hologram. This led to an irreversible breakdown of the insulation in the output voltage control potentiometer.

The appearance of the correlation plane of the optical system when carrying out the second (autocorrelation) stage of the Vander Lugt method is shown in Fig. 69. As would be expected of the autocorrelation of a grating-like structure, the main appearance is a set of straight parallel fringes of the same orientation as the original grating. Also, the number of fringes in Fig. 69 is, approximately at least, twice the number of ridges exposed in the input plane transparency (Fig. 67) which is also consistent with the theory of autocorrelations.

An interesting fainter structure was also visible in the correlation plane at this time, and is shown a little more clearly in Fig. 70 which is from the same negative as Fig. 69 but printed less heavily to emphasise the detail in the outlying parts of the correlation pattern. These details are shown diagramatically in Fig. 71b and consist of additional fringes, mostly aligned with the spaces between the fringes in the centre of the pattern (regions A of Fig. 71b). In certain places (regions B of Fig. 71b) the outlying fringes are straight and uninterrupted for the whole of their length.

A likely explanation of this outlying fringe structure is that it is indeed part of the true autocorrelation of

the ridge and furrow pattern, and is caused by the slight curvature at the end of each furrow. Such curvature is a characteristic feature of ridge and furrow (ref.52, p.82) and is believed to be caused by the need to start turning the team and plough before reaching the end of each furrow in order not to encroach upon the neighbouring strips of land when preparing to return the plough along the next furrow. It is known as the "reversed S" shape of ridge and furrow.

Fig. 71a shows diagramatically a grating of reversed S shaped elements seen through a circular aperture as was used in the input plane. From this we can make certain deductions about the form of its two dimensional autocorrelation if we visualise the shearing of Fig. 71a across itself in various directions.

For example, with small amounts of shear the main contribution to the autocorrelation will come from the straight part of the elements within the dotted circle of Fig. 71a, generating the strong fringe pattern seen in the central region of the correlation plane. However, large amounts of shear along the line of the ridge and furrow grating will cause coincidences between the parallel "shoulders" and "toes" (C) of the curved grating elements, giving additional weak fringes to the outlying part of the autocorrelation (Region A). There is no reason to suppose that these outlying fringes will align with the central fringes as their precise location will depend upon the amount of curvature of the grating elements.

In contrast to this, where large amounts of shear occur perpendicularly to the grating elements there can

20 mm.

Figure 72. Photograph of a transparency (whose scale is indicated) showing aerial views of
a) apparently random arrangement of trees, and
b) regular plantation of trees.

only be straight continuous fringes of a single alignment (Region B) as the grating elements (D) at the extreme edges of the aperture along this line are truncated by the circular aperture and show no curvature in their visible length.

It seems, then, that the appearance of Fig. 70 can probably be accounted for in some detail by comparisons with the expected autocorrelation and the optical autocorrelation method seems to provide reasonable performance with this particular type of input data.

9.5 Optical Autocorrelation in a more Practical Situation

A possible application for the autocorrelation operation is the recognition and analysis of symmetrical patterns amid a noisy background. This ability can easily find uses in connection with satellite and aerial photography, as symmetrical patterns in such images are frequently of artificial origin and rarely natural, providing a means of discriminating between the two in some cases.

An example of a comparison between two areas of an aerial photograph which exhibit different degrees of symmetry in their internal arrangements was carried out using the image shown in Fig. 72. This vertical air photo contains several woodland areas which display different degrees of symmetry in their arrangement. The area A appears to be a more or less random distribution of trees whereas area B, on close inspection, seems to contain trees which are planted on a rectangular matrix.

5 mm.

Figure 73. Photograph of the autocorrelation response obtained from the randomly afforested area (region a) of the transparency shown in Fig. 72.

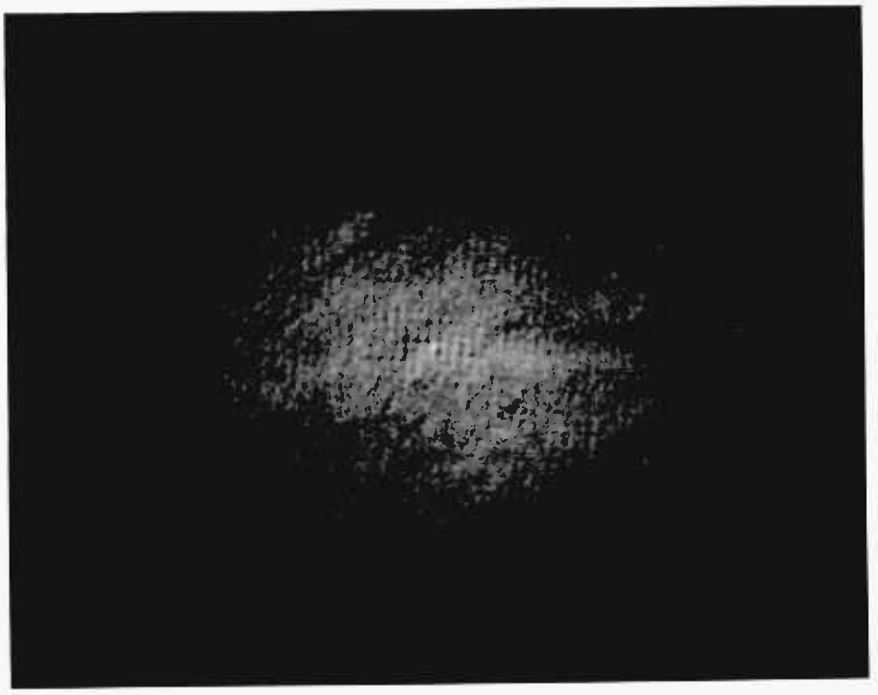

5 mm.

Figure 74. Photograph of the autocorrelation response obtained from the regularly planted area (region b) of the transparency shown in Fig. 72.

The autocorrelation of each of these two areas was carried out optically by the same method as before, thermoplastic holography in the simultaneous mode being used to form the holographic filter.

The appearance of the correlation plane of the optical bench found when autocorrelating areas A and B are shown in Figs. 73 and 74 respectively. Fig. 73 obtained from the apparently randomly arranged woodland shows a bright central region but little significant information away from this.

Fig. 74 on the other hand has a bright central point corresponding to the condition of "zero lag", surrounded by a matrix of fainter points. These suggest that an appreciable degree of correlation exists between the tree spacings in parts of the woodland separated from each other by up to twenty trees. The separation of the points in this autocorrelation matrix should also give a measure of the average separation of the trees.

It is not intended here to attempt to specify the degree of correlation which can be detected by this technique and it is not possible without a ground truth study to investigate either which types of woodland can be distinguished or the usefulness of such information in, say, forest surveys and management. However, we can at least see that holographic filtering is a technique which can extract information from continuous tone aerial photographs.

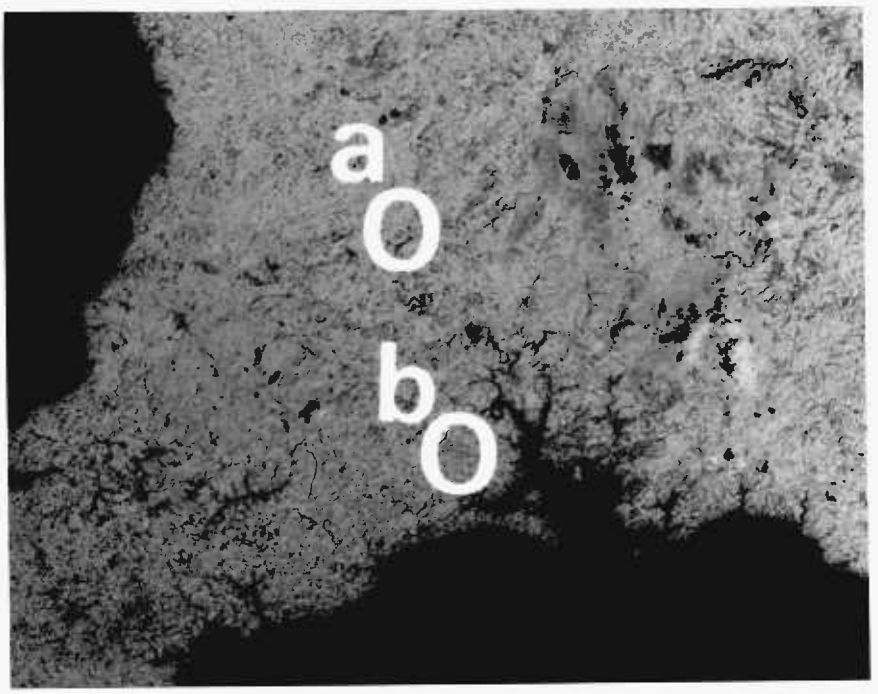

Figure 75. Photograph of an ERTS satellite transparency (whose scale is indicated) showing the areas a and b used in the autocorrelation expermints.

9.6 The Optical Autocorrelation of a Satellite Image Representing an Agricultural Area

As a further example of a possible application of holographic filtering to the analysis of continuous tone satellite imagery, the existence of different "textural signatures" for areas representing agricultural fields was tested. The type of signature considered here was concerned with the size, shape and orientation of the autocorrelation of the respective ERTS transparency area. If, for example, the fields in a certain area were all elongated in a particular direction we should expect their autocorrelation to be extended along that line. More typically, there may be wide variation in field size and shape, and in the orientation of their longest sides about some preferred arrangement. Therefore a technique, such as the use of autocorrelation which promises information about the average geometry of the fields, offers the possibility of producing a relatively simple characteristic signature for a region containing a complex field pattern.

The areas chosen for this exercise are shown in Fig. 75. These correspond with two agricultural regions in different types of terrain. Area A lies inland and close to Dartmoor, and area B lies in the valley of the River Tamar near the coast.

Each of these areas of the transparency was in turn autocorrelated optically using Vander Lugt filtering with a thermoplastic plate in the filter plane. Again the purpose-built Fourier transform lenses were used.

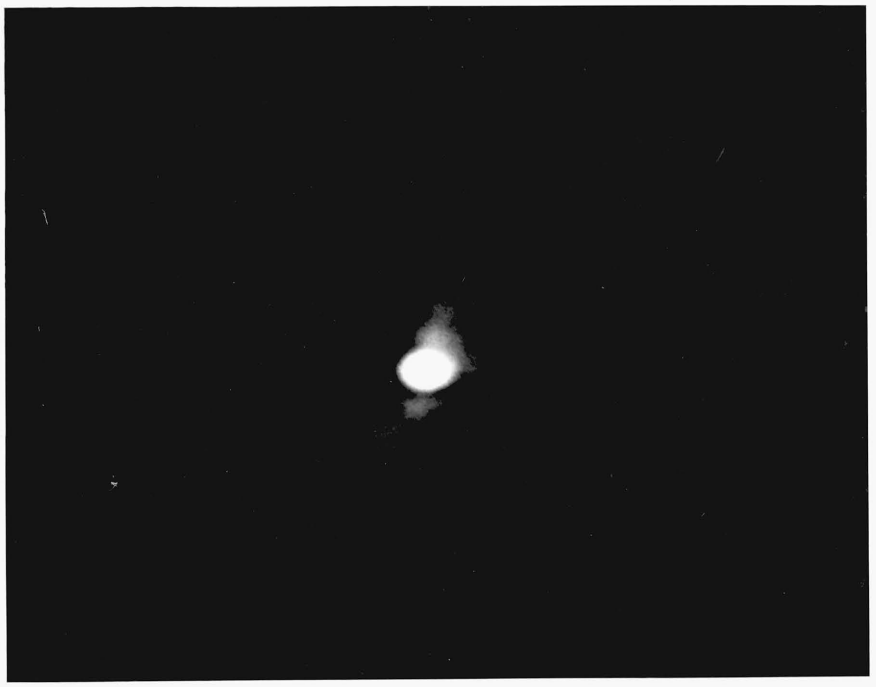

0·5mm.

Figure 76a. Photograph of the autocorrelation response obtained from region a of the transparency shown in Fig. 75.

0·5mm.

Figure 76b. Photograph of the autocorrelation response obtained from region b of the transparency shown in Fig. 75.

The appearance of the correlation plane during the second (correlation) stage of the procedure is shown in Fig. 76 for each of the two areas. In each case the brightest part of the structure is roughly elliptical, with a size of about 200 μm. This order of size corresponds to objects whose size is about 100 m. on the ground, the transparency used being of 1:1000000 scale, which suggests that objects about the size of a field are determining the appearance of the correlation response.

The ellipses in Fig. 76 are oriented differently suggesting different preferred arrangements in the geometry of the field layout in the two regions.

Whether the textural signatures apparently given by these autocorrelation responses characterise features of the terrain which are of significance to particular sections of society is a matter which can only be decided by linking this work with ground truth studies.

Also, more extensive work to examine the autocorrelation signatures of a number of different areas which are known to possess such significant features to various degrees is necessary. This would determine whether the simplification involved in averaging field geometries by autocorrelation permits the resulting signatures to retain sufficient information for adequately precise discrimination.

CHAPTER 10

CONCLUSION

10.1 The Thermoplastic Technique

Thermoplastic holography offers a useful laboratory tool for the investigation of holographic filtering and its application to particular problems. Its chief advantage is great convenience of operation in comparison with photographic materials.

The freedom from major mechanical displacement during development is of great practical assistance, although further study of the effects of thermal expansion of the hologram plate during heat development would be useful. If this were found a problem in any particular case it could be avoided by using the sequential mode of operation in which the recording and reconstruction stages take place with the hologram plate at the same temperature. The price would probably be a lower diffraction efficiency.

The apparent insensitivity to normal ambient room lighting levels is another practical aid. The exposure and development of the plate in the present work was carried out in negligible ambient lighting although this was not necessary judging by a few trials in more convenient lighting levels. Certainly, freedom from the need to handle and store holographic plates in darkness was found helpful in setting up the equipment for use.

The high diffraction efficiency of the thermoplastic device in comparison with the ordinary photographic

materials was, of course, also welcome.

A considerable disadvantage to the use of thermoplastic holography as described here is the presence of a carcinogenic compound. This imposes restrictions upon the handling and storage of the devices. It would be a great improvement for the technique if an equally effective but less dangerous photoconductor dopant material could be identified.

The principal inconvenience in the operation of thermoplastic holography is the need carefully to standardise the method used in preparing substrates, especially regarding the organic layers, in order to obtain repeatable results. In practice it would take a little time, a few weeks, say, to re-establish the degree of consistency achieved in this work, which would not be an excessive time during a research project, but this is clearly less desirable than the high degree of consistency reached by the manufacturers of photographic materials with virtually every batch of their readily available products.

The presence of high corona voltages during development is an additional hazard, although it appears to be a basic requirement of the method and not easy to avoid. At least this hazard is present only for short, clearly defined periods of time.

10.2 The Holographic Filtering Technique using Thermoplastic Materials

Naturally, the ideal aim of applied research is the creation of a routine tool for use in other disciplines.

It seems, however, that considerable development work would be necessary to simplify the operation of thermoplastic devices to the stage where they could be used routinely without the need for anything more than occasional attention from the operator.

However, as holographic filtering itself needs still considerable development before it becomes a routine technique in, say, satellite image interpretation, any technique such as thermoplastic recording which makes the study of holographic filtering easier is welcome.

We have seen, in previous chapters, illustrations of various avenues by which holographic filtering may be useful in extracting information from continuous tone imagery. The execution of these examples yielded the results given in Chapter 9 but also permitted some more general observations on the use of holographic filtering in connection with continuous tone image interpretation.

Perhaps the most striking point is the great extent to which Vander Lugt holographic filtering deviates from the ideal correlation operation when it is carried out in practice with any holographic recording material, thermoplastic or otherwise. This arises from saturation of the recording mechanism in the central bright area of the Fourier plane and possibly also from contrast reversal in this part of the Fourier plane during filter recording if the reference beam is not everywhere brighter than the Fourier transform being recorded. It would be quite difficult to arrange the beam ratios so that the Fourier transform was linearly recorded on the hologram, even for only that part which can be accommodated within the

available dynamic range of a photographic film whose characteristics are well known. To attempt this with the thermoplastic material, where the parameters involved in the material's characterisation are not even identified yet with certainty, would not be fruitful at present.

It is, however, probably because of the rather widespread reluctance to discuss practical difficulties of this type, that hopes for the Vander Lugt technique have, at least as yet, exceeded its actual applications. No doubt this reluctance stems from a desire not to detract from the elegance which the method has in principle. The introduction of thermoplastics to holographic filtering has, at any rate, largely overcome two of the practical difficulties: low holographic diffraction efficiency and the need for mechanical repositioning of the matched filter.

10.3 Suggestions for Further Work

Two improvements to the thermoplastic hologram recording equipment are desirable. The most urgent of these is undoubtedly the elimination of the carcinogenic dopant from the organic photoconductor. Until this is done, the technique is not likely to be popular among research workers and would certainly not be made available as a routine tool in other disciplines where the workers' level of awareness of the existence and nature of the hazard would probably be lower.

The other materials involved in the fabrication of the thermoplastic plates are relatively harmless and there appears to be little point in altering them until the

limitations of the materials become more apparent.

The second change in the equipment which may be useful concerns the corona charging device. The form used in the present work consisted of a single wire partially surrounded by an earthed cylinder. This charged a large central area of the plate quite uniformly, including the whole of the area of the Fourier transform which was likely to be within the dynamic range of the thermoplastic recording material. However, if it should be required to record over the whole of the hologram plate, then a charging device containing several parallel high tension wires would give better uniformity of charging over the larger area.

Two series of observations concerning the behaviour of the hologram plates would be useful. Firstly the response of the plates as a function of the charging voltage should be studied, and the optimum voltage used for further work. Absolute measurements of the voltage on the thermoplastic surface would be rather difficult and are not really necessary for optimising the process. What is needed is a means of varying the voltage to which the surface is charged (such as a voltage limiting wire grid between charging device and thermoplastic). However, a means of detecting variations in the voltage being applied to the surface as a result of fluctuations in, say, the ambient relative humidity would be useful in determining the extent of their influence.

Secondly, as it is necessary when setting up the thermoplastic processing procedure to identify the optimum thermoplastic thickness for the holographic spatial frequency to be used, a convenient method for plotting

quickly the characteristic of relative response against spatial frequency would be useful. The most promising solution to this is to record a hologram using plane reference wavefronts but spherical diverging wavefronts in the other beam. This would cause a range of spatial frequencies to be recorded across the plate. The plate would then be illuminated by the reference wavefronts alone and viewed by a closed circuit television system. If one line of the television raster were displayed on an oscilloscope it would show in effect a graph of relative holographic response against spatial frequency.

With regard to the behaviour of thermoplastic plates in holographic filtering, computation should be used to investigate further the effect of limited dynamic recording range of the hologram upon the form of the correlation response. This should be carried out in parallel with computations of the true autocorrelations of continuous tone transparencies for comparison.

References

1. Electrophotography, R. M. Schaffert, The Focal Press, 1965

2. Claus, C. J., Advances in Xerography: 1958-1962, Phot. Sci. & Eng. 7, No. 1, 5 (1963)

3. Glenn, W. E., Thermoplastic Recording, J. Appl. Phys. 30, No. 12, 1870, (1959)

4. Lardon, Lell-Döller and Weigl, Charge Transfer Sensitization of Some Organic Photoconductors based on Carbazole., Molecular Crystals, 2, 241 (1967)

5. Hayashi, Kuroda and Inami, Bull. Chem. Soc. Jap. 39, No. 8, 1660 (1966)

6. Hoegl, On Photoelectric Effects in Polymers and their Sensitization by Dopants, J. Phys. Chem., 69, no. 3, 775, (1965)

7. Gaynor, J. and Aftergut, S. Photoplastic Recording, Phot. Sci. & Eng. 7, No. 4, 209 (1963)

8. Gundlach, R. W. and Claus, C. J., A Cyclic Xerographic Method Based on Frost Deformation. Phot. Sci. & Eng. 7, No. 1, 14 (1963)

9. Vacuum Deposition of Thin Films, L. Holland, Chapman & Hall (1st edition, 1956)

10. Ilford Manual of Photography, 5th Edition

11. Urbach, J. C., Evaluation of Light-Scattering Images (Proceedings of the Conference on Photographic and Spectroscopic Optics 1964) Jap. J. Appl. Phys., 4, Supp. 1, (1965)

12. Urbach, J. C., The Role of Screening in Thermoplastic Xerography, Phot. Sci. & Eng., 10, No. 5, 287 (1966)

13. Marquet, M. and Tsujiuchi, J., Interpretation des aspects particuliers des images obtenues dans une expérience de détramage, Opt. Acta, 8, 267, (1961)

14. Urbach, J. C. and Meier, R. W., Thermoplastic Xerographic Holography, App. Opt., 5, No. 4, 666, (1966)

15. Leith, E. N. and Upatnieks, J., J. Opt. Soc. Am. 52, No. 10, 1123, (1962)

16. Queener, C. A., Use of an Organic Photoconductor in Xerography, Phot. Sci. & Eng. 15, No. 5, 423 (1971)

17. Schaffert, R. M., High Electrostatic Contrast in Electrophotography, Phot. Sci. & Eng. 15, No. 2, 148 (1971)

18. Electricity and Magnetism, Bleaney, B. I. and Bleaney, B., Oxford University Press, 2nd Edition.

19. Ionized Gases, von Engel, A., Oxford University Press, 2nd edition (1965)

20. Shahin, M. M., Characteristics of Corona Discharges and their application to Electrophotography, Phot. Sci. & Eng., 15, no. 4, 322 (1971)

21. Shahin, M. M. Mass-Spectrometric Studies of Corona Discharges in Air at Atmospheric Pressures. J. Chem. Phys. 45, 2600 (1966)

22. Sullivan, W. A. and Kneiser, J. J., Tone Reproduction by Frost Images, Phot. Sci. & Eng. 8, no. 4, 206 (1964)

23. Cressman, P. J., New Type of Thermoplastic Deformation, J. Appl. Phys., 34, no. 8, 2327 (1963)

24. Budd, H. F., Dynamical Theory of Thermoplastic Deformation, J. Appl. Phys., 36, no. 5, 1613 (1965)

25. Shahin, M. M., Nature of Charge Carriers in Negative Coronas. App. Opt. Supp. no. 3, 106 (1969)

26. Ost, J. and Moraw, R., Reversible Holographische Aufzeichnung in Photothermoplasten, Optik, 37, 357 (1973)

27. Lin, L. H. and Beauchamp, H. L. Write-Read-Erase in situ Optical Memory Using Thermoplastic Holograms, App. Opt., 9, 2088 (1970)

28. Lee, T. C. Holographic Recording on Thermoplastic Films, App. Opt., 13, 888, (1974)

29. Bergen, R. F. Characterization of a Xerographic Thermoplastic Holographic Recording Material, Phot. Sci. & Eng. 17, 473, (1973)

30. Credelle, T. L. and Spong, F. W., Thermoplastic Media for Holographic Recording, RCA Review 33, 206, (1972)

31. Stewart, W. C., Mezrich, R. S., Cosentino, L. S., Nagle, E. M., Wendt, F. S. and Lohman, R. D. An Experimental Read-Write Holographic Memory, RCA Review, 34, 3, (1973)

32. Lee, T. C., Recent Experimental Results of Alterable Holographic Storage in Thermoplastic-Photoconductor Devices, Digest of Technical Papers, Topical Meeting on Optical Storage of Digital Data, Optical Society of America, March 1973

33. Vander Lugt, A., Signal Detection by Complex Spatial Filtering, IEEE Trans. Inform. Theory, IT-10, 139, (1964)

34. Optical Holography, Collier, R.J., Burckhardt, C. B. and Lin, L. H., Academic Press, (1971)

35. Bulabois, J., Caron, A., Viénot, J. Ch., Selectivity of Hologram Filters as a Function of Pass Band Characteristics, Optics Technology, 191, August 1969

36. Dickinson, A. and Watrasiewicz, B. M., Critical Adjustment of Correlation Filters for Optical Character Recognition, Optics and Laser Technology, 229, November 1971

37. Peaker, A. R., and Horsley, B., Transparent Conducting Films of Antimony Doped Tin Oxide on Glass, Rev. Sci. Inst. 42, no. 12, 1825, (1971)

38. Preston, J. S., Constitution and Mechanism of the Selenium Rectifier Photocell, Proc. Roy. Soc. (A), 202, 449, (1950)

39. W. Edwards & Co. Ltd. Working Instructions for the Model 12 E Evaporating and Sputtering Plant

40. Gray, P. F. and Barnett, M. E. On Factors Affecting Diffraction Efficiency in Thermoplastic Hologram Recording, Optics Communications 12, 275, (1974)

41. Keyte, G. E. Limitation of the Photographic Process in the Preparation of Spatial Frequency Filters, AGARD XVIIth Avionics Panel Technical Symposium, Tonsberg, Norway, 24, (1969)

42. Lowenthal, S. and Belvaux, Y., Reconnaissance des formes par filtrage des fréquences spatiales, Opt. Acta. 14, 245, (1967)

43. The Fourier Transform and its Applications, Bracewell, R., McGraw-Hill, (1965)

44. Principles of Optics, Born, M. and Wolf, E. Pergamon Press, 4th edition (1970)

45. Rotz, F. B. and Greer, M. O., Photogrammetric and Reconnaissance Applications of Coherent Optics, Proc. Soc. Photo-Optical Instrumentation Engineers, 45, Coherent Optics in Mapping, 139, (1974)

46. Ilford Technical Sheet No. A 32. 2, Ilford Pan F 35 mm. Miniature Film

48. Gray, P. F. and Barnett, M. E., Matched Filtering of Continuous Tone Transparencies using Phase Media, Optics Communications, 14, 46 (1975)

49. Gray, P. F. and Barnett, M. E., Fourier Transform Holography and Optical Correlation using Thermoplastic Materials, Proceedings of ICO-10 Conference Prague 1975 (to be published)

50. Agfa-Gevaert Ltd., Photographic Materials for Holography, Technical Information (Scientific Photography) Sheet No. 21 7271 (771) (July 1971)

51. The Lost Villages of England, Maurice Beresford, Lutterworth Press, 1st Edition, Chapter 2, Plates 2 & 3

52. Fields in the English Landscape, Christopher Taylor, Dent, (1975).

Appendix 1

Processing used in the production of phase modulated transparencies using Agfa-Gevaert 8E75 or 10E75 Holographic Plates (From ref. 50)

Solutions used:-

Developer	Agfa-Gevaert G3p at normal dilution
Stop Bath	1% solution of Acetic Acid in water
Bleach	5 gm. Potassium Bichromate 5 ml. concentrated Sulphuric Acid 1 litre distilled water
Clearing agent	100 gm. Sodium Sulphite crystals 1 gm. Sodium Hydroxide 950 ml. distilled water
Desensitising agent	880 gm. Ethyl Alcohol 100 ml. distilled water 20 gm. Glycerine 120 mg. Potassium Bromide 200 mg. per litre Phenosafrinine

contd.

Appendix 1 (contd.)

Processing Stages:-

1. Develop for 5 minutes at 20° C (do not fix).
2. Immerse in stop bath for 2 minutes.
3. Wash in water for 5 minutes.
4. Bleach for 2 minutes.
5. Wash in water for 5 minutes.
6. Clear for 1 minute.
7. Wash in water for 5 minutes.
8. Desensitise (1 minute).
9. Rinse in Ethyl Alcohol.

Acknowledgements

I wish to thank Dr. M.E. Barnett of the Applied Optics Section, the supervisor of this work, for his support and advice throughout the project.

I am most grateful to my father, Mr. F.M. Gray, for the great assistance he provided by typing this thesis.

I should like also to thank Miss Lesley Knight for her help in the processing of photographs for the thesis, and Mr. R.M. Lee and Mr. J.D. Cleary for their helpful discussions and efforts in gathering the data for Figure 38.

The financial support of the Department of Industry for all stages of the work is also gratefully acknowledged.